

**ISTANBUL TECHNICAL UNIVERSITY ★ GRADUATE SCHOOL OF SCIENCE**  
**ENGINEERING AND TECHNOLOGY**

**FUNCTIONAL CONJUGATED POLYMERS**

**Ph. D.THESIS**

**Hüseyin AKBULUT**

**Department of Chemistry**

**Chemistry Programme**

**AUGUST 2015**



**ISTANBUL TECHNICAL UNIVERSITY ★ GRADUATE SCHOOL OF SCIENCE**  
**ENGINEERING AND TECHNOLOGY**

**FUNCTIONAL CONJUGATED POLYMERS**

**Ph. D. THESIS**

**Hüseyin AKBULUT**  
**(509112016)**

**Department of Chemistry**

**Chemistry Programme**

**Thesis Advisor: Prof. Dr. Yusuf YAĞCI**

**AUGUST 2015**



**İSTANBUL TEKNİK ÜNİVERSİTESİ ★ FEN BİLİMLERİ ENSTİTÜSÜ**

**FONKSİYONEL KONJUGE POLİMERLER**

**DOKTORA TEZİ**

**Hüseyin AKBULUT  
(509112016)**

**Kimya Anabilim Dalı**

**Kimyagerlik Programı**

**Tez Danışmanı: Prof. Dr. Yusuf YAĞCI**

**AĞUSTOS 2015**



**Hüseyin AKBULUT, a Ph.D. student of ITU Graduate School of Science Engineering and Technology** student ID 509112016, successfully defended the thesis entitled “**FUNCTIONAL CONJUGATED POLYMERS**”, which he prepared after fulfilling the requirements specified in the associated legislations, before the jury whose signatures are below.

**Thesis Advisor :**      **Prof. Dr. Yusuf YAĞCI**      .....

İstanbul Technical University

**Jury Members :**      **Prof. Dr. Turan ÖZTÜRK**      .....

İstanbul Technical University

**Prof. Dr. Mehmet EROĞLU**      .....

Marmara University

**Date of Submission : 27 July 2015**

**Date of Defense :**





*To my mother and father*



## FOREWORD

First of all, I would like to thank my thesis supervisor, Prof. Yusuf YAĞCI, for giving me the opportunity without football skills to work in his group. I am deeply indebted to him for his kind guidance, support, understanding, encouragements and help in academic and social life. Without his thoroughness and help, I would have never been able to accomplish the work of my graduate research. Always, I will remember his advice “You should be best whatever you do even playing a game”

Also i would like to many thanks the Prof. Dr. Suna Timur, Prof Dr. Takeshi Endo and Dr. Shuhei Yamada, without their knowledge and excellent skills, writing of this thesis would never be possible.

I would like to thank Prof. Dr. Turan Öztürk and Prof. Dr. Mehmet Erğolu for serving as my doctoral committee member and making valuable suggestions.

I would also like to express my deep thanks to all the past and present members of “Yagci Group” for their help, friendship and the nice environment they created not only inside, but also outside the lab. In particular, , Assoc. Prof. Dr. Baris Kiskan, Dr. Ömer Suat Taskin, Dr. Demet Çolak, Prof. Dr. Ioan Chianga, Cansu Aydoğan, Mustafa Arslan, Elyesa Murtezi, Senem Körk, Abdurrahman Musa, Sajjad Dadashi, Dr. Sean Doran, Semih Erdur, Semiha Bektaş, Betül Hanbeyoğlu, Elif Semerci, Ali Görkem Yılmaz, Mustafa Çiftçi, Umut Uğur Özköse, Merve Kara and Ozde Yetiskin with all of you, it has really been a great pleasure.

Finally, during all stages involved in the preparation of this thesis, I’m grateful to my mother Birsen and father Çetin Akbulut for their encouragement, understanding, patience and support all through my education.

The author thank the Scientific and Technical Research Council of Turkey (Tubitak) and the author was supported with scholarship by TUBITAK-BİDEB (2211-C).

AUGUST 2015

Hüseyin AKBULUT  
(M.Sc. Chemist)



## TABLE OF CONTENTS

	<u>Page</u>
<b>FOREWORD</b> .....	<b>ix</b>
<b>TABLE OF CONTENTS</b> .....	<b>xi</b>
<b>ABBREVIATIONS</b> .....	<b>xiii</b>
<b>LIST OF TABLES</b> .....	<b>xv</b>
<b>LIST OF FIGURES</b> .....	<b>xvii</b>
<b>SUMMARY</b> .....	<b>xix</b>
<b>ÖZET</b> .....	<b>xxiii</b>
<b>1. INTRODUCTION</b> .....	<b>1</b>
1.1 Purpose of Thesis.....	2
<b>2. ELECTROCHEMICAL DEPOSITION OF POLYPEPTIDE: BIO-BASED COVERING MATERIALS FOR SURFACE DESIGN</b> .....	<b>5</b>
2.1 Result and Discussion.....	7
2.1.1 Electroactive Polypeptide Macromonomer.....	7
2.1.2 Electrodeposition T-Pala and Enzyme Immobilization.....	9
2.1.3 Characterization of the PT-Pala Film.....	10
2.1.4 Surface Characterization.....	11
2.1.5 Biosensing applications.....	13
2.2 Experimental Section.....	19
2.2.1 Materials.....	19
2.2.2 Synthesis of thiophene-3-carbonitrile (1b).....	19
2.2.3 Synthesis of 3-(aminomethyl)thiophene (1c).....	19
2.2.4 Synthesis of L-Ala-N-(phenyloxycarbonyl) amino acid.....	20
2.2.5 Synthesis of T-Pala in the presence of 3-(aminomethyl)thiophene.....	20
2.2.6 Preparation of PT, PT-Pala, and PT-Pala/PT biosensors.....	20
2.2.7 Measurements.....	21
2.2.8 Electrochemical measurements.....	22
2.2.9 Antimicrobial activities.....	22
2.3 Conclusion.....	23
<b>3. SYNTHESIS AND CHARACTERIZATION OF POLYPHENYLENES WITH POLYPEPTIDE AND POLY(ETHYLENE GLYCOL) SIDE CHAINS</b> .....	<b>25</b>
3.1 Experimental.....	25
3.1.1 Materials.....	28
3.1.2 Measurements.....	28
3.1.3 Synthesis of 1,4-dibromo-2-(bromomethyl) benzene (1).....	29
3.1.4 Synthesis of 2-(2,5-dibromobenzyl)isoindoline-1,3-dione (2).....	29
3.1.5 Synthesis of (2,5-dibromophenyl) methan amine (MA-DBB).....	29
3.1.6 Synthesis of Urethane Derivatives of N $\epsilon$ -Carbobenzoxy-L-lysine (NCA-LL).....	30
3.1.7 Synthesis of polypeptide macromonomer (DBB-PLL).....	30
3.1.8 Synthesis of PEG macromonomer (DBB-PEG).....	31

3.1.9 Synthesis of PPP conjugated polymer bearing poly-L-lysine and PEG (PPP-g-PEG-PLL) .....	31
3.1.10 Synthesis of PPP conjugated polymer bearing primary amine and PEG (PPP-NH <sub>2</sub> -g-PEG) .....	32
3.1.11 Synthesis of PPP conjugated polymer bearing poly-L-lysine and PEG (PPP-g-PEG-PLL) by route 2 .....	32
3.2 Results and Discussion .....	33
3.2.1 Synthesis of PPPs with Polypeptide and PEG Side Chains .....	35
3.1.1 Materials .....	35
3.3 Conclusions .....	44
<b>4. SYNTHESIS, CHARACTERIZATION AND TARGETED CELL IMAGING APPLICATIONS OF POLY(P-PHENYLENE)S WITH AMINO AND POLY(ETHYLENE GLYCOL) SUBSTITUENTS .....</b>	<b>47</b>
4.1 Results and discussion .....	49
4.1.1 Synthesis of PPP with primary amine groups and PEG side chains .....	52
4.1.2 Bioconjugation of the FA to PPP-NH <sub>2</sub> -g-PEG .....	55
4.1.3 Cell culture .....	57
4.1.3.1 Cytotoxicity assay .....	57
4.1.3.2 Fluorescence microscope images .....	58
4.2 Experimental .....	60
4.2.1 Materials .....	60
4.2.2 Measurements .....	60
4.2.3 Synthesis of 1,4-dibromo-2-(bromomethyl)benzene (1) .....	61
4.2.4 Synthesis of 2-(2,5-dibromobenzyl)isoindoline-1,3-dione (2) .....	61
4.2.5 Synthesis of (2,5-dibromophenyl)methanamine (DBB-MA) .....	61
4.2.6 Synthesis of PEG macromonomer (DBB-PEG) .....	62
4.2.7 Synthesis of PPP conjugated polymer (PPP-NH <sub>2</sub> -g-PEG) .....	62
4.2.8 Bioconjugation of FA to PPP-NH <sub>2</sub> -g-PEG Polymer .....	62
4.2.9 Characterization of the FA/PPP-NH <sub>2</sub> -g-PEG conjugate .....	63
4.2.10 Cell culture .....	63
4.2.11 Cytotoxicity assay .....	63
4.2.12 Cell imaging via fluorescence microscopy .....	64
4.3 Conclusions .....	64
<b>5. CONCLUSIONS .....</b>	<b>67</b>
<b>REFERENCES .....</b>	<b>69</b>
<b>CURRICULUM VITAE .....</b>	<b>89</b>

## ABBREVIATIONS

<b>CDCl<sub>3</sub></b>	: Deuterated Chloroform
<b>CH<sub>2</sub>Cl<sub>2</sub></b>	: Dichloromethane
<b>DMF</b>	: <i>N,N</i> -dimethylformamide
<b>DMSO</b>	: Dimethyl Sulphoxide
<b>DSC</b>	: Differential Scanning Calorimetry
<b>EtOAc</b>	: Ethyl Acetate
<b>FT-IR</b>	: Fourier Transform Infrared Spectrophotometer
<b>GPC</b>	: Gel Permeation Chromatography
<b><sup>1</sup>H NMR</b>	: Hydrogen Nuclear Magnetic Resonance Spectroscopy
<b>PCL</b>	: Poly( $\epsilon$ -caprolactone)
<b>PEG</b>	: Poly(ethylene glycol)
<b>ROP</b>	: Ring-opening Polymerization
<b>TEA</b>	: Triethylamine
<b>THF</b>	: Tetrahydrofuran





## LIST OF TABLES

### Page

<b>Table 2.1 :</b> Comparison of some glucose biosensors constructed with different immobilization techniques, in terms of linearity and the relative standard deviation (RSD) in the literature.....	17
<b>Table 2.2 :</b> Antimicrobial activities of T-Pala, PT-Pala and standard antibiotics...	18
<b>Table 3.1 :</b> Solubility characteristics of the graft copolymers and precursors.....	38
<b>Table 3.2 :</b> Photophysical properties of PPP-g-PEG-PLL and its precursors.....	42
<b>Table 3.3 :</b> Molecular Weight Characteristics of the Graft Copolymers and Precursors .....	43



## LIST OF FIGURES

	<u>Page</u>
<b>Figure 2.1</b> : Preparation of 3-(aminomethyl)thiophene (1c).....	8
<b>Figure 2.2</b> : Synthetic route towards L-Ala-N-(phenyloxycarbonyl)amino acid (2c). .....	8
<b>Figure 2.3</b> : Synthesis of thiophene-polyalanine (T-Pala) .....	8
<b>Figure 2.4</b> : Schematic representation of PT-Pala film formation and construction of the PT-Pala film/GOx biosensor.....	9
<b>Figure 2.5</b> : FT-IR spectra of T-Pala and PT-Pala .....	10
<b>Figure 2.6</b> : CVs of the bare graphite electrode, PT-Pala-coated electrode, and GOx-immobilized PT-Pala-coated electrode.....	11
<b>Figure 2.7</b> : Cyclic voltammograms of prepared electrodes. (A) CVs of PT-Pala modified and (B) PT-Pala/GOx modified electrodes at the different scan rates, Inset: The correlation between the current and square root of the scan rate.....	12
<b>Figure 2.8</b> : SEM images of (A) PT-Pala-, (B) PT-Pala/PT-, and (C) PT-coated electrodes .....	13
<b>Figure 2.9</b> : Fluorescence microscope image of PT-Pala coated electrode .....	14
<b>Figure 2.10</b> : The effect of pH .....	14
<b>Figure 2.11</b> : Calibration curve for glucose .....	15
<b>Figure 2.12</b> : Calibration curve for glucose .....	16
<b>Figure 2.13</b> : Antimicrobial activity of PT-Pala .....	18
<b>Figure 3.1</b> : Synthesis of MA-DBB via Gabriel reaction.....	34
<b>Figure 3.2</b> : <sup>1</sup> H-NMR spectra of MA-DBB before (bottom) and after (top) proton exchange .....	34
<b>Figure 3.3</b> : Synthetic route for the urethane derivative of $\alpha$ -amino acid, NCA-LL.....	35
<b>Figure 3.4</b> : Synthesis of DBB-PLL by in situ NCA ring opening polymerization	35
<b>Figure 3.5</b> : <sup>1</sup> H-NMR spectrum of polypeptide macromonomer, DBB-PLL.....	36
<b>Figure 3.6</b> : <sup>1</sup> H-NMR spectrum of DBB-PEG .....	36
<b>Figure 3.7</b> : Synthesis of PEG macromonomer via Steglich esterification reaction.....	37
<b>Figure 3.8</b> : Synthesis of PPP polymer bearing poly-L-lysine and PEG side chains .....	38
<b>Figure 3.9</b> : <sup>1</sup> H-NMR spectrum of PPP-g-PEG-PLL in CDCl <sub>3</sub> .....	38
<b>Figure 3.10</b> : UV absorption spectra of DBB-PEG, DBB-PLL and PPP-g-PEG-PLL .....	39
<b>Figure 3.11</b> : Fluorescence excitation and emission spectra of PPP-g-PEG-PLL ..	40
<b>Figure 3.12</b> : The synthesis of PPP-NH <sub>2</sub> -g-PEG by Suzuki coupling polymerization .....	40
<b>Figure 3.13</b> : <sup>1</sup> H-NMR spectra of PPP-NH <sub>2</sub> -g-PEG .....	41

<b>Figure 3.14</b> : UV spectra of DBB-PEG, MA-DBB and PPP-NH <sub>2</sub> -g-PEG in DMF solution .....	41
<b>Figure 3.15</b> : The fluorescence spectra of PPP-NH <sub>2</sub> -g-PEG in DMF and water solution.....	42
<b>Figure 3.16</b> : <sup>1</sup> H-NMR spectrum of PPP-g-PEG-PLL (Route 2) .....	42
<b>Figure 3.17</b> : The synthesis of PPP-g-PEG-PLL by NCA ROP of NCA-LL by using PPP-NH <sub>2</sub> -g-PEG .....	44
<b>Figure 4.1</b> : Synthesis of amino functional monomer, DBB-MA .....	50
<b>Figure 4.2</b> : <sup>1</sup> H-NMR spectra of DBB-MA before (bottom) and after (top) proton exchange .....	51
<b>Figure 4.3</b> : Synthesis of water soluble macromonomer, DBB-PEG, via Steglich esterification.....	51
<b>Figure 4.4</b> : Synthesis of PPP-NH <sub>2</sub> -g-PEG via Suzuki condensation polymerization .....	52
<b>Figure 4.5</b> : <sup>1</sup> H-NMR spectra of PPP-NH <sub>2</sub> -g-PEG before (bottom) and after (top) proton exchange reaction .....	53
<b>Figure 4.6</b> : GPC traces of PPP-NH <sub>2</sub> -g-PEG and DBB-PEG.....	54
<b>Figure 4.7</b> : UV absorption spectra of PPP-NH <sub>2</sub> -g-PEG, DBB-PEG and DBB-MA in DMF, solution .....	54
<b>Figure 4.8</b> : Fluorescence excitation and emission spectra of PPP-NH <sub>2</sub> -g-PEG in water and DMF. ....	55
<b>Figure 4.9</b> : Schematic illustration of the bioconjugation .....	55
<b>Figure 4.10</b> : Fluorescence spectra of PPP-NH <sub>2</sub> -g-PEG and FA/PPP-NH <sub>2</sub> -g-PEG polymer conjugates.....	56
<b>Figure 4.11</b> : FT-IR spectrum of FA, PPP-NH <sub>2</sub> -g-PEG and FA/PPP-NH <sub>2</sub> -g-PEG .....	57
<b>Figure 4.12</b> : The effect of PPP-NH <sub>2</sub> -g-PEG and FA/PPP-NH <sub>2</sub> -g-PEG polymer on cell viability of HeLa cells (A) and A549 cells (B). ....	58
<b>Figure 4.13</b> : Fluorescence microscopy imaging of HeLa and A549 cells. ....	59

## FUNCTIONAL CONJUGATED POLYMERS

### SUMMARY

The considerable role of conjugated polymers (CPs) in emerging synthetic bio-applications, optical, electronic, diodes, and display technologies, represents the promising way in which considerable endeavors have been directed towards the realization of many aspects of conducting organic polymers.

Conducting polymers are known as “synthetic metals”, making them fundamental materials in many research fields because of their outstanding characteristics. They exhibit both excellent conductivity and high mechanical strengths and processability.

The use of CPs as an excellent immobilization platform for biomolecules led to the development of efficient biosensors, which were easy to process, had the ability to conduct electricity at any desired level, had a low cost, and straightforward preparation techniques. CPs provide high surface area, adjustable morphology by arranging the thickness of the polymer film and offer extensive stability of the enzymes incorporated in them.

Furthermore, these materials also facilitate structural and electronic modifications which can be used in detecting a target compound in any test solution. The polymer structure can be tuned to accomplish the desired properties, producing a sensitive and reproducible microenvironment for biological reactions to mimic the naturally occurring environments of the biological molecules.

Among vast number of CPs, poly(p-phenylene)s (PPP)s and polythiophenes (PT)s are the most promising class of polymer in terms of relatively high photoluminescence, electroluminescence quantum efficiencies and thermoxidative stability and so on.

Conjugated structure of CPs can create excellent one-dimensional surface for energy transport of electrons and strong UV absorption. Especially, their fluorescence feature is one of the most susceptible to environmental change and this allows for eminent selectivity in signaling reporter group materials and provides advantages for CPs to be used in sensor technologies including pH sensors, temperature sensors and recently developed biosensors.

Recent innovative strategies for the syntheses of functional polymeric structures bearing polypeptides, amino-rich and water soluble groups have received enormous interest in the fields of biomedicine, drug delivery, biomineralization, bioconjugations, and tissue engineering. Taking account of the unique advantages of these strategies, in this thesis, we focused on the combination of PPPs and PTs with polypeptide, amino and water soluble groups in the same conjugated backbone.

In the first part of thesis, a simple and efficient approach for the electrochemical deposition of polypeptides as bio-based covering materials for surface design is described. The method involves *N*-carboxyanhydride (NCA) ring-opening polymerization from its precursor to form a thiophene-functionalized polypeptide macromonomer (T-Pala), followed by electropolymerization.

The obtained conducting polymer, namely polythiophene-*g*- polyalanine (PT-Pala), was characterized and utilized as a matrix for biomolecule attachment. The biosensing applicability of PT-Pala was also investigated by using glucose oxidase (GOx) as a model enzyme to detect glucose. The designed biosensor showed a very good linearity for 0.01–1.0 mM glucose. Finally, the antimicrobial activities of newly synthesized T-Pala and PT-Pala were also evaluated by using the disc diffusion method.

In the second part of thesis, we report a novel approach for fabrication of multifunctional conjugated polymers, namely poly(*p*-phenylene)s (PPPs) possessing polypeptide (poly-L-lysine, PLL) and hydrophilic poly(ethylene glycol) (PEG) side chains. The approach is comprised of the combination of Suzuki coupling and in situ *N*-carboxyanhydride (NCA) ring-opening polymerization (ROP) processes.

First, polypeptide macromonomer was prepared by ROP of the corresponding NCA precursor using (2,5-dibromophenyl) methanamine as an initiator. Suzuki coupling reaction of the obtained polypeptide and PEG macromonomers both having dibromobenzene end functionality using 1,4-benzenediboronic acid as the coupling partner in the presence of palladium catalyst gave the desired polymer.

A different sequence of the same procedure was also employed to yield polymer with essentially identical structure. In the reverse sequence mode, low molar mass monomer (2,5-dibromophenyl)methanamine, and PEG macromonomer were coupled with 1,4- benzenediboronic acid in a similar way followed by ROP of the L-Lysine NCA precursor through the primary amino groups of the resulting polyphenylene.

In the third part of thesis, a novel approach for bioconjugation associated with a fluorescent conjugated polymer is demonstrated. For this purpose, a conjugated polymer, poly(*p*-phenylene) (PPP), with lateral substituents, namely primary amino groups and poly(ethylene glycol) (PEG) chains, as a potential building block for polymer bioconjugates was synthesized and characterized.

The synthesis was achieved through Suzuki polycondensation reaction in the presence of Pd(PPh<sub>3</sub>)<sub>4</sub> catalyst by using independently prepared PEG and amino functionalized dibromo benzenes in conjunction with benzene diboronic acid. For the evaluation of the bioactive PPP labeled with folic acid (FA) as a potential targeted cell imaging probe, HeLa and A549 cancer cells were used. Cytotoxicity assay showed that the polymer was not toxic to either of the cells.

Additionally, the fluorescence images showed that, depending on the level of the FA receptors on the cell surfaces, the fluorescent intensity in HeLa cells was obviously higher than A549 cells when treated with FA conjugated PPP-NH<sub>2</sub>-*g*-PEG polymer. The resulting FA/PPP-NH<sub>2</sub>-*g*-PEG conjugate was successfully used as a

bioconjugate for targeting and specifically imaging FA receptor positive HeLa human cervical cancer cells.

Summary, we successfully achieved the synthesis, characterization and some bioapplications of complex macromolecular architecture based on conjugated polymers bearing polypeptide, water soluble pendant PEG, and primary amine groups.

The synthesis of polypeptide sequences were achieved by NCA-ROP technique based on transformation of  $\alpha$ -amino acids to urethane derivatives which have possibility to obtain polypeptides in the well-designed and decisive control of molecular weight with one step intra-molecular cyclization reaction in the presence of primary amino functional initiators. We successfully used the primary amino functional thiophene and phenyl compounds as NCA-ROP initiator to obtain macromonomers having electropolymerization ability and possibility to give Suzuki coupling polymerization.

After the obtaining of conjugated polymers bearing polypeptide and primary amine groups based on PPP and PTs, some biofunctional material was used in the step of bioapplications.





## FONKSİYONEL KONJÜGE POLİMERLER

### ÖZET

Konjuge polimerlerin optik, elektronik, diyot ve biyolojik alanlardaki artan umut verici uygulamaları nedeniyle önemli oranda bilimsel çalışma konjuge polimerlerin bir çok açıdan yeni uygulamalarını araştırmaya yönlendirilmiştir. Sayısız konjuge polimerler içinde polipara fenilenler ve politiyofenler, fotolimunesans, electrolimunesans, kuantum verimi ve termal kararlılık açısından en çok gelecek vaad eden polimer sınıfındadırlar.

İletken polimerler yada sentetik metaller olarak adlandırılan konjuge polimerler sıradışı özellikleri nedeniyle birçok alanda temel malzeme haline gelmektedir. Ayrıca mükemmel iletkenlik, yüksek derecede mekanik dayanıklılık ve işlenebilirlik özellikleri ile öne çıkmaktadırlar.

Konjuge polimerlerin biyomoleküller için mükemmel bir immobilizasyon yüzeyi olarak kullanımı, düşük maliyetli, istenen seviyede, kolay işlenebilen ve iletkenlik özelliklerine sahip etkili biyosensör sistemlerinin gelişiminde etkili olmuştur.

Konjuge polimerler yüksek yüzey alanı, polimer film kalınlığının ayarlanabilme avantajıyla uygun yüzey morfolojisi ve üzerinde kararlı bir enzim tutunma alanı sağlayabilmektedir.

En son yapılan özgün çalışmalarda, üzerinde polipeptit, amince zengin ve suda çözünür gruplar içeren sentetik polimerler biyo-ilaç, ilaç taşıma, biyo mineralleşme, biyo konjugasyon ve doku mühendisliği alanlarında büyük ilgi görmektedir. Bu çeşit polimerlerin eşsiz özelliklerini dikkate alarak, bu tezde polipara fenilen ve politiyofen iskeleti üzerinde suda çözünür, amince zengin ve peptit içeren konjuge polimerler sentezledik.

Bu tezin ilk bölümünde, polipeptit kulanarak biyolojik temelli yüzey dizayni için basit ve etkili bir yöntem gösterilmektedir. Bu yöntem *N*-karboksianhidrid (NCA) hakla açılma polimerizasyonu ile tiyofen fonksiyonlu peptit makromonomer (T-Pala) sentezlendi ve elektropolimerizasyon ile son ürün elde edildi.

Elde edilen politiyofen-g-polialanin (PT-Pala) isimli iletken polimer karakterize edilerek biyomolekul bağlanması için bir matriks olarak kullanıldı. Polimerin biyosensör uygulanabilirliği glikoz algılama yönteminde model enzim olan glikoz oksidaz (GOx) kullanılarak incelendi. Bu sistem farklı pH aralıklarında en iyi biyosensör cevapları incelenerek GOX enzimi için de uygun değerlerde maksimum değere sahip olduğu görüldü.

Ayrıca polimer ve GOx enzimi hem kovalent bağlı hemde fiziksel bağlanma yöntemleri karşılaştırılarak incelendi. Dizayn edilen biyosensör sistemi 0.01–1.0 mM konsatrasyonda glikoz için çok iyi bir doğrulukta sonuç verdi.. Elde edilen biyokonjugasyon polimer sisteminin GOx ile sağladığı biyosensör özelliği literatürdeki diğer glukoz sensörü sistemlerle karşılaştırıldığında çok iyi değerlere sahip olduğu görüldü.

Yüzey özellikleri SEM analiz yöntemi ile sadece politiyofen, politiyofen ve PT-Pala graft yapısı ve sadece PT-Pala içeren üç farklı yüzey ile incelendi. Elde edilen farklı yüzey sonuçları ve floresans mikroskobunda alınan görüntüler ile konjuge polimerin yüzey yapısı detaylı bir şekilde aydınlatıldı.

Son olarak, sentezlenen T-Pala ve PT-Pala için antimikrobiyal aktivite disk difüzyon metodu ile incelendi. Grafit yüzey üzerindeki PT-pala kaplama Gram pozitive bakterilerine karşı önemli derecede antibakteriyel özellik gösterdiği görüldü.

İkinci bölümde, üzerinde polipeptit (poli-L-lisine, PLL) ve hidrofilik poli(etilen glikol) (PEG) yan grupları içeren çok fonksiyonlu konjuge polimer sentezi gösterilmektedir. Bu yaklaşım Suzuki kenetlenme reaksiyonu ve *N*-karboksianhidrid halka açılma polimerizasyonunu içermektedir.

İlk olarak, polipeptit makromonomer karşılık gelen monomer ve (2,5 dibromphenil) metilamine başlatıcısı kullanılarak NCA halka açılma polimerizasyonu ile sentezlendi. Daha sonra final polimer, peptit makromonomer, PEG makromonomer ve 1,4 benzendibronik acid ile Suzuki kenetlenme reaksiyonu kullanılarak sentezlendi.

Aynı polimer farklı bir yöntem ile tekrar sentezlendi. Bu yöntemde ilk olarak (2,5-dibromfenil) metilamine, PEG makromonomer ve 1,4 benzendibronik acid kullanılarak Suzuki reaksiyonu ile sentezlendi. Daha sonra polimer üzerindeki primer amine grupları başlatıcı olarak kullanılarak NCA halka açılma polimerizasyonu ile polipeptit zinciri polimer üzerinde sentezlendi.

Üçüncü bölümde, floresans konjuge polimer ile farklı bir biokonjugasyon uygulaması yapıldı. Suzuki kenetlenme polimerizasyonu ile sentezlenen, üzerinde primer amin ve PEG grupları içeren suda çözünür polipara fenilen konjuge polimer sentezlendi ve karakterize edildi.

Daha sonra folik acid ile işaretlenen potansiyel hücre hedefli görüntüleme probu incelemesi için, HeLa ve A549 kanser hücreleri kullanıldı. Sitotoksikite tahlili polimerin hücrede herhangi bir toksik etki göstermediğini ortaya koydu. Ayrıca floresans resimleri gösterdi ki; FA reseptörünün hücre yüzeyindeki seviyesine bağlı olarak, FA ile konjuge PPP-NH<sub>2</sub>-g-PEG polimeri ile muamele edildiğinde floresans yoğunluğu HeLa hücrelerinde A549 hücrelerinden açık şekilde daha yüksektir.

FA/PPP-NH<sub>2</sub>-g-PEG konjuge sistemi, FA reseptör pozitif HeLa rahim ağzı kanser hücrelerinin spesifik olarak görüntülenmesinde biokonjuge sistem olarak başarıyla kullanıldı.

Özet olarak, üzerinde polipeptit, suda çözünür grup, PEG, ve primer amin içeren kompleks yapıdaki çok fonksiyonlu konjuge polimerlerin sentezi, karakterizasyonu ve bazı biyouygulamaları başarıyla gerçekleştirildi.

Bu çalışmalarda biyouygulamaların temelini oluşturan peptit zincirlerinin sentezi NCA-ROP tekniği ile yapıldı. Polipeptit zincirinin molekül ağırlığının ve yapısının kontrollü bir şekilde elde edilmesine olanak sağlayan bu teknik  $\alpha$ -amino asitlerin üretilen türevlerine dönüştürülmesi prensibine dayanmaktadır. Polimerizasyon çok farklı özelliklere sahip primer amin başlatıcılarla tek basamaklı molekül içi halkalaşma reaksiyonu üzerinden yürümektedir. Bu çalışmada Suzuki kenetlenme ve eletropolimerizasyon reaksiyonlarına uygun fenil ve tiyofen bileşiklerinin primer amin içeren türevleri kullanıldı.



## 1. INTRODUCTION

Conducting polymers (CPs) are known as “synthetic metals”, making them fundamental materials in many research fields because of their outstanding characteristics. They exhibit both excellent conductivity and high mechanical strengths and processability. The use of CPs as an excellent immobilization platform for biomolecules led to the development of efficient biosensors, which were easy to process, had the ability to conduct electricity at any desired level, had a low cost, and straightforward preparation techniques. CPs provide high surface area, adjustable morphology by arranging the thickness of the polymer film and offer extensive stability of the enzymes incorporated in them. Furthermore, these materials also facilitate structural and electronic modifications which can be used in detecting a target compound in any test solution. The polymer structure can be tuned to accomplish the desired properties, producing a sensitive and reproducible microenvironment for biological reactions to mimic the naturally occurring environments of the biological molecules. With the help of the functional groups created, well organized matrices with the anticipated biosensor properties can be achieved.

Innovative approaches for the syntheses of polymeric structures bearing polypeptides or primary amines have received enormous interest in the fields of biomedicine, drug delivery, biomineralization, nanoscale self-assembly, and tissue engineering. Especially, the elaboration of polypeptides into polymeric structures opens new perspectives in the field of biotechnology as they are fascinating biomaterials mimicking natural proteins. Polypeptides, possessing wonderful biocompatibility as well as remarkable mechanical and biological durability, are used to create an excellent platform in biosensor fabrication. Furthermore, polypeptides are assumed to exhibit a three-dimensional (3-D) conformation under certain conditions. Therefore, combining synthetic polymers with polypeptide segments becomes a promising approach in the field of enzyme immobilization. The resulting feature reveals compelling selfassembling behavior and new versatile functions are created through the synergistic effect of polymeric structures with polypeptide units. Thus,

the novel design and synthesis of polypeptides containing conjugated polymers has attracted great interest.

In terms of economic and practical prospects, the ring-opening polymerization of the corresponding  $\alpha$ -amino acids of *N*-carboxyanhydrides (NCAs) appears to be the best technique for the synthesis of a considerable variety of polypeptides by using many different nucleophiles and bases. Although polymer chains grow linearly with monomer conversion without side reactions, the amine-based initiating systems suffer because of the requirement for extreme impurityfree conditions to achieve the decisive control of a certain molecular weight and terminal structure. It was recently shown that the precursor NCAs can be obtained via intramolecular cyclization of activated urethane derivatives of  $\alpha$ -amino acids by a simple procedure providing a practical and green way for polypeptide synthesis without the use and production of any toxic compounds. Quite recently, the method was further improved by taking advantage of consecutive NCA formation and polymerization processes from precursor urethane derivatives. Upon thermolysis in the presence of primary amines, in situ NCA formation and polycondensation with the elimination of phenol and CO<sub>2</sub> yields the desired polypeptides.

## 1.1 Purpose of The Thesis

The objective of the thesis is to synthesize and investigate some bioapplication of conjugated polymers which are namely poly(*p*-phenylene) (PPP) and polythiophene (PTs) bearing primary amines and polypeptide side chains. During this thesis, chromatographic (GPC), spectroscopic (<sup>1</sup>H-NMR, FT-IR), and microscopic (SEM) analyses are performed for the obtained polymers. This thesis is organized in such that each chapter has its own introduction, experimental, results and discussion, and list of references.

Chapter 1 discusses overall background information about the conjugated polymers and their recent novel applications, about the polypeptide preparation methods based on the ring-opening polymerization of the corresponding  $\alpha$ -amino acids of *N*-carboxyanhydrides (NCAs).

Chapter 2 describes a simple and efficient approach for the electrochemical deposition of polypeptides as bio-based covering materials for surface design is

described. The method involves *N*-carboxyanhydride (NCA) ring-opening polymerization from its precursor to form a thiophene-functionalized polypeptide macromonomer (T-Pala), followed by electropolymerization.

Chapter 3 gives a detailed account of a novel approach for fabrication of multifunctional conjugated polymers, namely poly(*p*-phenylene)s (PPPs) possessing polypeptide (poly-L-lysine, PLL) and hydrophilic poly(ethylene glycol) (PEG) side chains. The approach is comprised of the combination of Suzuki coupling and *in situ* *N*-carboxyanhydride (NCA) ring-opening polymerization (ROP) processes.

Chapter 4 involves an approach for bioconjugation associated with fluorescent conjugated polymer. A conjugated polymer, poly(*p*-phenylene) (PPP), with lateral substituents, namely primary amino groups and poly(ethylene glycol) (PEG) chains, as potential building block for polymer bioconjugates was synthesized and characterized.





## 2. ELECTROCHEMICAL DEPOSITION OF POLYPEPTIDE: BIO-BASED COVERING MATERIALS FOR SURFACE DESIGN

Innovative approaches for the syntheses of polymeric structures bearing polypeptides have received enormous interest in the fields of biomedicine, drug delivery, biomineralization, nanoscale self-assembly, and tissue engineering. The conjugation of synthetic polymers with polypeptides can result in novel biomaterials that possess the following characteristics: biorecognition-like properties similar to antibody/antigen interactions, biodegradability properties, biocatalyst activity, and compatibility with blood and/or tissue [1–5]. Polypeptides, showing three-dimensional conformations such as  $\alpha$ -helix,  $\beta$ -sheet, and random coil structures, could exhibit intriguing self-assembly behavior. Due to these unique features, they impart interesting properties and functions to any polymeric structure in which they are combined [6,7]. Traditionally, most peptides have been prepared [8] by ring-opening polymerization of the corresponding  $\alpha$ -amino acids of *N*-carboxyanhydrides (NCAs).

Generally, primary and secondary amines most favorably initiate NCA polymerization. Their “living” nature allows the decisive control of a certain molecular weight and terminal structure [7,9]. Although the “living” polymerization of NCA is a significant challenge in the synthesis of polypeptides based on natural or unnatural amino acids, the polymerization reaction requires extreme impurity-free conditions to achieve the polymerization without side reactions. Thus, extensive research worldwide has aimed at developing new methods for reliable syntheses of monomers that are appropriate for NCA polymerization. However, earlier attempts [10–16] on NCA synthesis involve either multistep reactions or the use of hazardous reagents such as phosgene, or lack sufficient monomer purity for polymerization. Moreover, the vulnerable nature of NCA in the presence of water contamination or under heating conditions is the main drawback, requiring the reaction to proceed under impractical conditions [4,9] Thus, research has been devoted to obtain NCAs from nontoxic materials with high purity and stability through the development of

new synthetic strategies. In related studies carried out in the laboratory of one of the authors of this paper, different NCAs were obtained via intramolecular cyclization of activated urethane derivatives of  $\alpha$ -amino acids by using a simple procedure [9,17–20]. The method offers a practical and green way for polypeptide synthesis without the use and production of any toxic compounds. Quite recently, the method was further improved by taking advantage of consecutive NCA formation and polymerization processes [9]. Thus, the precursor urethane derivatives were readily synthesized by a two-step procedure: (i) transformation of  $\alpha$ -amino acids into the corresponding ammonium salts and (ii) *N*-carbamylation of the salts with diphenyl carbonates. These compounds are stable at room temperature for months and can be converted into polypeptides simply by heating in dimethyl acetamide (DMAc) in the presence of primary amines through in situ NCA formation and polycondensation with the elimination of phenol and CO<sub>2</sub>.

Conjugated polymers, in particular those based on thiophene and its derivatives, have been extensively studied because of their applicability in the fabrication of electronics and electro-optic devices due to their characteristic electronic and optical properties [21]. These polymers have been synthesized by various coupling reactions as well as oxidative and electropolymerization processes, which provide films with different morphologies and, consequently, different physical and chemical properties [22]. Previously, it has been shown that polythiophenes (PTs) can be combined with conventional synthetic polymers through the combination of various chain polymerization processes with electropolymerization [23–33]. However, the corresponding conjugation of PT with biomolecules has been rarely investigated [34–38]. Reported examples involve a postmodification approach on the surface of PT films. For example, PT containing highly reactive *p*-benzenesulfonyl chloride groups was prepared by electropolymerization, and subsequent covalent protein immobilization was achieved by a nucleophilic reaction [34]. In another study, a peptide-modified PT biosensor was developed for electrochemical analysis of copper ions. The tripeptide Gly–Gly–His, which selectively recognizes copper ions, was covalently immobilized to the PT film [34]. In addition, besides covalent immobilization, [36,37]  $\pi$ – $\pi$  stacking interactions have been successfully used for the postmodification of PTs and other conjugated polymers [38].

Taking into consideration all of the above-mentioned views, herein we report the synthesis, characterization, and biosensing application of PT bearing polyalanine

homopeptide side chains (PT-Pala). This complex macromolecular architecture was prepared directly by NCA ring-opening polymerization reactions from its precursor to form the polypeptide macromonomer, followed by electropolymerization. To the best of our knowledge, no such conjugated graft copolymer with a variety of potential biological applications has been reported previously. As presented below, this combination has led to promising results in terms of biosensor and bioconjugation applications by taking advantage of the fluorescence features and reactivity of the amino side chains of PT and the polypeptide, respectively. Glucose oxidase (GOx) was used as a model enzyme, and immobilization of the biocomponent was carried out using glutaraldehyde, which forms a covalent bond between electrodeposited PT-Pala and the biomolecule through the amino groups of the polypeptide. The applicability of the PT-Pala film as an immobilization matrix was investigated by monitoring the electrochemical biosensor responses using glucose as the substrate. The surface features of the film were examined by Fourier transform infrared (FTIR) spectroscopy, scanning electron microscopy (SEM), and fluorescence microscopy. In addition, electrochemical characterization of the PT-Palacoated electrodes was performed. Finally, the antimicrobial activities of the newly synthesized thiophene-polyalanine macromonomer (T-Pala) and polymer (PT-Pala) were evaluated by using the disc diffusion method.

## **2.1 Result and Discussion**

### **2.1.1 Electroactive Polypeptide Macromonomer**

The possibility of NCA ring-opening polymerization with primary amines and electropolymerization of thiophene and its derivatives prompted us to combine these systems for the synthesis of PT-based graft copolymers with polypeptide side chains. Accordingly, graft copolymers were obtained in two discrete steps. In the first step, the polypeptide macromonomer T-Pala was synthesized via ring-opening polymerization of *L*-Ala- *N*-(phenyloxycarbonyl)amino acid with an amino initiator. As the thiophene polypeptide macromonomer was intended to be used in a further electropolymerization reaction, the synthetic strategy for the functional primary amino initiator was selected so as to preserve the 2- and 5-positions of the thiophene ring. Thus, 3-(aminomethyl)thiophene was readily synthesized according to the following reactions in high yields (Figure 2.1).

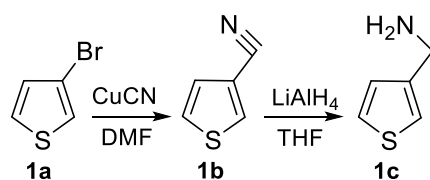


**Figure 2.1** : Preparation of 3-(aminomethyl)thiophene (1c) as the initiator of NCA polymerization.

The NCA precursor, *L*-Ala-*N*-(phenyloxycarbonyl) amino acid, i.e., the urethane derivative of an  $\alpha$ -amino acid, was synthesized by successive protection of the acid group of alanine (2a) by an ionic exchange reaction with the corresponding ammonium salt and *N*-carbamylation of the ammonium salt-protected amino acid (2b) via the nucleophilic attack of the active primary amino group of 2b toward the carbonyl group of diphenyl carbonate (DPC) (Figure 2.2).

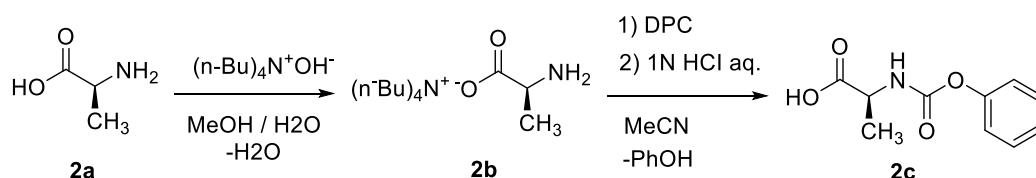


**Figure 2.2** : Synthetic route towards *L*-Ala-*N*-(phenyloxycarbonyl)amino acid (2c).

Polymerization of the NCA precursor (2c) proceeded in the presence of DMAc and 1c as the solvent and initiator, respectively, in a one-pot reaction through in situ intramolecular cyclization followed by a ring-opening reaction with CO<sub>2</sub> elimination (Figure 2.3).

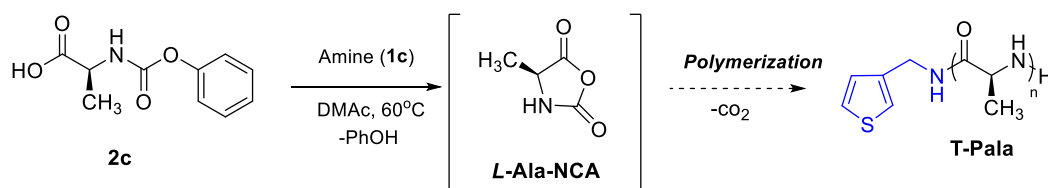


**Figure 2.3** : Synthesis of thiophene-polyalanine (T-Pala).

This strategy directly afforded the formation of NCA in the polymerization media and eliminated problems associated with the monomer purity and stability. The conditions of polymerization, i.e., a high concentration of the initiator with respect to the monomer, were chosen to obtain a low molecular weight polymer ( $M_n = 1140 \text{ g mol}^{-1}$ ), combined with a satisfactory conversion (80% yield) and polydispersity ( $M_w/M_n = 1.16$ ) suitable for the subsequent electropolymerization process. Although

the polyalanine chain has minimal steric hindrance among all types of polypeptides, high molecular weight polymers have low solubility in any solvent.

The structure of T-Pala was investigated by proton nuclear magnetic resonance ( $^1\text{H-NMR}$ ) and Fourier transform infrared (FTIR) spectroscopy. In the  $^1\text{H-NMR}$  spectrum of T-Pala, broad bands at 4.30–4.48 ppm and 1.45–1.65 ppm corresponding to  $-\text{CH}$  and  $-\text{NH}$  groups of the repeating unit indicate the polymeric structure. The terminal thiophene groups were confirmed by a doublet at 3.48 ppm, a doublet at 7.00 ppm, and singlets at 7.05 and 7.46 ppm. The  $-\text{NH}_2$  terminal group resonates at 7.68–7.74 ppm.

### 2.1.2 Electrodeposition T-Pala and Enzyme Immobilization

PT-Pala film formation was performed via electrochemical polymerization at a potential of +1.6 V vs. Ag/AgCl. The charge and the thickness of the electrodeposited PT-Pala film were calculated to be 248.8 mC and 5.53 mm, respectively. Afterwards, it was used as a functional platform containing the peptide handles on the surface for biomolecule immobilization. Gox was used as a model enzyme and was immobilized on the amino termini of the peptide chains on each thiophene unit by means of glutaraldehyde. Figure 2.4 describes each surface modification and the biosensor fabrication steps.

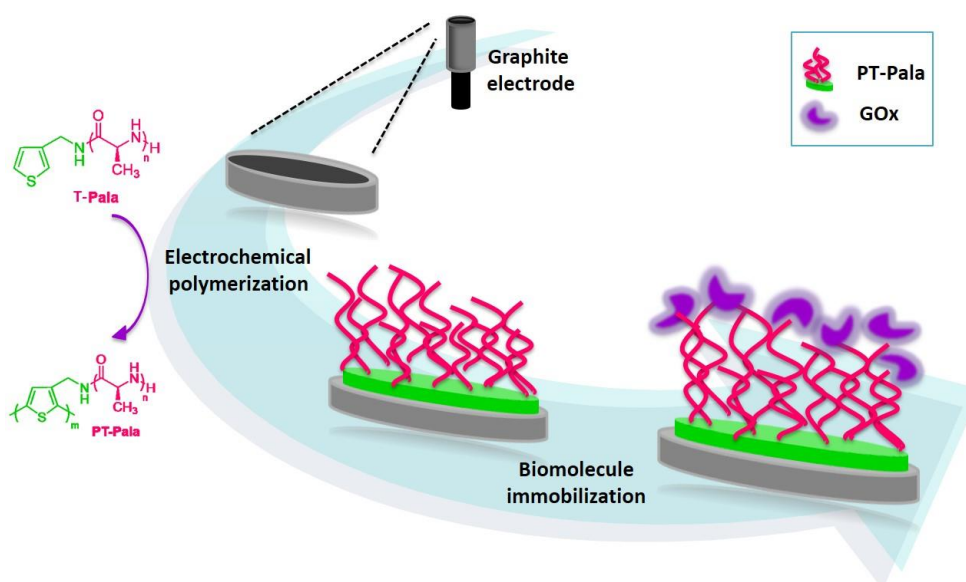


**Figure 2.4 :** Schematic representation of PT-Pala film formation and construction of the PT-Pala film/GOx biosensor.

### 2.1.3 Characterization of the PT-Pala Film

Both T-Pala and PT-Pala were characterized by FTIR spectral analysis. In the FTIR spectrum of the monomer, the following absorption peaks were identified:  $3266\text{ cm}^{-1}$  and  $3074\text{ cm}^{-1}$  (N–H vibration),  $2978\text{ cm}^{-1}$  and  $2874\text{ cm}^{-1}$  (aliphatic methylene stretching vibration),  $1624\text{ cm}^{-1}$  (C=O stretching vibration), and  $1222\text{ cm}^{-1}$  (C–C stretching vibration arising from a carbonyl group bonded to an alkyl group). The absorption bands at  $1532$ ,  $778$ , and  $698\text{ cm}^{-1}$  were due to the vibrations of C–H and C=C bonds of thiophene rings. The FTIR spectrum of the polymer revealed that electropolymerization of T-Pala was successfully achieved on the surface of the graphite electrode. The peak monitored at  $778\text{ cm}^{-1}$  indicated cis C–H wagging of the thiophene ring, and the band at  $698\text{ cm}^{-1}$  due to deformations of C–H out of the plane of the thiophene ring disappeared completely upon polymerization. In addition, new absorption bands became pronounced at  $760\text{ cm}^{-1}$  (thienylene C–H $\alpha$  tri-substituted ring bend) and  $1002\text{ cm}^{-1}$  (thienylene C–H $\alpha$  in-plane bend).

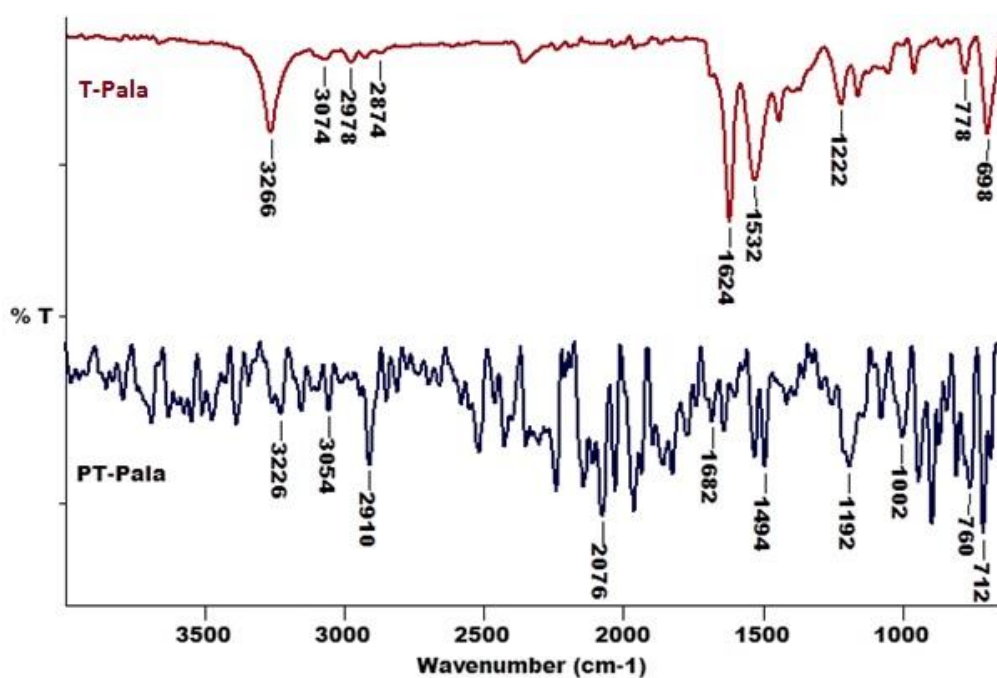


**Figure 2.5 :** FT-IR spectra of T-Pala and PT-Pala.

The strong peak observed at  $1192\text{ cm}^{-1}$  (S=O stretching vibration of  $\text{SO}_3^-$ ) was characteristic of the sodium dodecyl sulfate (SDS) dopant ion peak. The medium and broad peak monitored at  $1682\text{ cm}^{-1}$  was the C=O stretching vibration arising from the carbonyl group. The intensity of that peak was relatively low when compared to the intensity of the carbonyl peak of the monomer (Figure 2.5). It should also be pointed

out that the obtained polymer is expected to have a copolymer structure rather than a composite consisting of independent polymer chains. In the electrocopolymerization of such monomer and macromonomer couples, chemical linking of the segments occurs through the coupling reaction at 2 and 5, and unsubstituted 3 and 4 positions of the thiophene ring [23–33].

Cyclic voltammetry (CV) was used to investigate the electron transfer process on the biofilm surface. As well as CVs of bare graphite, PT-Pala- and PT-Pala/GOx-modified graphite electrodes were obtained in a mixture of 5.0 mM  $\text{Fe}(\text{CN})_6^{3-/4-}$  and 0.1 M KCl. As shown in Figure 2.6, the PT-Pala-modified graphite electrode had greater peak currents ( $38.514 \mu\text{A}$ ,  $\Delta E_{\text{Pc}} = 0.278 \text{ V}$ ) than the bare electrode ( $16.289 \mu\text{A}$ ,  $\Delta E_{\text{Pc}} = 0.268 \text{ V}$ ). This result is related to the enhanced conductivity of the polymer film, which is important for the biosensor response and can be attributed to the increased number of functional amino groups caused by electrodeposited peptides.

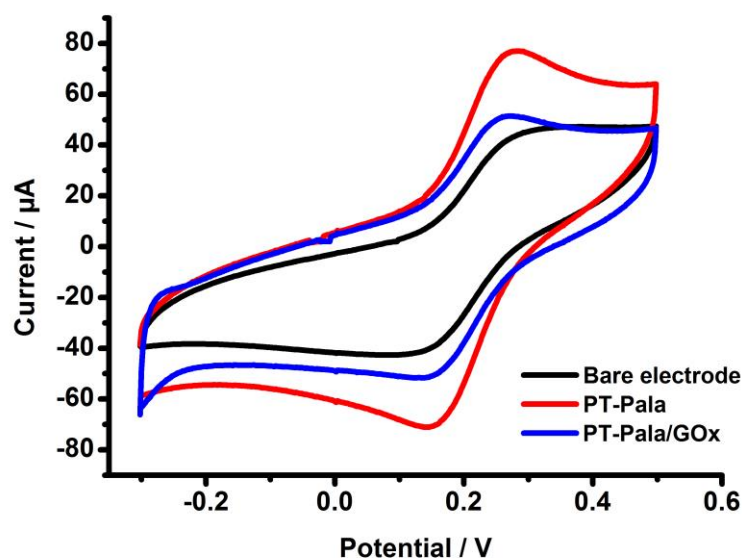


**Figure 2.6 :** CVs of the bare graphite electrode, PT-Pala-coated electrode, and GOx-immobilized PT-Pala-coated electrode (in 5.0 mM  $\text{Fe}_3(\text{CN})_6^{3-/4-}$ , at a scan rate of  $50 \text{ mV s}^{-1}$ )

Thus, negatively charged  $\text{Fe}(\text{CN})_6^{3-/4-}$  is attracted to the electrode surface. After biomolecule immobilization, the peak current ( $24.362 \mu\text{A}$ ,  $\Delta E_{\text{Pc}} = 0.296 \text{ V}$ ) decreased in comparison with the PT-Pala-coated graphite electrode. This result was

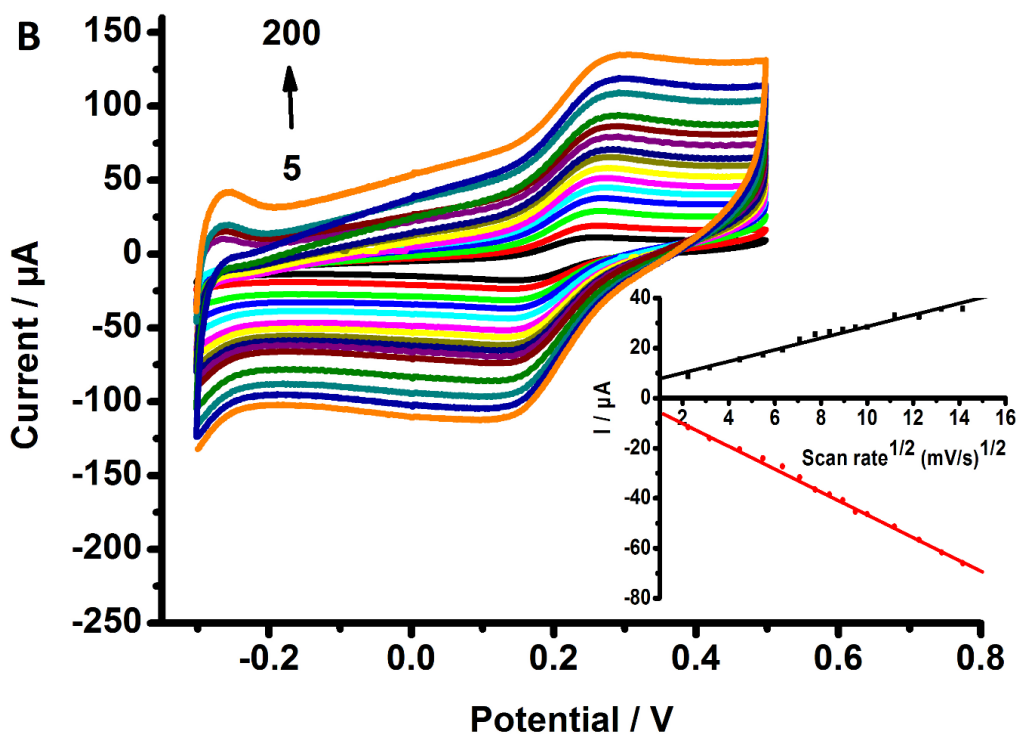
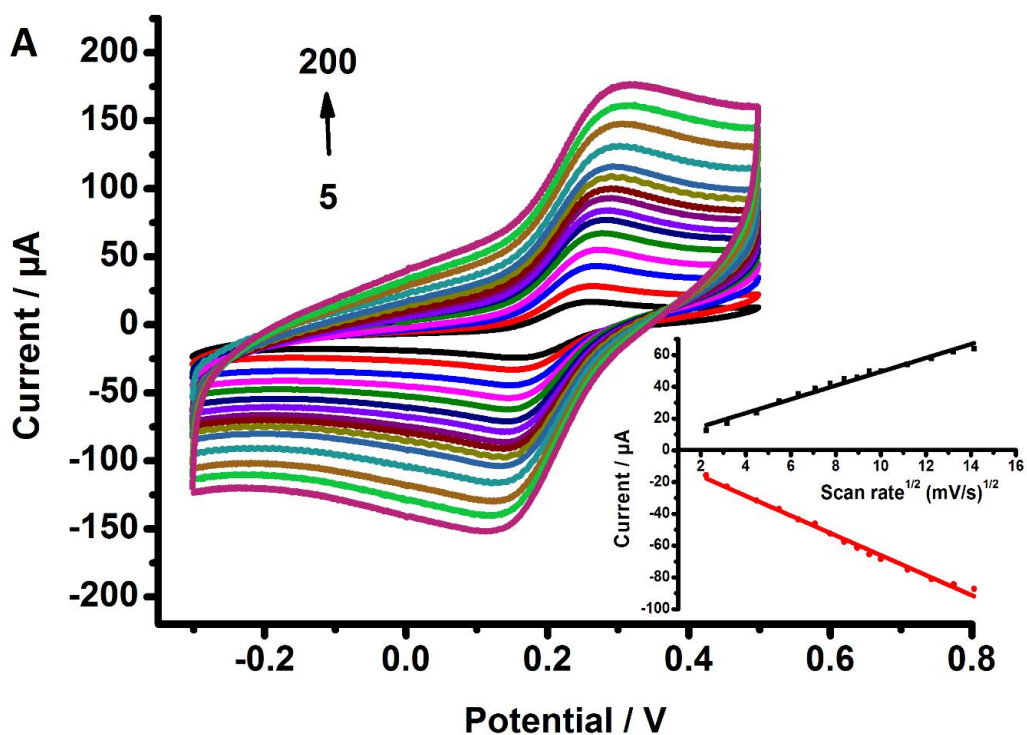


**Figure 2.7 :** Cyclic voltammograms of prepared electrodes. (A) CVs of PT-Pala modified and (B) PT-Pala/GOx modified electrodes at the different scan rates, Inset: The correlation between the current and square root of the scan rate.



expected due to the modification of the electrode surface with the biomolecule, which diminished the electron transfer properties because of a possible diffusion layer. The obtained results clearly confirm that the immobilization steps for biosensor fabrication were carried out successfully.

Furthermore, cyclic voltammograms of PT-Pala- and PT-Pala/ GO<sub>x</sub>-modified electrodes at different scan rates are shown in Figure 2.7. For PT-Pala-coated graphite, the square root of the scan rate-dependent anodic and cathodic linear equations is defined by  $y = -6.232x - 3.763$  ( $R^2 = 0.992$ ) and  $y = 4.336x + 6.103$  ( $R^2 = 0.981$ ), respectively. In the case of PT-Pala/GO<sub>x</sub>-modified graphite, the linearity of the anodic and cathodic signals is defined by the following equations:  $y = -4.634x + 0.061$  ( $R^2 = 0.996$ ) and  $y = 2.322x + 5.423$  ( $R^2 = 0.972$ ), respectively. Both the anodic and cathodic peak currents were linearly proportional to the square root of the scan rate, in the range from 5.0 to 200  $\text{mV s}^{-1}$  (Figure 2.7 (inset)), indicating a diffusion-controlled electrode process.

#### 2.1.4 Surface Characterization

The surface morphology of the PT-Pala film was monitored by SEM and compared with those of the electrodeposited PT and PT-Pala/PT copolymers. In the case of PT, granular morphology was observed; however, PT-Pala showed a completely different surface morphology. A homogeneous film was observed on the graphite surface; but when both PT and the PT-Pala/PT copolymer were used for the electrodeposition, a mixed structure of both PT and PT-Pala was obtained as shown in Figure 2.8. T-Pala deposition on indium tin oxide coated glass was also observed by fluorescence microscopy after formation (Figure 2.9). The polymer matrix can be seen clearly because of the fluorescent characteristic of the PT-Pala film.

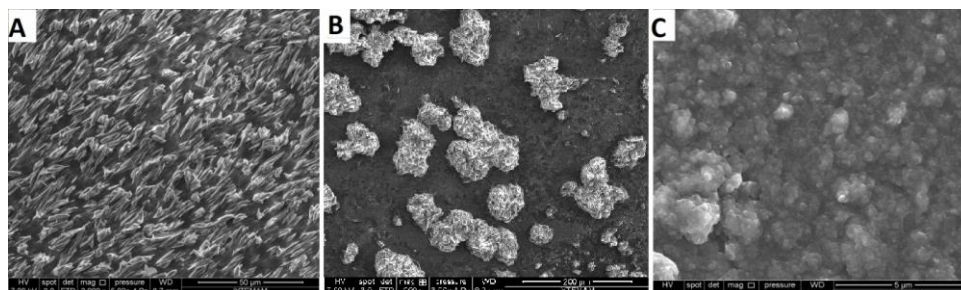


**Figure 2.8 :** SEM images of (A) PT-Pala-, (B) PT-Pala/PT-, and (C) PT-coated electrodes.

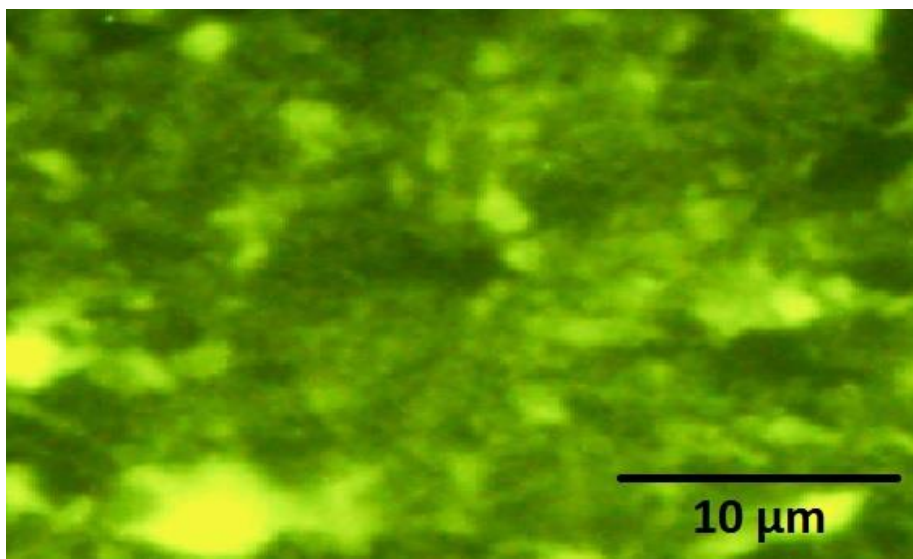


**Figure 2.9 :** Fluorescence microscope image of PT-Pala coated electrode.

### 2.1.5 Biosensing applications

The effect of pH on the sensitivity of the PT-Pala/GOx biosensor was optimized using 1.0mM glucose as the substrate. The pH of acetate buffer was varied from pH 3.5 to pH 5.5. The relative biosensor response (%) was plotted against different pH values. According to Figure 2.10, the maximum activity was at pH 4.5, which is close to the optimum pH for free GOx.

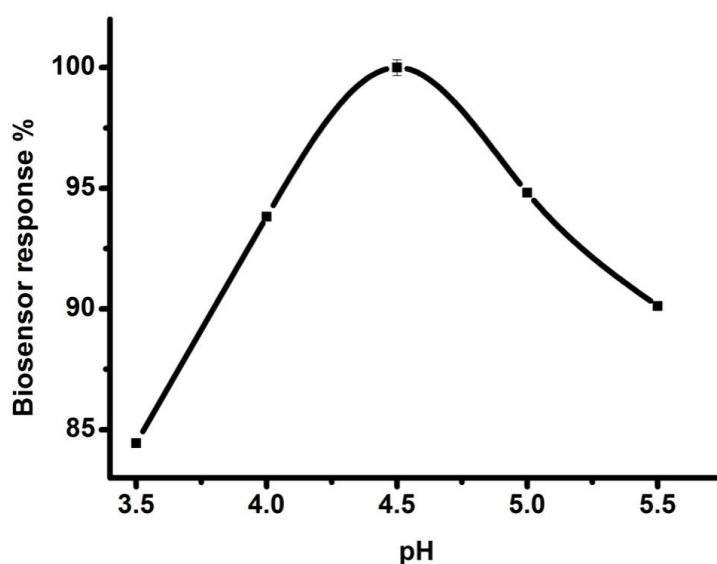


**Figure 2.10 :** The effect of pH. (in 50 mM sodium acetate, at pH 3.5-5.5, 25 °C, -0.7 V). Error bars show standard deviation.

Afterwards, chronoamperometric responses of the biosensor were recorded by adding standard solutions of glucose to reaction buffer solution. Figure 2.11 shows the calibration curve for glucose (the inset shows the linear range of the calibration curve). There was a linear relationship between the obtained current and the glucose concentration in the concentration range of 0.01–1.0 mM. To test repeatability, the biosensor signals corresponding to 0.5 mM glucose solutions were measured. The standard deviation and variation coefficient (%) were calculated to be  $\pm 0.016$  and 3.25%, respectively.

In addition, calibration curves were also plotted using Pt and PT-Pala/PT copolymer-coated graphite electrodes for the construction of GOx biosensors under identical experimental conditions. Insignificant response signals were obtained in a narrower linear range of glucose (0.01–0.8 mM) with a longer response time in comparison to the PT-Pala/GOx electrode.

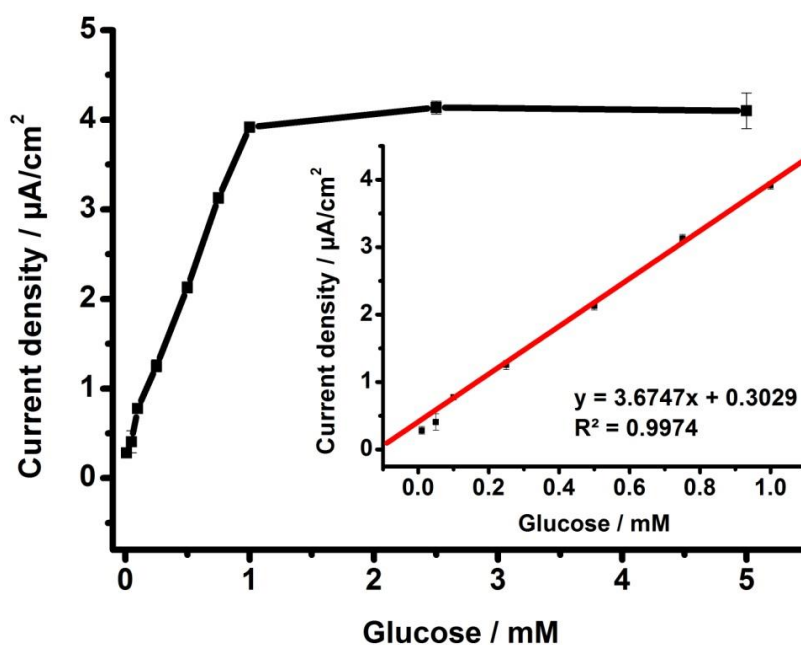


**Figure 2.11** : Calibration curve for glucose. PT-Pala/GOx in 50 mM sodium acetate, pH 4.5, 25 °C,  $-0.7$  V. Error bars show the standard deviation of three measurements (the inset shows the linear range).

To observe the effect of covalent immobilization on the current responses, another biosensor was prepared by the physical adsorption. In this case, the enzyme electrode was constructed without using glutaraldehyde and a calibration graph was plotted to compare the response characteristics with the GOx electrode obtained by using the

covalent immobilization procedure (Figure 2.12). The linearity was obtained from 0.05 to 1.0 mM for glucose, with the equation of  $y = 2.415x + 0.366$  ( $R^2: 0.989$ ). Moreover, the biosensing performance was tested by successively measuring the responses by the addition of glucose (0.5 mM).

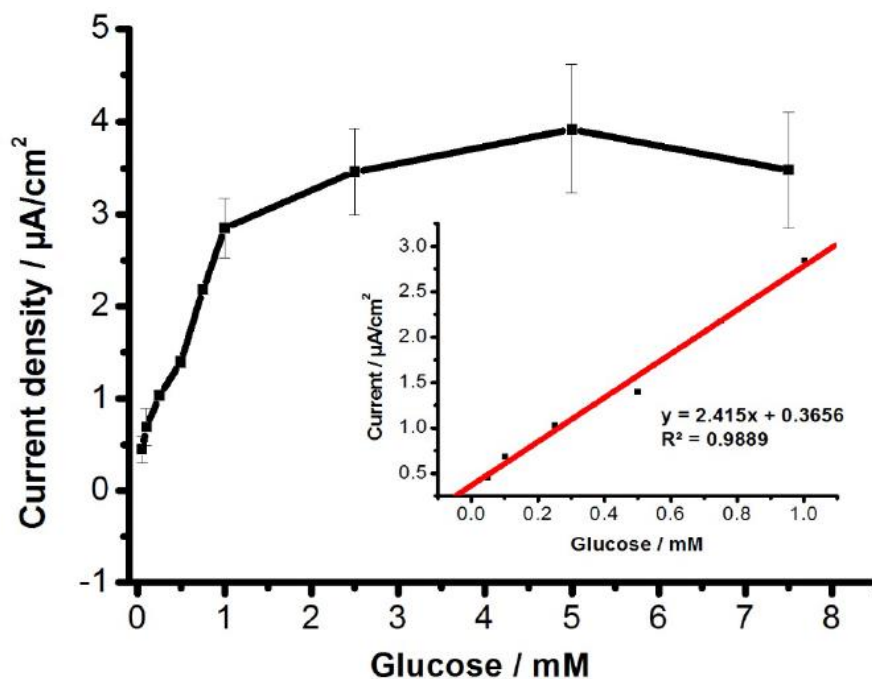


**Figure 2.12 :** Calibration curve for glucose. PT-Pala/GOx biosensor constructed without glutaraldehyde in 50 mM sodium acetate, pH 4.5, 25 °C,  $-0.7$  V. Error bars show the standard deviation of three measurements (the inset shows the linear range).

The variation coefficient was calculated to be 16.12%. The results showed that the biosensor constructed by the physical adsorption exhibited lower sensitivity (as can be seen from the slopes of the linear plots) and unacceptable RSD value which shows non-repetitive signals. It could be explained by the weak interactions between the biomolecule and the surface as a result of a short incubation time (90 min). Thus, the leakage of the biomolecules from the surface occurred easily and it caused unreproducible response signals after each trial. On the other side, these findings show that the polymer matrix could have potential for the biomolecule adsorption, but in that case, longer incubation times in the immobilization procedures are required. Also, the adsorption time as well as the enzyme amount should be optimized as the important parameters to have more reproducible and reliable response signals.

Electrode	Immobilization method	Linear range (mM)	RSD (%)	Ref.
SPCE	Adsorption	0.2–7.5	ND	40
GCE	Adsorption	0.05–10.50	ND	41
GCE	Adsorption	0.1–5.0	3.79	42
PDE	Adsorption	0.2–9.1	3.6	43
Fe working electrode	Entrapment	0.025–3.0	3.5	44
CNT paste electrode	Entrapment	Up to 0.8	ND	45
Au electrode	Crosslinking	0.05–12	2.2	46
BDD electrode	Crosslinking	0–25	ND	47
GCE	Affinity	1.8 x 10 <sup>-3</sup> -5.15	2.5	48
Pt microelectrode	Affinity	Up to 2.4	ND	49
GE	Covalent immobilization	0.02–1.20	ND	50
GE	Covalent immobilization	0.025–1.25	5.87	51
GE	Covalent immobilization	0.01–1.0	3.25	This work

<sup>a</sup> SPCE: The screen-printed carbon electrode, GCE: glassy carbon electrode, CNT: carbon nanotube, PDE: platinum disk electrode, BDD: borondoped diamond, Pt: platinum, GE: graphite electrode, and ND: not detected.

**Table 2.1** : Comparison of some glucose biosensors constructed with different immobilization techniques, in terms of linearity and the relative standard deviation (RSD) in the literature<sup>a</sup>

In addition to covalent immobilization, there are different immobilization techniques including adsorption, entrapment, and cross-linking which present different advantages and drawbacks. Among these techniques, covalent immobilization depending on the formation of chemical bonds between functional groups of the enzyme and the matrix has some advantages such as a stable and compact structure, short response time and no diffusion barrier [39]. Table 2.1 presents a comparison of some glucose biosensors constructed using different immobilization techniques that were reported in the literature. Also, antimicrobial activities of the novel thiophene-polyalanine macromonomer (T-Pala) and polymer (PT-Pala) were evaluated by using

the disc diffusion method (Table 2.2 and Figure 2.13). The results showed that PT-Pala exhibited moderate antibacterial activity towards Gram-positive bacteria. Graphite covered with PT-Pala also showed significant antibacterial activity against Gram-positive *S. aureus* ATCC 25923.

**Table 2.2** : Antimicrobial activities of T-Pala, PT-Pala and standard antibiotics.

OFX: ofloxacin; AMC: amoxycillin/clavulanic acid (2:1); IPM: imipenem; E: erythromycin; (–) not active. a)  $\mu\text{g}/6.0$  mm paper disc; b) graphite disc coated with electropolymer of PT-Pala (3.0 mm diameter).

Tested microorganisms	Zones of inhibition (mm)					
	Tested materials		Standard antibiotics			
	T-Pala (75) <sup>a</sup>	PT-Pala <sup>b</sup>	OFX (5) <sup>a</sup>	AMC (30) <sup>a</sup>	IPM (10) <sup>a</sup>	E (15) <sup>a</sup>
<i>Escherichia coli</i> ATCC 25922	–	–	26	16	20	10
<i>Staphylococcus aureus</i> ATCC 25923	–	7	22	30	>30	20

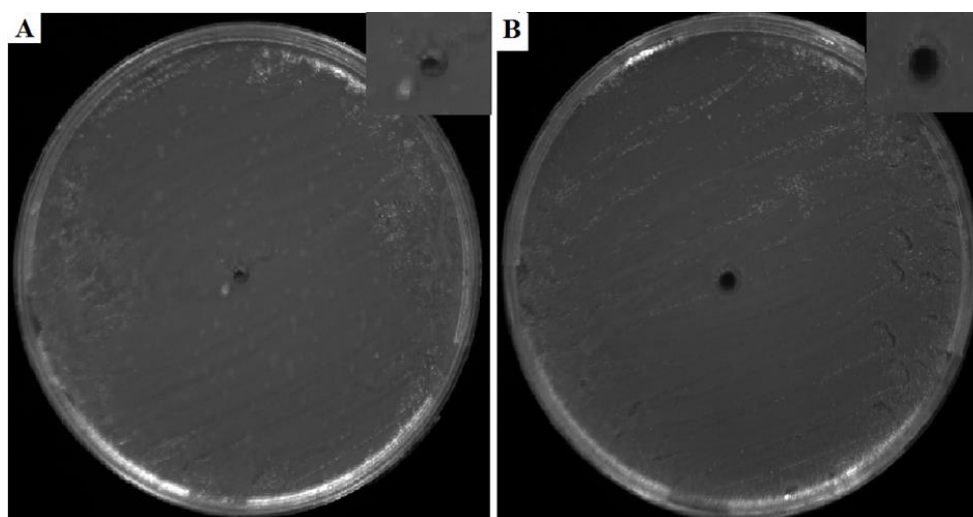


**Figure 2.13** : Antimicrobial activity of PT-Pala against *S. aureus* ATCC 25923 (A) graphite disc (B) graphite disc coated with PT-Pala.

## 2.2 Experimental Section

### 2.2.1 Materials

3-Bromothiophene, copper(I) cyanide, lithium aluminium hydride, L-alanine, tetrabutylammonium hydroxide, and diphenyl carbonate were purchased from Sigma-Aldrich and were used as received. DMAc and DMF were purified by heating at 60 °C for 1 h over calcium hydride (CaH<sub>2</sub>), followed by fractional distillation before use.

### 2.2.2 Synthesis of thiophene-3-carbonitrile (1b)

3-Bromothiophene (1a; 1.63 g, 10 mmol) and CuCN (3.58 g, 40 mmol) dissolved in 15 mL of DMF were placed in a Schlenk tube under a nitrogen atmosphere, and the mixture was stirred at 150 °C for 18 h. Then, the temperature was allowed to drop to room temperature and 40 mL of 14% NaOH was added to the mixture. Next, 300 mL of diethyl ether was added to the aqueous phase, and the mixture was vigorously stirred at room temperature for 30 min. Afterwards, the organic layer was washed with water and dried over NaSO<sub>4</sub>. After evaporation of the solvent until near dryness, the residue was purified by flash chromatography (silica gel, 1 : 1 chloroform–hexane as the eluent) to provide 765 mg of product in ~70% overall yield. <sup>1</sup>H-NMR (CDCl<sub>3</sub>, 500 MHz): δ 7.89 (s, 1H), 7.38 (d, 1H), 7.18 (d, 1H).

### 2.2.3 Synthesis of 3-(aminomethyl)thiophene (1c)

To a solution of lithium aluminum hydride (417 mg, 11 mmol) in 15 mL of dry THF at 0 °C, thiophene-3-carbonitrile (1b; 1.0 g, 9.16 mmol) in 15 mL of dry THF was added over 20 min under a nitrogen atmosphere, and the mixture was warmed to 50 °C over 2 h. The reaction mixture was cooled to 0 °C, and 2.0 mL of 15% NaOH was added dropwise before 6.0 mL of water was added to the mixture. The aqueous layer was extracted with diethyl ether (50 mL x 5). Then, the organic layer was concentrated by evaporation. The oily residue was purified by fractional distillation under vacuum to give 870 mg of product as a colorless oil in ~70% overall yield. <sup>1</sup>H-NMR (CDCl<sub>3</sub>, 500 MHz): δ 7.31 (d, 1H), 7.15 (s, 1H), 7.03 (d, 1H), 3.90 (s, 2H), 1.47 (s, 2H).

### 2.2.4 Synthesis of L-Ala-N-(phenyloxycarbonyl) amino acid

To a stirred solution of L-alanine (1.78 g, 20 mmol) in methanol (30 mL), tetrabutylammonium hydroxide (37% in methanol, 13.8 g, 20 mmol) was slowly added at room temperature. After stirring for 1 h, the reaction mixture was concentrated under reduced pressure. The resulting residue was dissolved in acetonitrile (20 mL). The solution was added dropwise over 10 min to a stirred solution of DPC (4.2 g, 20 mmol) in acetonitrile (25 mL) under ambient conditions, and then the reaction mixture was stirred for 3 h. To the reaction mixture, 1.0 M HCl aqueous solution (20 mL) was added. The mixture was transferred into a separatory funnel containing distilled water (30 mL), and the organic fractions were combined, washed with brine, dried over Na<sub>2</sub>SO<sub>4</sub>, filtered, and concentrated under reduced pressure. The crude products were purified by flash column chromatography with a gradient from 50–70% ethyl acetate in n-hexane as the eluent, followed by recrystallization with ethyl acetate–n-hexane to yield 2.5 g of product as a white powder in 60% yield. <sup>1</sup>H-NMR (CDCl<sub>3</sub>, 500 MHz): δ 1.55 (d, J = 7.2 Hz, 3H), 4.49 (dt, J = 14.0, 6.9 Hz, 1H), 5.60 (d, J = 7.1 Hz, 1H), 7.14 (d, J = 7.9 Hz, 2H), 7.21 (t, J = 7.4 Hz, 1H), 7.36 (t, J = 7.8 Hz, 2H).

### 2.2.5 Synthesis of T-Pala in the presence of 3-(aminomethyl)thiophene

L-Ala-N-(phenyloxycarbonyl)amino acid (2c) (206 mg, 1.0 mmol) dissolved in 1.0 mL of dry DMAc and 3-(aminomethyl)-thiophene (1c)/DMAc solution (20 μL, 1.0 × 10<sup>-2</sup> mmol μL<sup>-1</sup>) was placed into a flame-dried Schlenk tube. The polymerization was carried out at 60 °C for 48 h under a nitrogen atmosphere. Next, the reaction mixture was cooled to room temperature, and the white blurry solid was poured into diethyl ether and stirred for 2 h at room temperature to eliminate the unreacted monomer and other contaminants. The white precipitates were collected by filtration and dried under vacuum to yield 73 mg of T-Pala in 80% yield. Mn: 1140, *M<sub>w</sub>/M<sub>n</sub>* = 1.16. <sup>1</sup>H-NMR (CDCl<sub>3</sub>, 500 MHz): δ 1.45–1.65 (br, 3H), 3.45–3.52 (br, 2H), 4.10–4.25 (br, 1H), 4.27–4.52 (br, 3H), 6.98–7.30 (br, 1H), 7.13–7.15 (br, 1H), 7.27–7.30 (br, 1H).

### 2.2.6 Preparation of PT, PT-Pala, and PT-Pala/PT biosensors

Initially, spectroscopic grade graphite electrodes were polished on emery paper and washed thoroughly with distilled water to be used in the polymerization reaction. In



order to achieve electrochemical polymerization, T-Pala was initially subjected to chronoamperometry by applying +1.6 V in 0.1 M SDS in 30 : 70 water-acetonitrile solutions for 20 min. For electrochemical copolymerization of T-Pala/thiophene, 0.1 M thiophene was added to the solution and the same reaction conditions were applied. In the case of a bare PT matrix, 0.1M thiophene, 0.1M SDS, and 10 mL of distilled water were used and +1.6 V was applied. For enzyme immobilization, an appropriate amount of Gox (1.0 mg in 5.0  $\mu$ L, 50 mM sodium phosphate buffer, pH 7.0) was spread over the polymer-coated electrodes, glutaraldehyde (5.0 mL, 0.1% in 50 mM sodium phosphate buffer, pH 7.0) was added, and the electrodes were allowed to stand under ambient conditions to dry for 90 min. To confirm the efficiency of the covalent immobilization to the biosensor response, a control experiment in the absence of glutaraldehyde under identical experimental conditions was also performed.

### 2.2.7 Measurements

$^1\text{H-NMR}$  spectra were recorded with an Agilent VNMRS 500 MHz, and chemical shifts were recorded in ppm units using tetramethylsilane as an internal standard. For amperometric measurements, the radiometer electrochemical measurement unit (VoltaLab PGP201, Lyon, France) was used with a traditional three-electrode configuration. A graphite electrode (Ringsdorff Werke GmbH, Bonn, Germany, type RW001, 3.05 mm diameter and 13% porosity) as the electrode for biomolecule attachment, a Ag/AgCl electrode as the reference electrode, and a platinum electrode as the counter electrode were used during electrochemical measurements, and all potentials were reported with respect to the Ag/AgCl reference electrode. A Palm Instruments potentiostat (PalmSens, Houten, The Netherlands, <http://www.palmsens.com>) with three electrode configurations was used for the CV experiments. FTIR-attenuated total reflection (ATR) spectra were recorded in the wavenumber range from 4000–650  $\text{cm}^{-1}$  with a Spectrum BX-II Model instrument (Perkin Elmer, Norwalk, CT, USA) and an attached MIRacle ATR diamond crystal unit (Pike Technologies, Madison, WI, USA). A resolution of 4  $\text{cm}^{-1}$  and 50 scans per sample were used. An Olympus BX53F Fluorescence microscope with an Olympus DP72 camera and an Uplanapo 100x objective and SEM (FEI QUANTA250 FEG) were used for surface imaging of the prepared electrodes. For determination of the number average molecular weight ( $M_n$ ) and polydispersity

index ( $M_w/M_n$ ) for the synthesized polymers, a gel permeation chromatography (GPC) analysis was performed on an Agilent 1100 Series instrument, including a pump, NUCLEOGEL® GPC columns, and a differential refractive index (RI) detector, at a flow rate of  $0.7 \text{ mL min}^{-1}$  using  $0.01 \text{ M LiBr/DMF}$  as the eluent and  $50 \text{ }^\circ\text{C}$ . Toluene was chosen as the flow marker, and the RI detector was calibrated with poly(methyl methacrylate) standards having a molecular weight of  $2.500\text{--}270.000 \text{ g mol}^{-1}$ .

### **2.2.8 Electrochemical measurements**

Amperometric determination of the biosensor response was performed under ambient conditions by applying a constant potential at  $-0.7 \text{ V}$  and following the oxygen consumption as a result of enzymatic activity in the bioactive surface. The enzyme electrodes were initially equilibrated in  $10 \text{ mL}$  of sodium acetate ( $\text{pH: } 4.5$ ) as a working buffer. When the background current reached a steady state, the substrate solution was added to the electrochemical cell, then the current change was monitored as current density ( $\mu\text{A cm}^{-2}$ ), and the steady-state current values were recorded.

In all amperometric studies, each measurement was repeated three times, and standard deviations were calculated. All reported data were given as the average of three measurements  $\pm$  standard deviation. In the figures, error bars show standard deviation. The experiments were conducted at ambient temperature ( $25 \text{ }^\circ\text{C}$ ).

### **2.2.9 Antimicrobial activities**

Antimicrobial activities of the thiophene-polyalanine macromonomer (T-Pala) and polymer (PT-Pala) were evaluated by using the disc diffusion method [52,53] T-Pala and electropolymer of T-Pala (PT-Pala) that were successfully coated on the surface of graphite electrode were evaluated for *in vitro* antibacterial activity against Gram-positive *Staphylococcus aureus* ATCC 25923 and Gram-negative *Escherichia coli* ATCC 25922 (strains belonging to the American Type Culture Collection, LGC Standarts GmbH, Wesel, Germany). Antimicrobial activity was investigated according to the recommendation of the National Committee for Clinical Laboratory Standards (NCCLS) by using disk diffusion method [24]. It was performed on Nutrient Agar (NA, Oxoid) plates. Plates were dried at approximately  $36 \text{ }^\circ\text{C}$  for about  $30 \text{ min}$  in an incubator before inoculation. Three to five freshly grown colonies

of bacterial strains were inoculated into 25 mL of Nutrient Broth (NB, Oxoid) medium in a rotary shaker at 200 rpm for 4 to 6 h until a turbidity of 0.5 McFarland ( $1 \times 10^8$  CFU/mL) was reached. Final inocula were adjusted to  $5 \times 10^5$  CFU/mL using a spectrophotometer. 50  $\mu$ L of inoculum from the final inocula was applied to each of agar plates and were uniformly spread with a sterilized cotton spreader over the surface. Absorption of excess moisture was allowed to occur for 30 min before application of sterile filter-paper discs (6 mm in diameter, Oxoid, England,). The paper discs were impregnated with 15  $\mu$ L of the T-Pala sample solutions in dimethylsulphoxide (DMSO) which include 5.0 mg per 1.0 mL of DMSO (solution was filter-sterilized using a 0.45  $\mu$ m membrane filter) and electropolymer of PT-Pala coated graphite disc (3 mm diameter) were applied to the agar surface. These plates were incubated at 37 °C for 24 h. At the end of the incubation time, the diameters of the inhibition zones were measured in millimeters using an inhibition zone ruler. Standard antibiotic discs (all from Oxoid) of ofloxacin (OFX, 5  $\mu$ g/disc), amoxicillin/clavulanic acid (2:1) (AMC, 30 mg/disc), imipenem (IMP, 10 mg/disc), erythromycin (E, 15  $\mu$ g/disc) were individually evaluated as positive controls, while the disc imbued with 15  $\mu$ L of pure DMSO and graphite discs were accepted as negative control.

### **2.3 Conclusion**

In conclusion, we designed and demonstrated a facile and generally applicable technique for the formation of a novel, biofunctional immobilization platform on graphite for use as a matrix for biomolecule attachment via ring-opening polymerization of NCA directly from the precursor and subsequent electropolymerization. This technique is experimentally facile and can be applied to various types of polypeptides. In the present work, the concept was successfully tested for the preparation of the functional PT-Pala and subsequent GOx attachment. Further experiments demonstrated the biosensing applicability of the electroactive conjugated polymers. The bioapplication of these types of polymers is unprecedented. Moreover, the described strategy is not restricted to the model peptide employed here and can be potentially extended to a very broad range of peptides by using their NCA precursors in the related ring-opening polymerization. Thus, the properties of the side chain polypeptides on the conducting layer can be tuned for various bio-applications, such as cell culture on a chip.



### **3. SYNTHESIS AND CHARACTERIZATION OF POLYPHENYLENES WITH POLYPEPTIDE AND POLY(ETHYLENE GLYCOL) SIDE CHAINS**

The extensive role of conjugated polymers (CPs) in emerging synthetic bio-applications [54,55], optical [56], electronic [57-59], diodes [60,61], and display technologies [62] represents the promising way in which considerable endeavors have been directed towards the realization of many aspects of conducting organic polymers. The conducting properties of CPs arise from having delocalized  $\pi$ -electron bonding along the polymer backbone bearing a framework of alternating double and single carbon-carbon bonds along which electrons can flow [54,63-67]. The mechanical flexibility, tunable optical properties, excellent conductivity, high mechanical strengths and processability of some conducting polymers make them potentially useful materials for new applications such as high-contrast organic light-emitting displays and low-cost organic photovoltaic solar cells [68-74]. Conjugated structure of CPs can create excellent one-dimensional surface for energy transport of electrons and strong UV absorption [75-79]. Especially, their fluorescence feature is one of the most susceptible to environmental change and this allows for eminent selectivity in signaling reporter group materials and provides advantages for CPs to be used in sensor technologies including pH sensors, temperature sensors and recently developed biosensors [80-82]. In CPs, the adjusting molecular morphology can lead to high surface area and extensive stability of the enzymes incorporated. Variations at surface properties depend on types of pendent groups, allowing for the production of polymers which are water soluble or exceptionally compatible with biomolecules [83,84].

Among vast number of CPs, poly(p-phenylene)s (PPP)s are the most promising class of polymer in terms of relatively high photoluminescence, electroluminescence quantum efficiencies and thermoxidative stability [85-87]. PPPs can easily be functionalized to give a wide range of derivatives due to the fact that their syntheses generally include phenyl compound monomers readily

allowing for many chemical modifications. Unfortunately, PPPs suffer from insolubility in many solvents, which limit their processability [88-90]. However, the addition of conformational alkyl or water soluble pendants or polymers as side chains to the backbone can lead to the obtainment of soluble PPPs with high molecular weight. In related studies in the authors' laboratory, it has been shown that PPPs can be combined with conventional synthetic polymers through the combination of various chain polymerizations with coupling processes to give soluble graft copolymers while preserving the conjugated backbone properties [84,91,92].

Innovative approaches including the combination of polypeptides with polymeric structures have received enormous interest in the fields of biomedicine, drug delivery [94,95], tissue engineering [96] and they are regarded as impressive biomaterial mimicking natural proteins [97]. Such conjugation systems can also open new perspectives for the fabrication of novel biomaterials that possess antibody/antigen, biocatalyst activity, compatibility with blood and/or tissue properties [98-100]. Polypeptides, existing in three-dimensional conformations such as  $\alpha$ -helix,  $\beta$ -sheet, and random coil shapes, exhibit intriguing morphological surface and excellent properties, such as low toxicity, biodegradability and biocompatibility [101,102]. Recent novel studies involving the synthesis of polymers such as polyether, polyester, chitosan, polysiloxane etc., combined with polypeptide segments, have the potential to revolutionize today's morphological structures and biomedical applications [103]. Considering conventional methods which have some drawbacks such as, multistep reactions, the use of hazardous reagents such as phosgene, lack of sufficient monomer purity and sensitivity to water contamination or heating conditions, the ideal synthetic pathway for polypeptides is the ring-opening polymerization (ROP) of the corresponding  $\alpha$ -amino acids of *N*-carboxyanhydrides (NCAs) [104-110]. In this technique, the polymerization can readily be induced with primary or secondary amines and their living nature allows the decisive control of molecular weight and terminal structure. The precursor urethane derivatives as monomer are readily synthesized by a two-step procedure: (i) transformation of  $\alpha$ -amino acids into the corresponding ammonium salts and (ii) *N*-carbamylation of the salts with diphenyl carbonates. These urethane derivatives of  $\alpha$ -amino acids are stable for

several months at room temperature [104]. It should be noted that high stability and ease of polymerization of these molecules with amines provides the possibility to form polypeptide-polythiophene copolymers as bio-based covering materials and ethanol biosensors [92].

Although polymers bearing bound polypeptides provide unique properties and advantage as regards bio-functionalization, the use of soluble support is a more essential requirement in biological application [111-116]. Water solubility can be achieved by the incorporation of polyethers, such as poly(ethylene glycol) (PEG). Polypeptide-PEG combinations as well as glycopeptides [117-120] with various topological structures receive great attention due to their excellent solubility in both water and organic solvents, and their biocompatibility. Moreover, they exhibit no antigenicity, immunogenicity, or toxicity towards the human body and is approved by the US-American Food and Drug Administration (FDA) [121,122].

Herein, we report a novel approach for the synthesis of PPP copolymers bearing both PEG units and polypeptide groups by the combination of Suzuki coupling and in situ NCA-ROP processes. This amine compound was used as initiator for NCA polymerization in the synthesis of polypeptide macromonomers and also used as monomer for the synthesis of PPP copolymer bearing primary amine groups and PEG. We provide two strategies to obtain PPP polymers bearing PEG and poly-L-lysine (PLL) side chains; (1) Suzuki coupling polymerization between PEG and polypeptide macromonomers, (2) NCA graft polymerization over the PPP backbone bearing the primary amine and PEG groups. To investigate the structure of the polymers and monomers, <sup>1</sup>H-NMR was applied. UV-vis and fluorescence spectra of PPP polymers are accepted as evidence of the formation of  $\pi$ -conjugated backbone. The polymers obtained with the characteristic features they possess could in the future be applied to various bio mimicking and other bio applications.

## 3.1 Experimental

### 3.1.1 Materials

Tetrakis (triphenylphosphine) palladium(0) ( $\text{Pd}(\text{PPh}_3)_4$ ), Poly(ethylene glycol) mono methyl ether ( $M_{n,RI} = 550 \text{ g mol}^{-1}$ ) (Me-PEG<sub>2000</sub>), *N*-*boc*-L-lysine, tetrabutylammonium hydroxide (37% in methanol) 2,5-Dibromo-benzoic acid, *N,N*-dimethylacetamide (DMAc) 1,4-benzene-diboronic acid, *N*-bromosuccinimide (NBS), 4-(*N,N'*-dimethyl) amino pyridine (DMAP), dicyclohexylcarbodiimide (DCC), poly(ethylene glycol) mono methyl ether (PEG<sub>2000</sub>), Phthalimide potassium salt, hydrazine monohydrate (98%) and Benzoyl peroxide are from Sigma-Aldrich and used without any further purification. All solvents were purified and dried.

### 3.1.2 Measurements

<sup>1</sup>H-NMR spectra were performed with an Agilent VNMRS 500 MHz, and chemical shifts were recorded in ppm units using tetramethylsilane as an internal standard. UV/vis absorbance measurements were recorded on a Shimadzu UV-1601 spectrometer. Fluorescence measurements were performed with a model LS-50 spectrometer from PerkinElmer at room temperature. The fluorescence quantum yields were determined according to IUPAC technical report using coumarine 1 (7-Diethylamino-4-methylcoumarin) as standard [123]. Gel-permeation chromatography (GPC) measurements were carried out in Viscotek GPCmax auto sampler system. Instrument was equipped with a pump (GPCmax, Viscotek Corp., Houston, TX), light-scattering detector ( $\lambda_0 = 670 \text{ nm}$ , Model 270 dual detector, Viscotek Corp.) consisting of two scattering angles: 7° and 90° and the refractive (RI) index detector (VE 3580, Viscotek Corp.). Both detectors were calibrated with PS standards in the narrow molecular weight distribution. Three ViscoGEL GPC columns (G2000HHR, G3000HHR and G4000HHR) employed with THF in the 1.0 mL min<sup>-1</sup> flow rate at 30 °C. All data were analyzed using Viscotek OmniSEC Omni-01 software.



### 3.1.3 Synthesis of 1,4-dibromo-2- (bromomethyl) benzene (1)

2,5-Dibromotoluene (2.55 ml, 18.5 mmol), NBS (6.2 g, 24.8 mmol) and 0.1 g of benzoyl peroxide were added to dry 40 mL of CCl<sub>4</sub> under nitrogen atmosphere. The solution was refluxed with condenser under nitrogen and 200 W light for 4 h. Heating started from 65 °C and temperature was increased by 10 °C per hour and in the last one hour temperature was kept at 95 °C. After that, the precipitate was filtered and washed with a supplementary amount of CCl<sub>4</sub> and finally with a small quantity of CH<sub>2</sub>Cl<sub>2</sub>. The organic layer was washed with water several times, and then dried over NaSO<sub>4</sub>. The solvent was evaporated in vacuo. Then the remaining crude material was purified by flash column chromatography (SiO<sub>2</sub>, Et<sub>2</sub>O) and recrystallized in petroleum ether to yield (1) (3.04 g, 50%, white crystal). <sup>1</sup>H-NMR (CDCl<sub>3</sub>, 500 MHz): δ 4.54 (s, 2H), 7.30 (dd, J = 8.5, 2.4 Hz, 1H), 7.45 (d, J = 8.5 Hz, 1H), 7.60 (d, J = 2.3 Hz, 1H).

### 3.1.4 Synthesis of 2-(2,5-dibromobenzyl)isoindoline-1,3-dione (2)

To the solution of (1) (2.9 g, 8.8 mmol) in 10 ml dry DMF, potassium phthalimide (2.45 g, 13.22 mmol) were added. After stirring for 12 h at 160 °C in a schlenk tube under nitrogen atmosphere, the reaction mixture was poured into water. The precipitate was washed with water, purified by flash column chromatography (SiO<sub>2</sub>, CH<sub>2</sub>Cl<sub>2</sub>), precipitated in ethanol and dried under vacuum to yield (2) (2.56 g, 74%, white solid). <sup>1</sup>H-NMR (CDCl<sub>3</sub>, 500 MHz): δ 4.94 (s, 2H), 7.26 (dd, J = 5.7, 2.5 Hz, 1H), 7.28 (d, J = 2.3 Hz, 1H), 7.45 (d, J = 8.3 Hz, 1H), 7.79 (dd, J = 5.5, 3.0 Hz, 2H), 7.92 (dd, J = 5.5, 3.1 Hz, 2H).

### 3.1.5 Synthesis of (2,5-dibromophenyl) methan amine (MA-DBB)

The solution of (2) (0.381 g, 0.95 mmol) in 25 ml absolute ethanol with 3 ml hydrazine were stirred at 90 °C for 5 h. After allowing to cool to room temperature, the mixture was extracted with CH<sub>2</sub>Cl<sub>2</sub> and 10 % NaHCO<sub>3</sub>. The organic layer was dried over Na<sub>2</sub>SO<sub>4</sub> and reduced in vacuo. The residue was purified by column chromatography (Al<sub>2</sub>O<sub>3</sub> (neutral), THF) to yield (3) (145 mg,

57%, yellow oil). <sup>1</sup>H-NMR (CDCl<sub>3</sub>, 500 MHz): δ 1.59 (br, 2H), 3.87 (s, 2H), 7.23 (dd, J = 8.4, 2.4 Hz, 1H), 7.38 (d, J = 8.4 Hz, 1H), 7.54 (d, J = 2.4 Hz, 1H).

### 3.1.6 Synthesis of Urethane Derivatives of Nε-Carbobenzoxy-L-lysine (NCA-LL)

To a stirred solution of Nε-carbobenzoxy-L-lysine (3.5 g, 12.5 mmol) in methanol (35 mL) and distilled water (5 mL), tetrabutylammonium hydroxide (37% in methanol) (8.77 g, 12.5 mmol) was slowly added at room temperature. After stirring for 1 h, the mixture was concentrated under reduced pressure. The residues were dissolved in acetonitrile (25 mL). The solution was added dropwise over 10 min to a stirred solution of DPC (2.68 g, 12.5 mmol) in acetonitrile (25 mL) at room temperature, and then the mixture was stirred overnight. To the reaction mixture, 1N of HCl aqueous solution (20 mL) was added. The mixture was put into a separating funnel containing distilled water (30 mL) and ethyl acetate (30 mL). The aqueous layer was extracted with ethyl acetate (3 x 30 mL) and the organic layers were combined, dried over Na<sub>2</sub>SO<sub>4</sub> and concentrated under reduced pressure. The crude products were purified by flash column chromatography (SiO<sub>2</sub>, chloroform:acetone:acetic acid = 7:3:0.1, as eluent), and then recrystallized with ethyl acetate/ *n*-hexane to yield 3.4 g (68%), as white solids. <sup>1</sup>H NMR (500 MHz, CDCl<sub>3</sub>): δ 1.34–1.58 (m, 4H), 1.67– 1.83 (m, 1H), 1.84–1.96 (m, 1H), 3.15 (m, 2H), 4.39 (m, 1H), 4.86(s, 1H), 5.08 (s, 2H), 5.84 (d, 1H, J = 8.1 Hz),, 7.09 (d, 2H, J =7.8 Hz), 7.15 (t, 1H, J =7.4 Hz), 7.28–7.37 (m, 7H).

### 3.1.7 Synthesis of polypeptide macromonomer (DBB-PLL)

To the solution of Nε-carbobenzoxy-L-lysine (0.4 mg in 1ml DMAc) in a flame-dried Schlenk tube, the amine initiator, MA-DBB, (5.3 mg in 0.5 ml DMAc) was added. The reaction mixture was stirred at 60 °C for 120 h under argon atmosphere. After the polymerization, mixture was cooled to room temperature and poured into diethyl ether. The precipitates were filtrated, and then dried under vacuum to yield 230 mg (80%), as white solids. <sup>1</sup>H-NMR (CDCl<sub>3</sub>, 500 MHz): δ 1.29-1.77 (broad), 1.78-2.01 (broad), 2.93-3.27 (broad), 3.49 (dd, J = 14.0, 7.0 Hz,

2H), 3.78-3.98 (broad), 4.85-5.25 (broad), 5.32-5.64 (broad), 6.84 (d,  $J = 7.9$  Hz, 1H), 7.06 (s, 1H), 7.17-7.36 (broad), 7.39 (d,  $J = 8.5$  Hz, 1H).

### 3.1.8 Synthesis of PEG macromonomer (DBB-PEG)

2,5-Dibromo-benzoic acid (4g, 14.3 mmol), DMAP (174.7 mg, 1.43 mmol), Me-PEG<sub>2000</sub>-OH (25.74 g, 12.87 mmol) were dissolved in 80 ml of dry CH<sub>2</sub>Cl<sub>2</sub> under nitrogen atmosphere. To this solution was added DCC (3.246 g, 15.7 mmol) in 20 ml dry CH<sub>2</sub>Cl<sub>2</sub> drop-wise under nitrogen. Then, the reaction mixture was stirred for 5 days at room temperature. After that, the mixture was filtered and washed with 250 ml of CH<sub>2</sub>Cl<sub>2</sub>. The organic phase was quenched with 10% NaHCO<sub>3</sub> and brine, and then dried over Na<sub>2</sub>SO<sub>4</sub>. The solution was concentrated and passed through a silica-gel column using CH<sub>2</sub>Cl<sub>2</sub> as eluent. After removal of solvent in vacuo, the polymer was precipitated in cold diethyl ether to yield 26 g (95%). <sup>1</sup>H-NMR (CDCl<sub>3</sub>, 500 MHz):  $\delta$  3.85 – 3.46 (broad), 3.38 (broad), 7.45 (dd,  $J = 8.5$ , 2.4 Hz, 1H), 7.52 (d,  $J = 8.5$  Hz, 1H), 7.93 (d,  $J = 2.4$  Hz, 1H).

### 3.1.9 Synthesis of PPP conjugated polymer bearing poly-L-lysine and PEG (PPP-g-PEG-PLL)

DBB-PLL (0.18 g), DBB-PEG (0.8 g) and benzene-1,4-diboronic acid (74.58 mg, 0.45 mmol) was dissolved in a solution of 2 ml of 2.0 M K<sub>2</sub>CO<sub>3</sub> (aq.) and 3 ml of THF in a Schlenk tube. The mixture was bubbled with nitrogen over a period of 30 min and then, Pd(PPh<sub>3</sub>)<sub>4</sub> (26 mg, 0.226 mmol) was added. The reaction mixture was stirred at 70 °C for 4 days in the absence of oxygen and light. After polymerization, the reaction mixture was extracted with water and CH<sub>2</sub>Cl<sub>2</sub>. Organic phase was collected and dried over Na<sub>2</sub>SO<sub>4</sub>. After the concentration of mixture under reduced pressure, the final polymer was precipitated in cold diethyl ether and dried under vacuum to yield 0.556 g (55%). <sup>1</sup>H-NMR (CDCl<sub>3</sub>, 500 MHz):  $\delta$  1.01-1.68 (broad), 1.69-2.09 (broad), 2.97-3.24 (broad), 3.40 (d,  $J = 15.2$  Hz, 3H), 3.41-3.71 (broad), 3.81 – 3.76 (m, 2H), 3.82-3.92 (broad), 4.19-4.36 (broad), 4.93-5.12 (broad), 5.37-5.52 (broad), 7.12-7.36 (broad), 7.35-8.36 (broad).

### **3.1.10 Synthesis of PPP conjugated polymer bearing primary amine and PEG (PPP-NH<sub>2</sub>-g-PEG)**

The reaction solution was prepared with 30 ml THF and 20 ml of aqueous K<sub>2</sub>CO<sub>3</sub> solution under nitrogen. Prior use, this solution was degassed by bubbling nitrogen over a period of 30 min. In the 10 ml of the reaction solution, MA-DBB (0.8 g, 3 mmol), DBB-PEG (2.3 g), benzene-1,4-diboronic acid (0.663 g, 4 mmol), Pd(PPh<sub>3</sub>)<sub>4</sub> (0.092 g, 0.08 mmol) was dissolved under nitrogen and stirred at 70°C for 4 days in the Schlenk tube under vacuum. After stirring, the reaction mixture extracted with CH<sub>2</sub>Cl<sub>2</sub> and small amount of water. Organic phase was concentrated and precipitated in excess diethyl ether to yield 1.85 g, white powder. <sup>1</sup>H-NMR (CDCl<sub>3</sub>, 500 MHz): δ 2.06 (broad), 3.38 (broad), 3.45-3.8 (broad), 7.92-8.20 (broad), 7.6-7.9 (broad), 7.2-7.6 (broad).

### **3.1.11 Synthesis of PPP conjugated polymer bearing poly-L-lysine and PEG (PPP-g-PEG-PLL) by route 2**

PPP-NH<sub>2</sub>-g-PEG (0.9 g) was charged into flame-dried Schlenk tube and then dissolved in 1 ml of DMAc, followed by addition of NCA precursor (NCA-LL)/DMAc solution (0.3 g/1 ml). The reaction mixture was stirred at 60 °C for 48 h under argon atmosphere. After the NCA ROP polymerization, the mixture was cooled to room temperature and then precipitated in cold diethyl ether. The resulting precipitates were filtered and dried under vacuum to yield 0.523 g (95%). <sup>1</sup>H-NMR (CDCl<sub>3</sub>, 500 MHz): δ 1.07-1.66 (road), 1.75-2.15 (broad), 2.91-3.20 (broad), 3.55 ( t, 3H), 3.56-3.68 (broad), 3.77 – 3.72 (m, 2H), 3.81-4.07 (broad), 4.18-4.37 (broad), 4.91-5.11 (broad), 5.43-5.60 (broad), 7.08-7.36 (broad), 7.34-8.39 (broad).

### 3.2 Result and Discussion

The crucial part of the approach for the synthesis of PPPs with macromolecular side chains is to obtain dibromobenzene functionalized polymers or low molar mass related components since applied Suzuki coupling reactions utilize dibromobenzenes in conjunction with the benzene diboronic acids and derivatives. Thus, primary amino functional dibromobenzene possessing suitable functionalities for both polypeptide incorporation and Suzuki coupling processes was synthesized via Gabriel reaction [124-129]. 2,5-Dibromotoluene was chosen as starting material because it can readily react with *N*-bromosuccinimide (NBS) to afford the allylic bromination of the methyl group in the presence of peroxide. After obtaining **1** in good yield, the substitution reaction with the conjugate base of phthalimide gave the corresponding *N*-alkyl phthalimide, 2-(2,5-dibromobenzyl)isoindoline-1,3-dione, (**2**). The efficiency of the reaction was increased by using preformed potassium salt of phthalimide, instead of phthalimide, facilitating the reaction to be conducted in a polar protic solvent such as DMF under homogenous conditions. Treatment of the imide derivative, **2** with hydrazine in methanol results in the formation of phthalhydrazide and (2,5-dibromophenyl) methanamine (MA-DBB) through intramolecular substitution. By using column chromatography, the desired amine compound MA-DBB could be separated from the side product phthalhydrazide. The overall synthetic pathway is outlined in Figure 3.1. The structure of MA-DBB was confirmed by <sup>1</sup>H-NMR analysis (Figure 3.2). Singlet peak at 1.59 ppm was assigned to –NH<sub>2</sub> protons, which was further confirmed by the examination of the hydrogen–deuterium exchange reaction. After the deuterium exchange using D<sub>2</sub>O, the peak at 1.59 ppm disappeared and a new singlet peak at 4.72 ppm appeared.

As stated previously, polypeptides can be synthesized from the corresponding NCA precursors. For our convenience, we have selected L-lysine based NCA precursor, *L*-lysine-*N* (phenyloxycarbonyl) amino acid (NCA-LL). This urethane derivatives of  $\alpha$ -amino acid, was synthesized in two reaction steps; (i) the transformation of  $\alpha$ -amino acid into the corresponding ammonium salt by an ionic exchange reaction and (ii) *N*-carbamylation of the ammonium salt-protected

amino acid via nucleophilic attack of the active primary amino group to the carbonyl group of diphenyl carbonate (Figure 3.3).

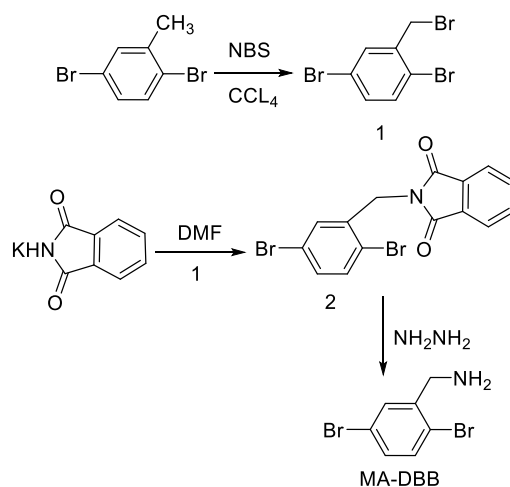


**Figure 3.1** : Synthesis of MA-DBB via Gabriel reaction.

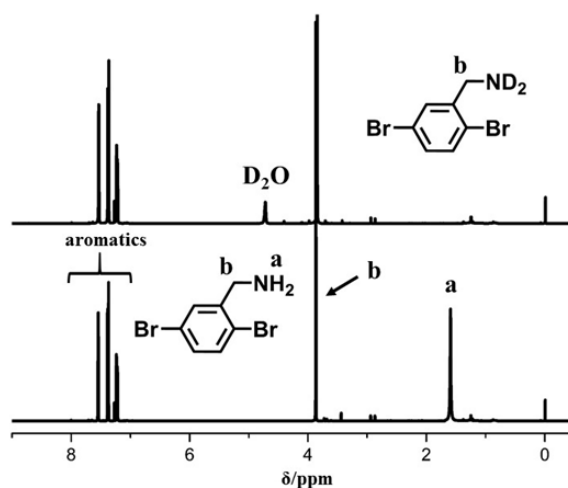


**Figure 3.2** :  $^1\text{H-NMR}$  spectra of MA-DBB before (bottom) and after (top) proton exchange.

The final product NCA-LL is stable and can be stored for several months at room temperature. Starting material of *N*-(phenoxy carbonyl) amino acid was synthesized according to the described procedure.

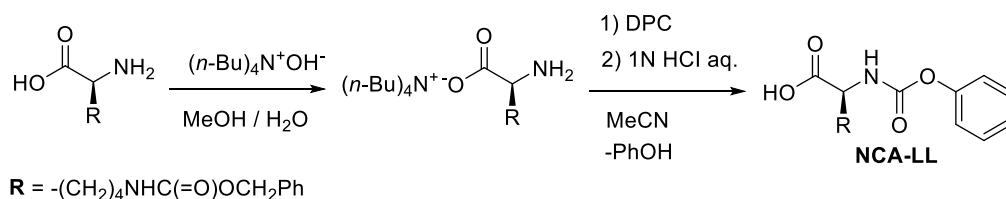


**Figure 3.3 :** Synthetic route for the urethane derivative of  $\alpha$ -amino acid, NCA-LL.

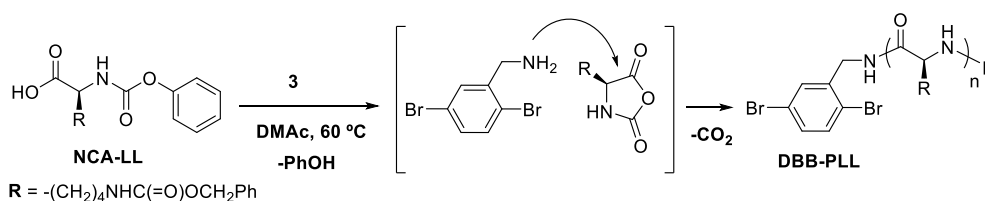


**Figure 3.4 :** Synthesis of DBB-PLL by in situ NCA ring opening polymerization.

### 3.2.1 Synthesis of PPPs with Polypeptide and PEG Side Chains

In order to develop the protocol for the synthesis of the final polypeptide bioconjugate, Suzuki coupling and in situ NCA ROP were combined in two different sequences. In the first route, polypeptide macromonomer (DBB-PLL) was prepared by ROP of NCA-LL using MA-DBB as an initiator (Figure 3.4). In earlier studies, we have shown that at high amine concentration, the monomer is rapidly consumed and polymerization proceeds in a controlled manner [104]. In the polymerization process, the NCA ring is formed by the elimination of phenol. Then, the primary amine group of the initiator attacks to the carbonyl carbon of NCA ring to form an amide bond between initiator and monomer with the evolution of  $\text{CO}_2$ , and the other activated amine side of the opened NCA ring ensues polypeptide chain growth. The structure of the polypeptide and presence of the terminal dibromobenzene group were confirmed by  $^1\text{H-NMR}$  analysis. As can be seen from Figure 3.5, aromatic protons of the end group resonate at 7.47, 7.06 and 6.84 ppm. Characteristic aromatic protons corresponding to the repeating unit appear between 7.13-7.42 ppm.

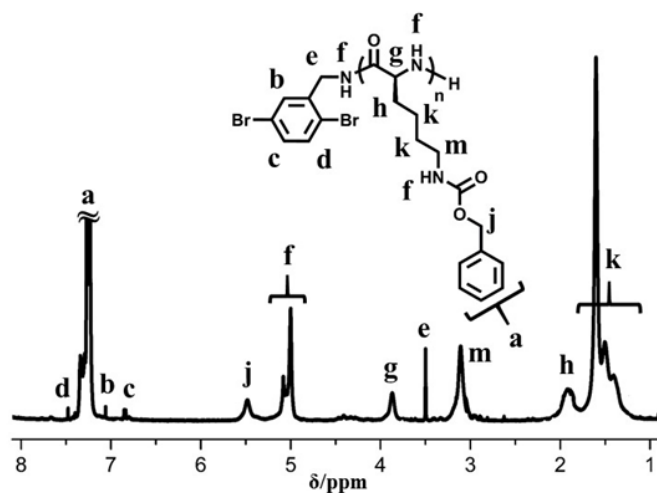


**Figure 3.5 :**  $^1\text{H-NMR}$  spectrum of polypeptide macromonomer, DBB-PLL.

The other polymeric coupling component, PEG macromonomer was synthesized by the well-known Steglich esterification method under mild conditions with the favorable catalytic action of 4-dimethylaminopyridine (DMAP) [84] (Figure 3.7).  $^1\text{H-NMR}$  spectral analysis of DBB-PEG evidenced the presence of both PEG repeating units and end group (Figure 3.6).

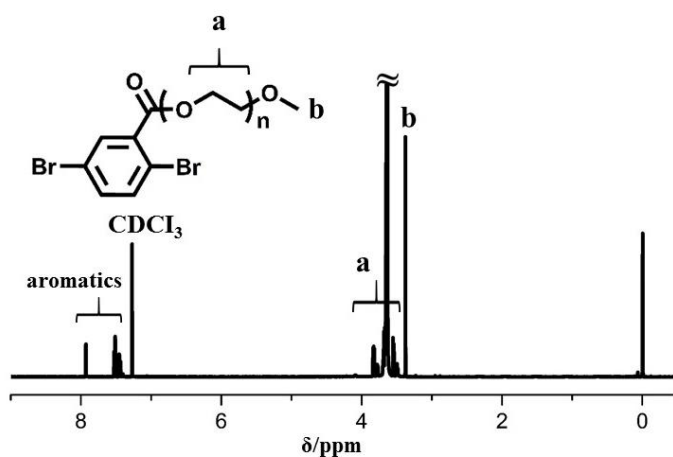


**Figure 3.6 :**  $^1\text{H-NMR}$  spectrum of DBB-PEG



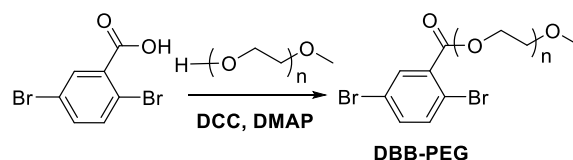


**Figure 3.7 :** Synthesis of PEG macromonomer via Steglich esterification reaction.

The assembling of PEG and polypeptide side chains on the PPP backbone was achieved by Suzuki condensation polymerization that provides molecular design flexibility. In this connection, it should be pointed out that Yamamoto coupling of only macromonomers without any spacer units is expected to yield much lower chain growth due to the steric hindrance of the bulky polymer chains. In the applied strategy, hydrophilic and biorelated segments can be incorporated to the PPP structure through the sequence adjustment using a spacer benzene ring. In the Suzuki polymerization, macromonomers and the coupling partner 1,4-benzenediboric acid in homogeneous suspension of THF/water with potassium carbonate were reacted in the presence of palladium catalyst (Figure 3.8). The polymerization time was deliberately prolonged to 4 days to overcome steric limitations of the macromonomers and obtain graft copolymers with adequate molecular weight. As polypeptides have tendency to form helical structures affecting the solubility properties, the molar ratio of PEG macromonomer to polypeptide macromonomer was deliberately kept low (mol/mol; 6/1) so as to provide sufficient solubility (Table 3.1). <sup>1</sup>H-NMR spectrum of the resulting graft copolymer, PPP-g-PEG-PLL, presented in Figure 3.9, clearly verifies the presence of both PPP backbone and side chains. Conjugated phenyl protons of PPP backbone appear as broad signals at 8.3-7.34 ppm. While phenyl protons of PLL segment are detected at 7.32 and 7.16, the broad signals at 3.74 and 3.42 are attributed to the CH<sub>2</sub> protons of PEG side-chain.

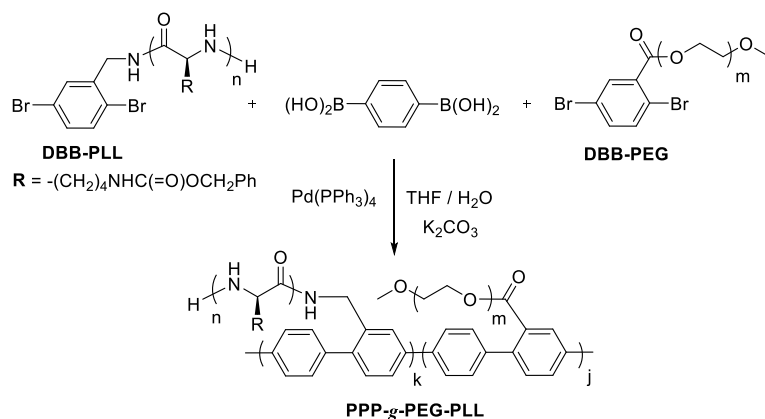


**Figure 3.8** : Synthesis of PPP polymer bearing poly-L-lysine and PEG side chains.

**Table 3.1** : Solubility characteristics of the graft copolymers and precursors; S = soluble, NS = not soluble, SS = slightly soluble.

Polymer	THF	H <sub>2</sub> O
DBB-PLL	S	NS
DBB-PEG	S	S
PPP- <i>g</i> -PEG-PLL (Route 1)	S	SS
PPP-NH <sub>2</sub> - <i>g</i> -PEG	S	S
PPP- <i>g</i> -PEG-PLL (Route 2)	S	SS

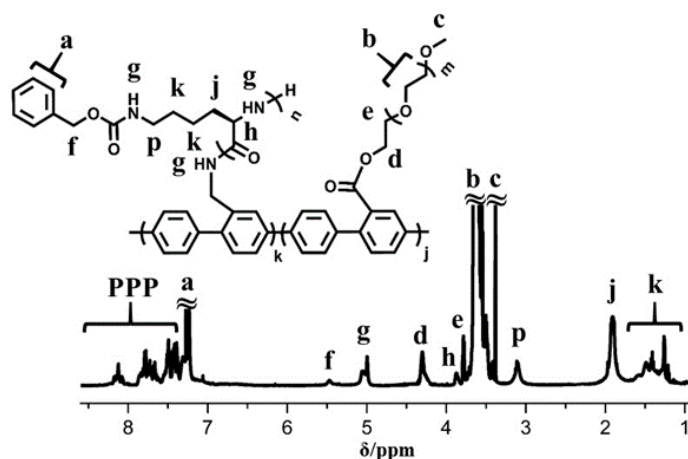


**Figure 3.9** : <sup>1</sup>H-NMR spectrum of PPP-*g*-PEG-PLL in CDCl<sub>3</sub>.

Photophysical characteristics of the graft copolymer were also investigated. UV-Vis absorption of spectra of PPP-*g*-PEG-PLL and its precursors, PEG and PLL

macromonomers registered in DMF with the same concentration are presented in Figure 3.10. As can be seen, DBB-PLL macromonomer has relatively stronger absorption than that of the DBB-PEG macromonomer due to the aromatic phenyl groups in the structure.

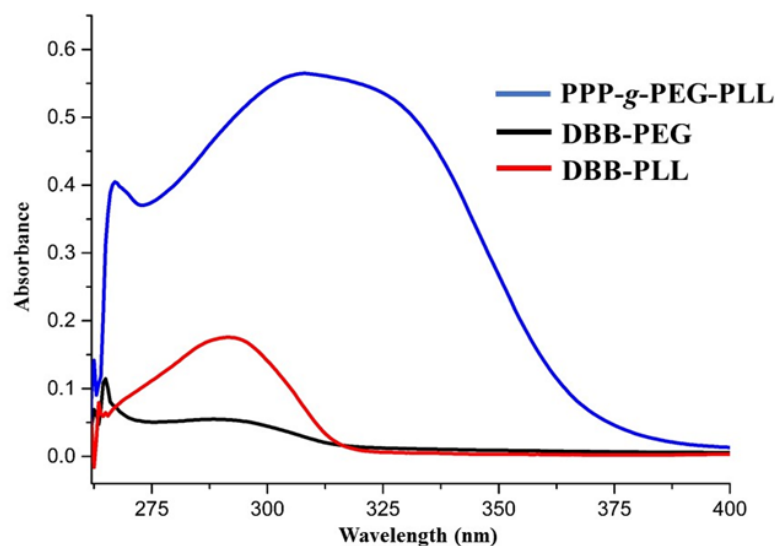


**Figure 3.10** : UV absorption spectra of DBB-PEG, DBB-PLL and PPP-g-PEG-PLL in DMF solution ( $0.1 \text{ mg.ml}^{-1}$ ).

Expected strong absorption band of PPP-g-PEG-PLL was due to the presence of supplementary conjugated phenylene rings in the main chain. Figure 3.11 shows the fluorescence spectra of PPP-g-PEG-PLL. The influence of starting macromonomers was very low in the observed spectrum of the graft copolymer, as their independent fluorescence intensities are rather weak and a nearly mirror-image-like relation between absorption and emission spectra was observed. It should also be noted that the fluorescence spectrum has a small shoulder emission at lower wavelength which may arise from the random placement of the macromonomer sequences in the backbone. Moreover, the aggregations that are taking place during the nanoparticles formation through self-assembling of PPP backbones in solution create the red shifted shoulders in asymmetric shape [130,131]. In the second route, the sequence of the processes of the already described strategy was reversed. The usual Suzuki coupling reaction described in the first route using MA-DBB, DBB-PEG and *p*-benzenediboronic acid under similar experimental conditions yielded PPP with amino groups in the structure (Figure 3.12).

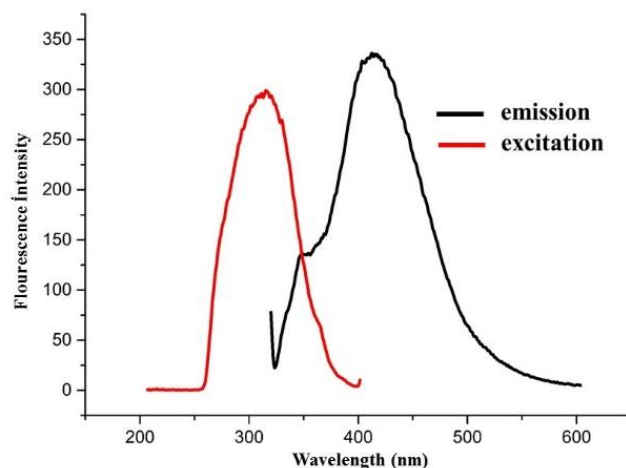


**Figure 3.11 :** Fluorescence excitation and emission spectra of PPP-g-PEG-PLL in DMF ( $1.43 \text{ mg}\cdot\text{L}^{-1}$ ).

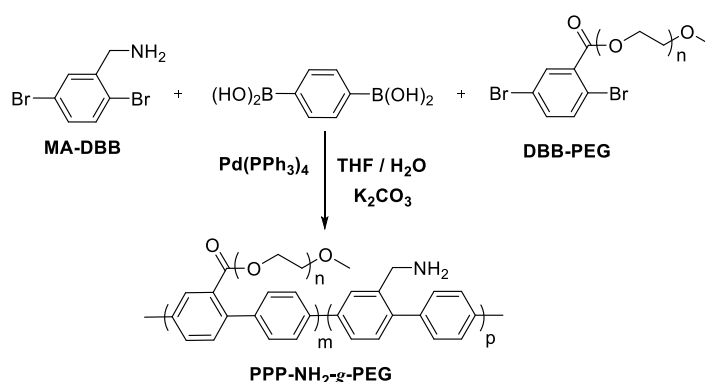


**Figure 3.12 :** The synthesis of **PPP-NH<sub>2</sub>-g-PEG** by Suzuki coupling polymerization.

In the process, the mole ratio of MA-DBB to DBB-PEG was 3/1 so as to obtain polymers with longer chain length. As the relative amount of DBB-PEG is increased, due to its polymeric nature and steric hindrance, limited chain growth is expected. The structure of the amino-functional PEG grafted PPP (PPP-NH<sub>2</sub>-g-PEG) was confirmed by <sup>1</sup>H-NMR analysis and Figure 3.13 exhibits the typical proton signals of PEG and PPP units as well as that of the primary amine at 1.96 ppm. Notably, the latter protons disappear after D<sub>2</sub>O proton exchange reaction. Compared to the precursors, PPP-NH<sub>2</sub>-g-PEG shows strong UV absorbance and fluorescence emission at higher wavelengths due to the extended conjugation arising from the PPP structure (Figures 3.14 and 3.15) Photophysical properties of the polymers investigated in dilute DMF and water solutions are depicted in Table 3.2.

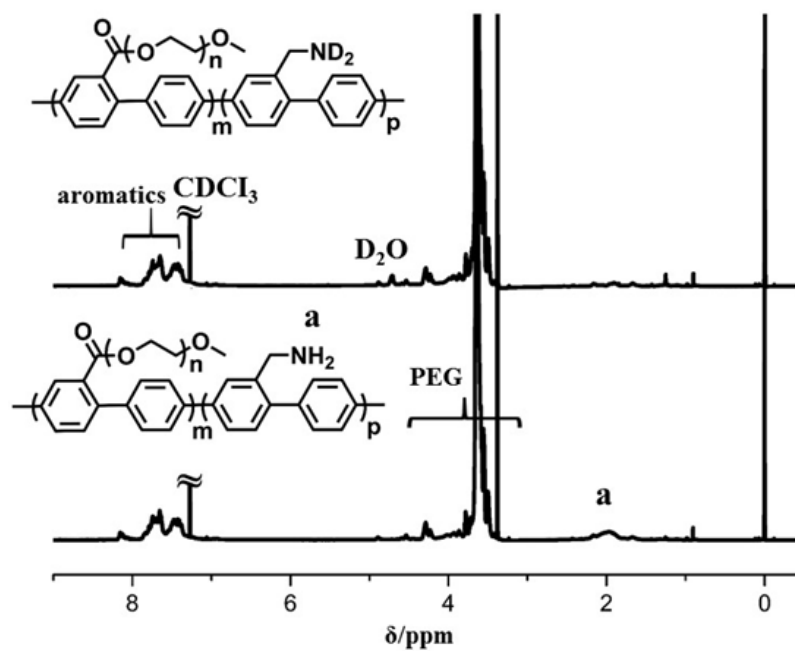


**Figure 3.13 :**  $^1\text{H-NMR}$  spectra of PPP- $\text{NH}_2$ -g-PEG before (bottom) and after (top) proton exchange.

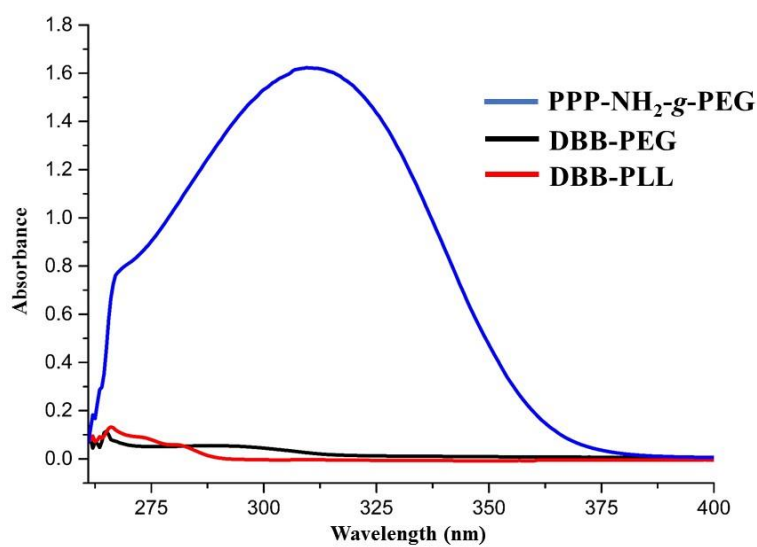


**Figure 3.14 :** UV spectra of DBB-PEG, MA-DBB and PPP- $\text{NH}_2$ -g-PEG in DMF solution ( $0.1 \text{ mg}\cdot\text{ml}^{-1}$ ).

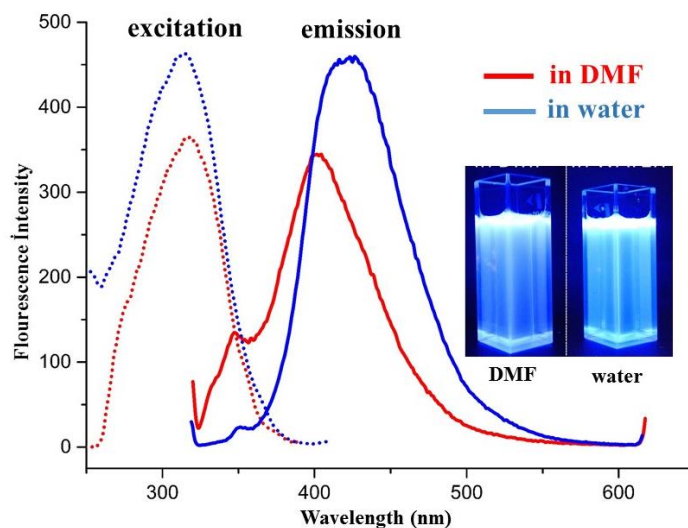


**Figure 3.15 :** The fluorescence spectra of PPP-NH<sub>2</sub>-g-PEG in DMF and water solution (0.3 mg.L<sup>-1</sup>).

**Table 3.2.** Photophysical properties of PPP-g-PEG-PLL and its precursors.

Polymer	$\epsilon^a$ (L.mol <sup>-1</sup> .cm <sup>-1</sup> )	$\Phi_f$ in Water	$\Phi_f$ in DMF
DBB-PLL	155998	-	-
DBB-PEG	3371	-	-
PPP-g-PEG-PLL (Route 1)	668542	0.34	0.49

<sup>a</sup> Measured at 290 nm in DMF solutions.

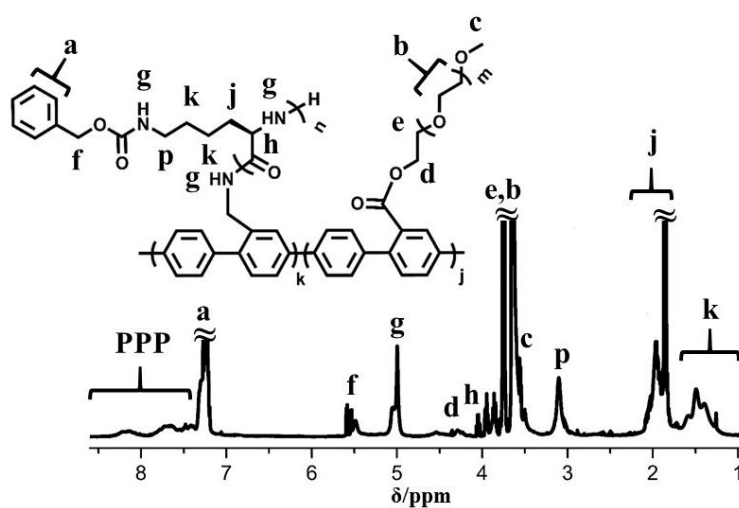


**Figure 3.16 :** <sup>1</sup>H-NMR spectrum of PPP-g-PEG-PLL (Route 2).

**Table 3.3** : Molecular Weight Characteristics of the Graft Copolymers and Precursors

Polymer	$M_w^a$ [g mol <sup>-1</sup> ]	$M_w/M_n^a$	DP <sup>a</sup>
DBB-PLL	86660	2.01	328
DBB-PEG	6880	1.24	150
PPP-g-PEG-PLL (Route 1)	140450	1.85	--
PPP-NH <sub>2</sub> -g-PEG	34430	1.41	--
PPP-g-PEG-PLL (Route 2)	41810	2.41	--

<sup>a</sup> Determined by GPC with light scattering detector according to polystyrene standards.

In the final step for the synthesis of PPP bearing PEG and PLL side chains, NCA ROP of NCA-LL was conducted through the primary amino groups of PPP-NH<sub>2</sub>-g-PEG exactly under the same polymerization conditions described in the first route. The overall reaction is depicted in Scheme 3.17. The <sup>1</sup>H-NMR spectrum of the graft copolymer exhibited almost the same spectral characteristics to that obtained by the first route since both methods yield essentially structurally identical polymers.

However, the aromatic protons corresponding to the PPP backbone were broader and more intense (Figure 3.16). This is expected since the Suzuki coupling reaction was carried out with low molar mass monomer, MA-DBB, facilitates longer PPA chain growth. This was further confirmed by the molecular weight measurements. As can be seen from Table 3.3, where molecular weight characteristics of the graft copolymers obtained by the two routes and intermediate polymers formed at various stages are compiled. The overall molecular weight of the polymer synthesized by the second route is much lower. The NCA ROP from the amine groups of the PPP results in the formation of shorter polypeptide chains.

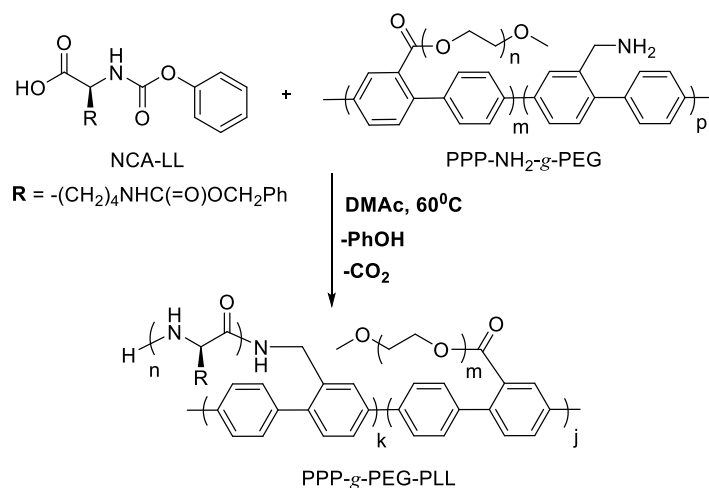


**Figure 3.17 :** The synthesis of PPP-*g*-PEG-PLL by NCA ROP of NCA-LL by using PPP-NH<sub>2</sub>-*g*-PEG.

### 3.3 Conclusion

In conclusion, in this work we presented a design principle to fabricate conjugated PPP graft copolymers with hydrophilic PEG and polypeptide side chains by the combination of NCA ROP and Suzuki polycondensation processes via two routes. In the first route, the dibromo benzene functional PEG and PLL macromonomer obtained by in situ NCA ROP were used in a Suzuki coupling reaction using benzene diboronic acid as the antagonist Suzuki coupling agent. In the other route, the same reactions were conducted in a different sequence. First, PPP with primary amine and PEG side groups was formed by Suzuki reaction. The NCA ROP through the pendant amino groups yielded the desired PPP graft copolymers. The described approach via Suzuki coupling conjugated polymers and polypeptides (Figure 3.18). In principle, it should not matter which route is employed first as both methods essentially yield structurally identical polymers as evidenced by spectral characterization. Highly emissive nature of the backbone and hydrophilic and bio-character of the side chains make these polymers an interesting class of bio-related emitting materials to be further evaluated in biosensor and functional materials. Such applications were previously demonstrated for electrochemically formed polythiophene derivatives [83,84]. Further studies in this line are now in progress.



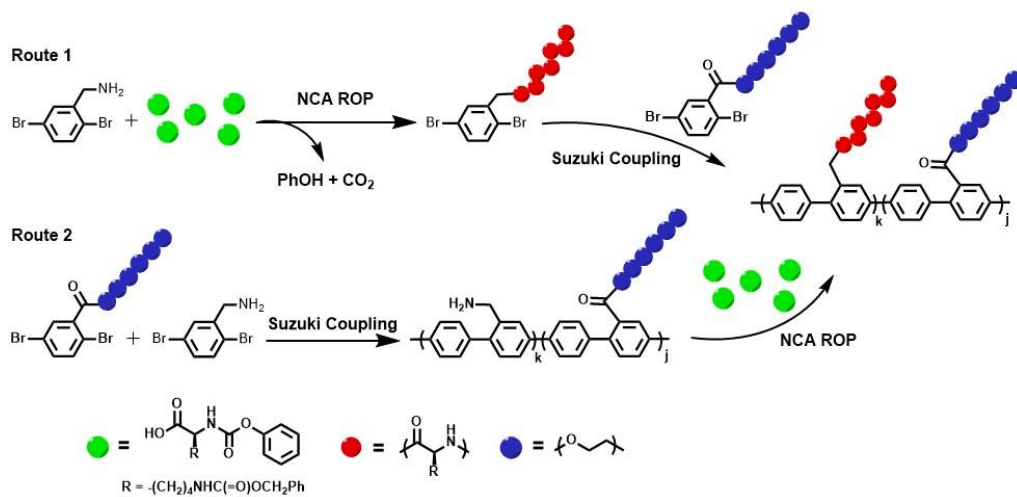


**Figure 3.18** : Total reaction pathways for route first and second



#### **4. SYNTHESIS, CHARACTERIZATION AND TARGETED CELL IMAGING APPLICATIONS OF POLY(P-PHENYLENE)S WITH AMINO AND POLY(ETHYLENE GLYCOL) SUBSTITUENTS**

Bio-functionalization of polymers of synthetic origin have played a challenging role over the past decades in the wide range of bioconjugation applications including the covalently incorporation of synthetic polymers with biological materials such as antibodies, peptides, proteins, enzymes, carbohydrates, viruses or cells [132]. Conceptually, this complementary strategies over conjugation of peptides, proteins or enzymes with synthetic polymers to design the versatile molecular biomaterials, had been first considered as essential topic in pharmaceutical chemistry for a few decades [133-136]. In line with recent discoveries of nanotechnology and biotechnology, polymer bioconjugates have gone far the field of biomaterial and gained enormous attraction in material science consisting of artificial enzymes, biometrics, light-harvesting systems, biosensors, photonics and nano-electronic devices [137-139]. To generate a bioconjugation system with synthetic polymer and biomaterial through covalent linkage, the most common method is the carbodiimide-mediated coupling reaction. As cross-linking agents, carbodiimides (EDC or DCC)/*N*-hydroxysuccinimide (NHS) gives coupling reaction between the primary amine groups in polymer and the carboxyl groups in biomaterial or vice versa positions. Other similar approaches based on chemical modification of primary amine groups to make them appealing different bioconjugation pathways [140-142]. Recent applications related to amino-based systems include, in situ enzymatic photo-patterning for manipulation of cell [143], amine-modified carbon nanotubes and nonporous carbon in controlled drug releasing [144-145], non-natural amino acid-mediated protein and polysaccharide conjugation for synthetic biology purposes [146], bio-based covering material for surface design and biosensor fabrication [147-148]. Amino-rich polymer-based nanoparticles for imaging-guided drug delivery and therapy [149], biological labelling application of protein by aminated luminescent nanoparticles [150], polyamine conjugates in systematic

in vivo short interfering RNA delivery therapeutics [151], surface initiated living polymerization of *N*-carboxyanhydride (NCA) to obtain polypeptides by grafting [152-154] are the other typical uses and numerous other studies remain.

Although the existence of amine group on polymer provides a unique property and advantage in bio-functionalization process, water-solubility is essential additional requirement in biological application. Water solubility can be achieved by water soluble supports such as poly(ethylene glycol) (PEG), which comes to the forefront from a highly versatile class of polyethers. PEG was also approved by the US-American Food and Drug Administration for the consuming in human body, exhibiting no antigenicity, immunogenicity, or toxicity [155-164].

Besides the effective role of PEG in bio-applications, advances in the field of bio-imaging have profoundly impacted the use of water soluble bio-polymers and concerns significantly focused on the fabrication of fluorescence-based organic conjugated polymers relying on  $\pi$ -electron delocalization features [165]. Among the vast number of conjugated polymers, PPP is the most promising polymer in terms of relatively high photoluminescence (PL), electroluminescence (EL) quantum efficiencies and thermos-oxidative stability. PPP can be easily functionalized to form a wide range of its derivatives due to fact that in the synthesis processes, generally the monomer is chosen as phenyl compounds allowing to many chemical modification readily [166-171]. Unfortunately, the main drawback, PPP has, is the insolubility in many solvents, which limits their processability. However, the addition of conformationally appropriate alkyl or water soluble pendants to backbone can lead to obtain soluble PPPs with sufficiently high molecular weight [172-180].

Nowadays, the goal and the content of the studies in biomedical field are focused on increasing delivery of the variety of drugs, gene therapy agents, and radiopharmaceuticals to the target tissue. A variety of ligands has been examined for the development of efficient targeted imaging, drug delivery and tracking systems [181]. The folate receptor has been proven as a highly selective overexpressed tumor marker in epithelial lineage tumours such as ovarian, colorectal, and breast cancer by the side of healthy tissue [182]. Besides, it is

well-known that folic acid (FA) has a high affinity to the folate receptors and is widely used as a targeting ligand for tumor-specific delivery. The inclusion of FA to the targeting system simplifies the internalization of the molecules by the receptor overexpressed cancer cells via receptor-mediated endocytosis [183].

In this study, we describe design and synthesis of fluorescent conjugated polymer possessing amino and PEG side groups (PPP-NH<sub>2</sub>-*g*-PEG) suitable for cell-targeting and imaging studies. In this connection, it should be pointed out that there exist several other promising approaches for surface modification or targeting tissues of interest utilizing acid functionalized polymers or anionic polysaccharides-based nanoparticlesref. However, the benefits of our system are several folds. In our approach, both amine and hydrophilic PEG functionalities are attached using the same chemistry that facilitates bio-functionality and water solubility, respectively.

The obtained polymers have excellent photophysical properties that can be benefited for the image proposes without any additional fluorophore. Besides, the some problems associated with the nanoparticles are eliminated due to the fully organic and biocompatible polymeric structure.

As will be shown below, the obtained water-soluble polymer was decorated with FA for the targeting and specifically imaging of FA receptor positive HeLa human cervixes cancer cells. The FA conjugated PPP-NH<sub>2</sub>-*g*-PEG polymer was obtained by a simple bioconjugation method called EDC/NHS chemistry. The resulted conjugates were characterized by several methods such as FTIR and fluorescence spectroscopy. Finally, the cellular internalization of fluorescent-based polymer was visualized by fluorescence microscopy.

#### **4.1 Results and discussion**

The instruction of bioactive polymer embodying amino and PEG lateral substituents on the same linear conjugated chain needs two different functional monomers in the time that Suzuki polycondensation was chosen as the polymerization technique. Suzuki coupling reaction providing more

straightforward access to obtain polymer with changeable sequence ratio between amino functional and PEG monomers was used to adjust the higher contribution of amino monomer than PEG macromonomer to PPP structure. Amino functionality is the crucial part of this study for the utilization of the polymer for bioconjugation. By this association, the preparation of primary amine functional monomer via Gabriel synthesis is based on the transformation of the primary alkyl halides into the primary amines [184-191]. To obtain primary alkyl halide, starting material was chosen as 2,5-dibromotoluene as it can readily react with *N*-bromosuccinimide (NBS) to afford allylic bromination of methyl group of toluene in the presence of peroxide. In the first stage, the reaction between 1 and conjugate base of phthalimide gives the corresponding *N*-alkyl phthalimide. The efficiency of the reaction was increased by using preformed potassium salt of phthalimide instead of phthalimide. Reaction proceeded with a polar protic solvent DMF under homogenous condition and the substitution product methyldibromophenyl phenothiazine (2) was obtained in a higher state of purity and in a shorter period of time. Second stage, named as hydrazinolysis, is the treatment of imide with hydrazine in methanol, results phthalhydrazide and DBB-MA through intramolecular substitution. With the column chromatograph, the amino compound purified and eliminated from the side product of phthalhydrazide (Figure 4.1).

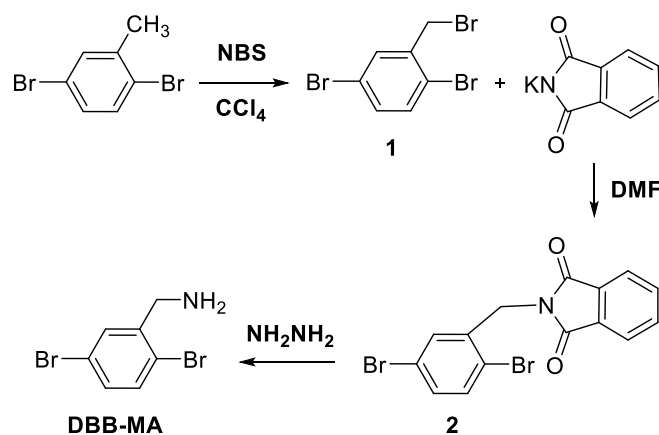


**Figure 4.1** : Synthesis of amino functional monomer, DBB-MA.

DBB-MA was characterized by <sup>1</sup>H-NMR analysis. Singlet peak at 1.59 ppm was assigned to -NH<sub>2</sub> protons. To further confirm the existence of primary amine,

hydrogen–deuterium exchange reaction was performed. Notably, after the deuterium exchange with D<sub>2</sub>O, this peak disappears. The detailed assignment of the all characteristic peaks is presented in Figure 4.2.

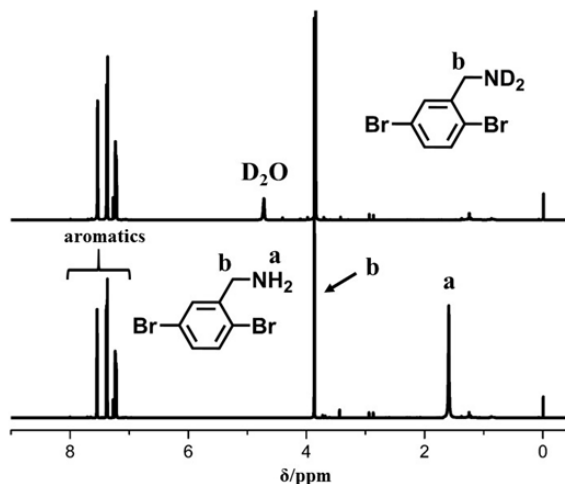


**Figure 4.2 :** <sup>1</sup>H-NMR spectra of DBB-MA before (bottom) and after (top) proton exchange.

The other dibromo benzene component for the subsequent Suzuki coupling, water soluble macromonomer was obtained by mild Steglich method with the favorable catalytic action of 4-dimethylaminopyridine (DMAP) [192].

Esterification reaction between PEG monomethylether and 2,5-dibromobenzoic acid under the standard condition gave the desired product in good yield (Figure 4.3). After the elimination of the excess amount of dicyclohexylcarbodiimide (DCC) and unreacted PEG monomethylether by column chromatography, the macromonomer with  $M_n = 5550 \text{ g mol}^{-1}$  and  $M_w/M_n = 1.24$  was obtained.

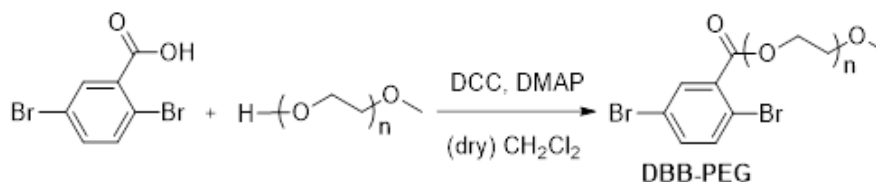


**Figure 4.3 :** Synthesis of water soluble macromonomer, DBB-PEG, via Steglich esterification.

#### 4.1.1 Synthesis of PPP with primary amine groups and PEG side chains

The combination of PEG and amine functional monomer on the PPP backbone was achieved by Suzuki condensation polymerization using 1,4-benzenediboronic acid as the coupling partner in the presence of palladium catalyst (Figure 4.4).

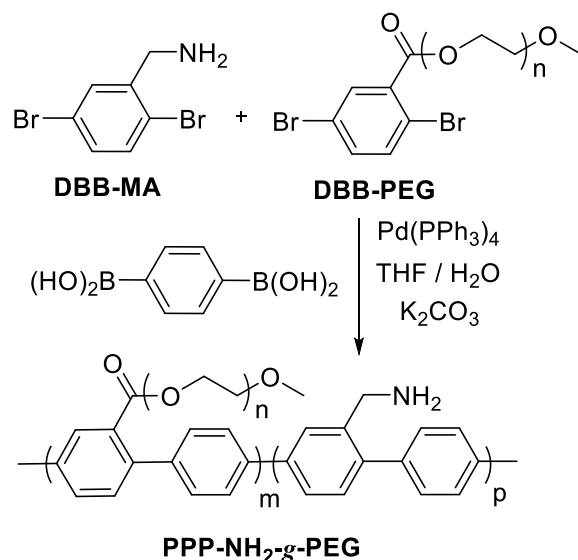


**Figure 4.4 :** Synthesis of PPP-NH<sub>2</sub>-g-PEG via Suzuki condensation polymerization.

Obviously, if desired, the polymer may further be modified by the same reaction through terminal boronic acid or bromobenzene groups [192-193]. Addition of coupling partner makes it possible to arrange the sequence proportion of the components in the conjugated polymer. In our work, we deliberately used the molar ratio of DBB-PEG/DBB-MA as 1/3 to achieve sufficient chain growth since DBB-PEG is relatively less reactive due to the polymeric and hydrophilic nature. Moreover, once adequate hydrophilicity is achieved, the amino functionality is crucial for the subsequent bioconjugation. In the <sup>1</sup>H-NMR spectrum, characteristic benzyl amine protons appear at 1.96 ppm as a broad peak which shifts to 4.71 ppm after D<sub>2</sub>O exchange (Figure 4.5).



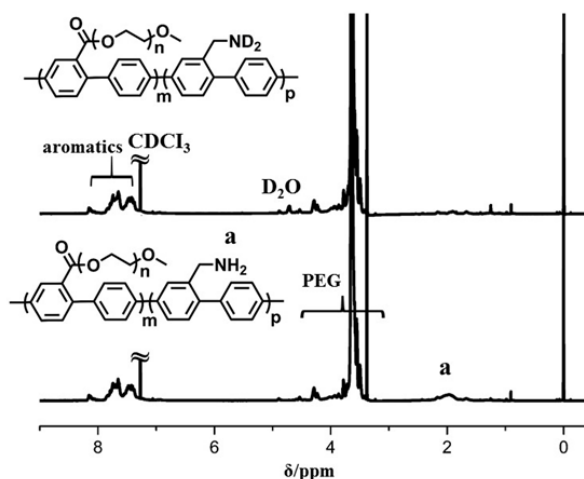


**Figure 4.5 :**  $^1\text{H-NMR}$  spectra of PPP- $\text{NH}_2$ -g-PEG before (bottom) and after (top) proton exchange reaction.

The  $M_n$  and  $M_w/M_n$  values of PPP- $\text{NH}_2$ -g-PEG soluble polymer were found to be  $24500 \text{ g mol}^{-1}$  and 1.41 as determined by gel permeation chromatography (GPC). This value should be taken as the minimum estimation [194-195] since the polymer has hydrophilic side chain and comb-like structure and the GPC system was calibrated with linear polystyrene standards. Figure 4.6 shows the GPC traces of the macromonomer and the final conjugated polymer. The trace of the conjugated polymer consists a weak shoulder at high elution volume pertaining to the unreacted PEG macromonomer. This may arise from the difficulty to achieve exact equimolarity particularly when Suzuki coupling components with different molecular weights are used. Due to the similar solubility properties, the separation of the macromonomer by extraction was not possible. However, the presence of small but some macromonomer in the conjugated polymer would not affect the ultimate use in the bioconjugation process, since PEG is known to be a biocompatible polymer.

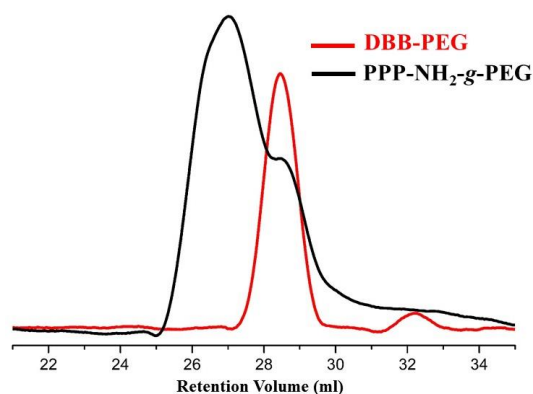


**Figure 4.6 :** GPC traces of PPP-NH<sub>2</sub>-g-PEG and DBB-PEG.

UV-Vis absorption spectra of the components of the coupling polymerization and the final polymer are shown in Figure 4.7. Expected strong absorption band of PPP-NH<sub>2</sub>-g-PEG was due to the presence of supplementary conjugated phenylene rings in the main chain that can be regarded as the further evidence for the formation of PPP backbone.

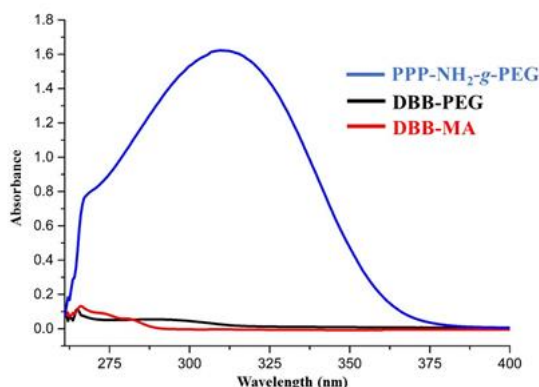


**Figure 4.7.** UV absorption spectra of PPP-NH<sub>2</sub>-g-PEG, DBB-PEG and DBB-MA in DMF, solution (0.1 g/L).

The excitation and fluorescence emission spectra of PPP-NH<sub>2</sub>-g-PEG in DMF and water were recorded (Figure 4.8). As can be seen, while the excitations in both solvents present similar trend, the corresponding emission in water is slightly blue shifted relative to that in DMF. Moreover, the aggregations that are taking place during the nanoparticles formation through self-assembling of PPP backbones in solution create the red shifted shoulders in asymmetric shape [196-197].

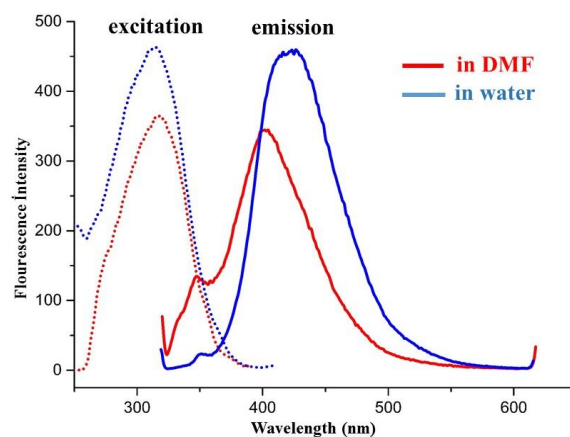


**Figure 4.8.** Fluorescence excitation and emission spectra of PPP-NH<sub>2</sub>-g-PEG in water and DMF (0.3 mg.L<sup>-1</sup>).

Normally, as in the case of most conjugated polymer, PPP derivatives have a rigid structure which causes the insolubility problem in common organic solvents. The grafting of relatively long and flexible side chains to the polymer backbone has been a major approach to deal with this problem. On the other hand, the side chains features may change the optical and electronic properties of PPP backbone [165]. In our approach, the solubility is achieved without considerable negative effect on the fluorescence properties of PPP backbone.

#### 4.1.2 Bioconjugation of the FA to PPP-NH<sub>2</sub>-g-PEG

The polymer and obtained bioconjugate were characterized by various spectroscopic and microscopic investigations. PPP-NH<sub>2</sub>-g-PEG was conjugated with FA via a chemical method outlined in Figure 4.9.

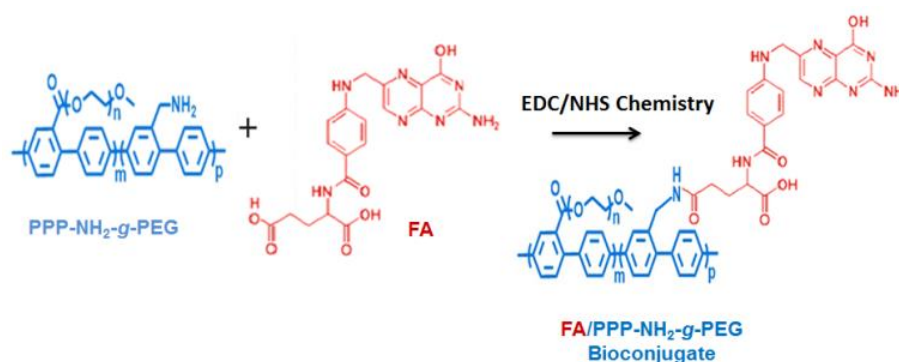


**Figure 4.9 :** Schematic illustration of the bioconjugation.

Fluorescence properties of PPP-NH<sub>2</sub>-g-PEG polymer before and after bioconjugation were evaluated. As can be seen from the fluorescence spectra illustrated in Figure 4.10, PPP-NH<sub>2</sub>-g-PEG has a maximum emission at 410 nm. Upon conjugation, the fluorescence profile of the polymer retained without any major changes. However, conjugation step caused a significant decrease in the fluorescence intensity. However, the remained fluorescence signal is still high enough to use the system for in vitro cell imaging experiments, which cannot be realized by conventional fluorophores.

FTIR analysis was used to confirm the incorporation of the FA in the PPP-NH<sub>2</sub>-g-PEG, which is shown in Figure 4.11. FA is formed from a pteridine ring, *p*-amino benzoic acid and glutamic acid residue. As can be seen from the FTIR analysis of pure FA, the most characteristic peak absorption which was attributed to -COOH and carbonyl groups (C=O) and aromatic C=C structures on both phenyl and pteridine rings was clearly demonstrated itself at the 1684 and 1606 cm<sup>-1</sup>. After the conjugation of FA with PPP-NH<sub>2</sub>-g-PEG (which will be then called as FA/PPP-NH<sub>2</sub>-g-PEG), the absorption peaks at 1684 and 1611 cm<sup>-1</sup> may belong to the C=O stretching which is related to amide-I bond. Furthermore, the absorption band between 3300 and 3600 may have belonged to hydroxyl stretching bands that comes from FA.

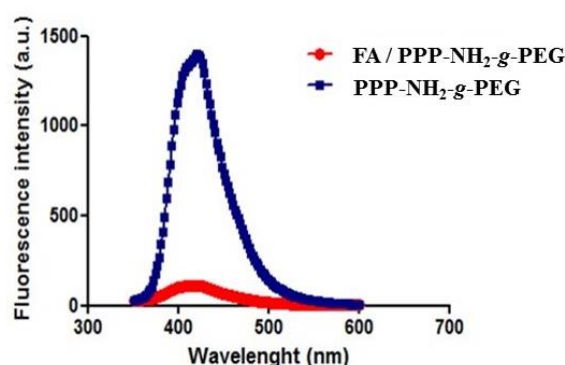


**Figure 4.10 :** Fluorescence spectra of PPP-NH<sub>2</sub>-g-PEG and FA/PPP-NH<sub>2</sub>-g-PEG polymer conjugates.

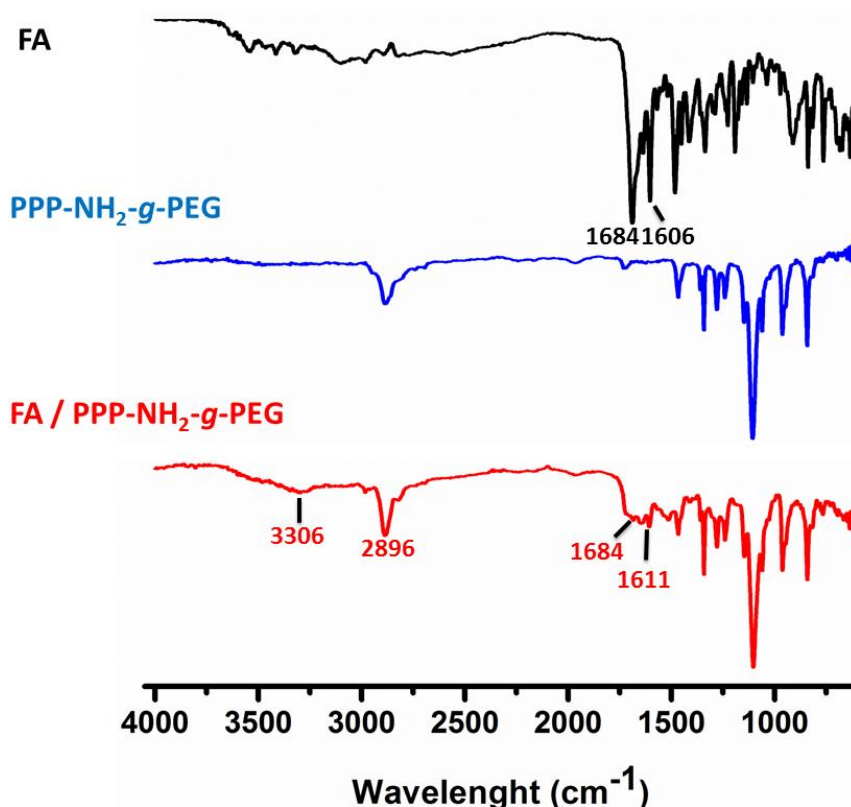


**Figure 4.11** : FT-IR spectrum of FA, PPP-NH<sub>2</sub>-g-PEG and FA/PPP-NH<sub>2</sub>-g-PEG.

### 4.1.3 Cell culture

#### 4.1.3.1 Cytotoxicity assay

Cytotoxic effects of PPP-NH<sub>2</sub>-g-PEG and FA/PPP-NH<sub>2</sub>-g-PEG polymer at different concentrations were examined by MTT assay on A549 and HeLa cells. As demonstrated in the Figure 4.12, the MTT assay results for HeLa and A549 cells, toxicity of the FA/PPP-NH<sub>2</sub>-g-PEG polymer was slightly higher than non-conjugated polymer on HeLa cell lines, while both of them showed similar toxicity on A549 cell lines. The differences between toxicity of FA conjugated and non-conjugated polymer may depend on the cellular uptake of the samples. Recently, the expression levels of FA receptors on the surfaces of both cell lines were investigated by using both genomic and proteomic approaches, PCR and flow cytometry analysis, and were found to be overexpressed on surface of HeLa cells compared to A549 cell lines [198]. It is attributed that the increase in cytotoxicity was caused by enhanced

cellular uptake of FA conjugated polymer in FA receptor positive HeLa cells via receptor-mediated endocytosis.

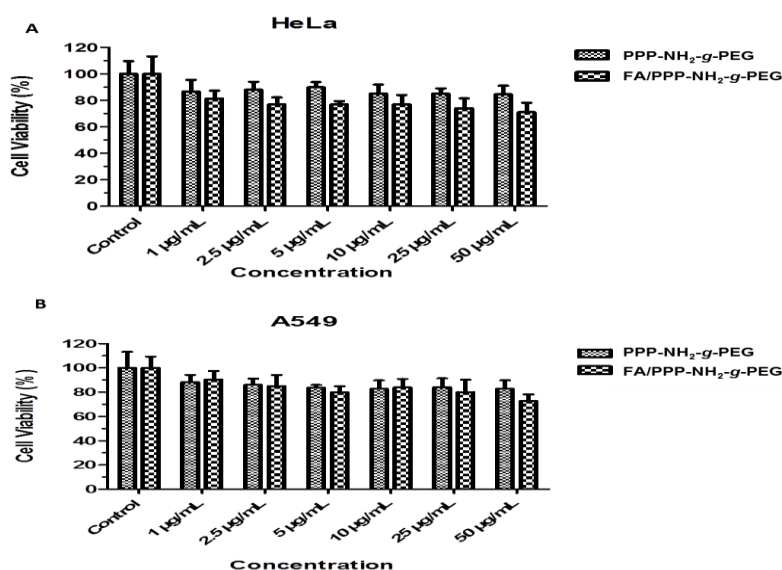


**Figure 4.12 :** The effect of PPP-NH<sub>2</sub>-g-PEG and FA/PPP-NH<sub>2</sub>-g-PEG polymer on cell viability of HeLa cells (A) and A549 cells (B). Values are the mean  $\pm$  standard deviation (n = 6).

#### 4.1.3.2 Fluorescence microscope images

FA receptor positive cells have no pores or channels for the diffusion of the polymeric materials into the cells. In order to achieve more efficient therapy and imaging studies, it is important to use of membrane permeable agents [68]. FA functionalized materials constitute a considerable target for tumor specific delivery of variety of drugs, gene therapy agents, and radiopharmaceuticals for FA receptor rich cell lines such as HeLa [200]. For the investigation of FA/PPP-NH<sub>2</sub>-g-PEG conjugate as a potential targeted cell imaging probe, fluorescence microscope images of the HeLa and A549 cells were taken after incubation of the samples. The fluorescence images of HeLa and A549 cells treated with the FA/PPP-NH<sub>2</sub>-g-PEG polymer and non-conjugated polymer were given in Figure 4.13. According to fluorescence microscope images of cells, the visual fluorescence signal is increased in HeLa cells after being treated with FA/PPP-NH<sub>2</sub>-g-PEG polymer in comparison with non-conjugated polymer. As shown in Figure 4.13-A, functionalization of the PPP-NH<sub>2</sub>-g-PEG polymer with FA increased the cellular uptake in HeLa cells

through FA receptors on cell surfaces while the non-conjugated polymer was not endocytosed (Figure 4.13-B). In contrast to this, for FA receptor poor A549 cells, no differences were observed between the fluorescence signal both of FA conjugated and non-conjugated polymer samples (Figure 4.13A-B). As it can be seen from the fluorescence images, the fluorescent intensity in HeLa cells was obviously higher than A549 cells, depending on the uptake selectivity of FA conjugated polymer. Also, fluorescence intensity of the FA/PPP-NH<sub>2</sub>-g-PEG polymer in FA pre-treated HeLa cells significantly decreased because of the saturation of FA receptors with free FA. Based on these results it can be said that the internalizing of the polymer by the HeLa cells is dependent on endocytosis via FA receptors. Besides, all of this data is coherent with the cytotoxicity assay results.

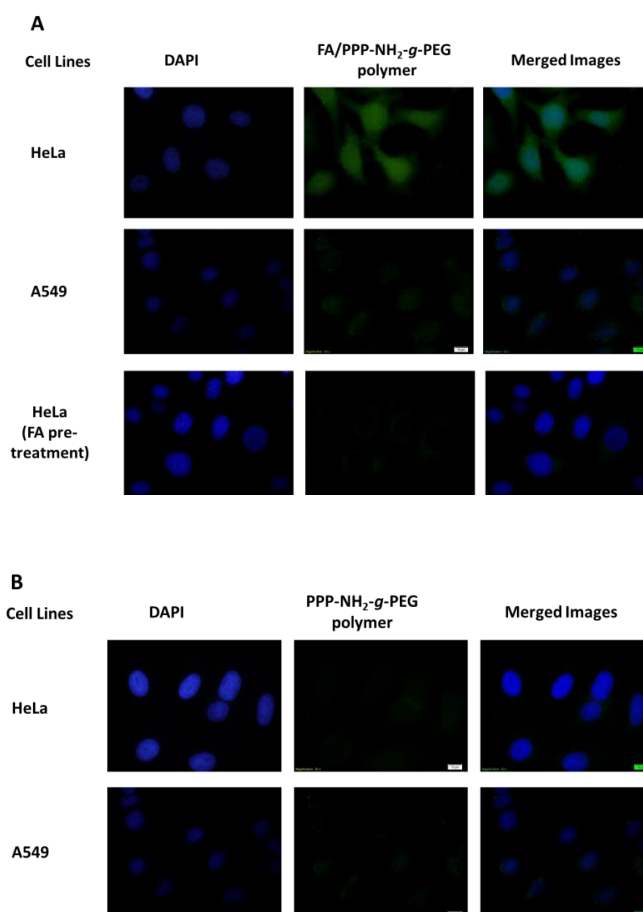


**Figure 4.13 :** Fluorescence microscopy imaging of HeLa and A549 cells. Cells were treated with FA/PPP-NH<sub>2</sub>-g-PEG polymer directly and after being pre-treated with free FA (A). Cells were treated with non-conjugated PPP-NH<sub>2</sub>-g-PEG polymer (B) for 2 h at 37°C, overlap of two images, control nuclei staining with DAPI.

## 4.2 Experimental

### 4.2.1 Materials

Tetrakis(triphenylphosphine)palladium(0) (Pd(PPh<sub>3</sub>)<sub>4</sub>), 2,5-Dibromo-benzoic acid, 1,4-benzene-diboronic acid, *N*-Bromosuccinimide (NBS), 4-(*N,N'*-dimethyl) amino pyridine (DMAP), dicyclohexylcarbodiimide (DCC), poly(ethylene glycol) mono methyl ether (PEG<sub>2000</sub>), Phthalimide potassium salt, hydrazine monohydrate (98%) and Benzoyl peroxide, Folic acid, *N*-(3-dimethylaminopropyl)-*N'*-ethylcarbodiimide hydrochloride, Sigma *N*-Hydroxysuccinimide, 3-(4,5-dimethylthiazol-2-yl)-2,5-diphenyl tetrazolium bromide, sodium dodecyl sulfate, Diamino-2-phenylindol were purchased from Sigma-Aldrich and used without any further purification. All solvents were purified and dried. Water was purified in a Milli-Q plus System (Millipore).

### 4.2.2 Measurements

<sup>1</sup>H-NMR spectra were performed with an Agilent VNMR5 500 MHz, and chemical shifts were recorded in ppm units using tetramethylsilane as an internal standard. UV/vis absorbance measurements were recorded on a Shimadzu UV-1601 spectrometer. Fluorescence measurements were performed with a model LS-50 spectrometer from Perkin Elmer at room temperature. Gel-permeation chromatography (GPC) measurements were carried out in Viscotek GPCmax auto sampler system. Instrument was equipped with a pump (GPCmax, Viscotek Corp., Houston, TX), light-scattering detector ( $\lambda_0 = 670$  nm, Model 270 dual detector, Viscotek Corp.) consisting of two scattering angles: 7° and 90° and the refractive (RI) index detector (VE 3580, Viscotek Corp.). Both detectors were calibrated with PS standards in the narrow molecular weight distribution. Three ViscoGEL GPC columns (G2000HHR, G3000HHR and G4000HHR) employed with THF in the 1.0 mL min<sup>-1</sup> flow rate at 30°C. All data were analyzed using Viscotek OmniSEC Omni-01 software.



#### 4.2.3 Synthesis of 1,4-dibromo-2-(bromomethyl)benzene (1)

2,5-Dibromotoluene (2.55 mL, 18.5 mmol), NBS (6.2 g, 24.8 mmol) and 0.1 g of benzoyl peroxide were added to dry 40 mL of CCl<sub>4</sub> under nitrogen atmosphere. The solution was refluxed with condenser under nitrogen and 200 W light for 4 h. Heating started from 65 °C and temperature was increased by 10 °C per hour and in the last one h temperature was kept at 95°C. After that, the precipitate was filtered and washed with a supplementary amount of CCl<sub>4</sub> and finally with a small quantity of CH<sub>2</sub>Cl<sub>2</sub>. The organic layer was washed with water several times, and then dried over NaSO<sub>4</sub>. The solvent was evaporated in vacuo. Then the remaining crude material was purified by flash column chromatography (SiO<sub>2</sub>, Et<sub>2</sub>O) and recrystallized in petroleum ether to yield (1) (3.04 g, 50%, white crystal). <sup>1</sup>H-NMR (CDCl<sub>3</sub>, 500 MHz): δ 4.54 (s, 2H), 7.30 (dd, J = 8.5, 2.4 Hz, 1H), 7.45 (d, J = 8.5 Hz, 1H), 7.60 (d, J = 2.3 Hz, 1H).

#### 4.2.4 Synthesis of 2-(2,5-dibromobenzyl)isoindoline-1,3-dione (2)

To the solution of 1 (2.9 g, 8.8 mmol) in 10 mL dry DMF, potassium phthalimide (2.45 g, 13.22 mmol) were added. After stirring for 12 h at 160 °C in a schlenck tube under nitrogen atmosphere, the reaction mixture was poured into water. The precipitate was washed with water, purified by flash column chromatography (SiO<sub>2</sub>, CH<sub>2</sub>Cl<sub>2</sub>), precipitated in ethanol and dried under vacuum to yield (2) (2.56 g, 74%, white solid). <sup>1</sup>H-NMR (CDCl<sub>3</sub>, 500 MHz): δ 4.94 (s, 2H), 7.26 (dd, J = 5.7, 2.5 Hz, 1H), 7.28 (d, J = 2.3 Hz, 1H), 7.45 (d, J = 8.3 Hz, 1H), 7.79 (dd, J = 5.5, 3.0 Hz, 2H), 7.92 (dd, J = 5.5, 3.1 Hz, 2H).

#### 4.2.5 Synthesis of (2,5-dibromophenyl)methanamine (DBB-MA)

The solution of 2 (0.381 g, 0.95 mmol) in 25 mL absolute ethanol with 3.0 mL hydrazine were stirred at 90 °C for 5 h. After allowing cooling to room temperature, the mixture was extracted with CH<sub>2</sub>Cl<sub>2</sub> and 10% NaHCO<sub>3</sub>. The organic layer was dried over Na<sub>2</sub>SO<sub>4</sub> and reduced in vacuo. The residue was purified by column chromatography (Al<sub>2</sub>O<sub>3</sub> (neutral), THF) to yield (DBB-MA) (145 mg, 57%, yellow

oil). ). <sup>1</sup>H-NMR (CDCl<sub>3</sub>, 500 MHz): δ 1.59 (br, 2H), 3.87 (s, 2H), 7.23 (dd, J = 8.4, 2.4 Hz, 1H), 7.38 (d, J = 8.4 Hz, 1H), 7.54 (d, J = 2.4 Hz, 1H).

#### 4.2.6 Synthesis of PEG macromonomer (DBB-PEG)

2,5-Dibromo-benzoic acid (4.0 g, 14.3 mmol), DMAP (174.7 mg, 1.43 mmol), Me-PEG<sub>2000</sub>-OH (25.74 g, 12.87 mmol) were dissolved in 80 ml of dry CH<sub>2</sub>Cl<sub>2</sub> under nitrogen atmosphere. To this solution was added DCC (3.246 g, 15.7 mmol) in 20 mL dry CH<sub>2</sub>Cl<sub>2</sub> drop-wise under nitrogen. Then, the reaction mixture was stirred for 5 days at room temperature. After that, the mixture was filtered and washed with 250 mL of CH<sub>2</sub>Cl<sub>2</sub>. The organic phase was quenched with 10% NaHCO<sub>3</sub> and brine, and then dried over Na<sub>2</sub>SO<sub>4</sub>. The solution was concentrated and passed through a silica-gel column using CH<sub>2</sub>Cl<sub>2</sub> as eluent. After removal of solvent in vacuo, the polymer was precipitated in cold diethyl ether to yield 26 g (95%). <sup>1</sup>H-NMR (CDCl<sub>3</sub>, 500 MHz): δ 3.85 – 3.46 (broad), 3.38 (broad), 7.45 (dd, J = 8.5, 2.4 Hz, 1H), 7.52 (d, J = 8.5 Hz, 1H), 7.93 (d, J = 2.4 Hz, 1H).

#### 4.2.7 Synthesis of PPP conjugated polymer (PPP-NH<sub>2</sub>-g-PEG)

The reaction solution was prepared with 30 mL THF and 20 mL of 2.0 M aqueous K<sub>2</sub>CO<sub>3</sub> solution under nitrogen. Prior use, this solution was degassed by bubbling nitrogen over a period of 30 min. In the 10 mL of the reaction solution, DBB-MA (0.8 g, 3.0 mmol), DBB-PEG (2.3 g), benzene-1,4-diboronic acid (0.663 g, 4.0 mmol), Pd(PPh<sub>3</sub>)<sub>4</sub> (0.092 g, 0.08 mmol) was dissolved under nitrogen and stirred at 70°C for 4 days in the Schlenk tube under vacuum. After stirring, the reaction mixture extracted with CH<sub>2</sub>Cl<sub>2</sub> and small amount of water. Organic phase was concentrated and precipitated in excess diethyl ether to yield 1.85 g, white powder. <sup>1</sup>H-NMR (CDCl<sub>3</sub>, 500 MHz): δ 2.06 (broad), 3.38 (broad), 3.45-3.8 (broad), 7.92-8.20 (broad), 7.6-7.9 (broad), 7.2-7.6 (broad).

#### 4.2.8 Bioconjugation of FA to PPP-NH<sub>2</sub>-g-PEG Polymer

FA/PPP-NH<sub>2</sub>-g-PEG polymer conjugates were prepared by conventional EDC/NHS chemistry. FA was conjugated to the polymer through the reaction between amino

group of the polymer and carboxyl group of FA. Briefly, FA (25 µg/mL) dissolved in PBS (pH 7.4) reacted with EDC (0.5 M, in 25 mM, pH 5.5 MES buffer) and NHS (0.125 M, in 25 mM, pH 5.5 MES buffer) for the activation of the carboxyl group of FA. Then, the activated FA was reacted with PPP-NH<sub>2</sub>-g-PEG polymer containing amino group for 4 h at room temperature. Finally, the conjugates were washed with PBS three times by using 10 kDa membrane filter (Sartorius Stedim Biotech).

#### **4.2.9 Characterization of the FA/PPP-NH<sub>2</sub>-g-PEG conjugate**

The structure of polymer can be easily modified with FA due to the presence of functional amino groups in the structure. To verify the successful conjugation of polymer and FA, the fluorescence intensity of polymer was monitored with microplate reader (Thermo Scientific, Varioskan Flash Multimode Reader, USA) step by step. Also, the conjugation was confirmed FTIR analyses. FT-IR spectra were recorded on a PerkinElmer FT-IR Spectrum One spectrometer.

#### **4.2.10 Cell culture**

A549 (human lung cancer) and HeLa (human cervix cancer) cell lines were obtained from ATCC. Cells were cultured on DMEM containing 10% FCS and 1.0% penicillin/streptomycin and were incubated at 37°C in a 5.0% CO<sub>2</sub> and 95% air humidified atmosphere.

#### **4.2.11 Cytotoxicity assay**

Determination of the dose dependent cytotoxicity of the PPP-NH<sub>2</sub>-g-PEG polymer and prepared conjugates was carried out via 3-(4,5-dimethylthiazol-2-yl)-2,5-diphenyl tetrazolium bromide (MTT) assay.<sup>67</sup> Cells were removed from flask to 96-well-tissue plates and were cultivated in the wells until reaching confluence. After completion of cultivation, the medium was removed and the cells were washed with PBS. Following the washing of wells, the cells were treated with the PPP-NH<sub>2</sub>-g-PEG and FA/PPP-NH<sub>2</sub>-g-PEG polymers at 50 µg/mL, 25 µg/mL, 10 µg/mL, 5.0 µg/mL, 1.0 µg/mL concentrations, for 24 h. Then the samples were removed completely by washing with PBS and 10% MTT solution was added to the wells.

Afterwards, cells were incubated with MTT for 4 h and 100  $\mu\text{L}$  SDS (1.0 g SDS in 10 mL 0.01 M HCl) was added per well for dissolving formazan which was occurred inside the cells as a result of MTT treatment. After 24 h of incubation, the optical densities of each well were measured by using a spectrophotometric plate reader (Bio-Tek Instruments, Winooski, VT, USA).

#### **4.2.12 Cell imaging via fluorescence microscopy**

For the purpose of examination of the interactions between the targeted and non-targeted fluorescence probes with both FA receptor negative and positive cell lines, A549 and HeLa cells were imaged via fluorescence microscope (Olympus BX53F) equipped with a CCD camera (Olympus DP72) by utilizing the fluorescence properties of the polymer. In order to obtain cell images, FA conjugated polymer and non-conjugated polymer (10  $\mu\text{g}/\text{mL}$  as the polymer amount) were diluted with medium 1:1 and were added to cells cultivated on a chamber slide for 2 days. The cells were incubated for 2 h at 37°C and were washed twice with PBS. At the end of the incubation time, the cells were stained with DAPI. Additionally, for the saturation of the FA receptors with free FA prior to treatment with FA/PPP-NH<sub>2</sub>-g-PEG, first FA (500  $\mu\text{g}/\text{mL}^{-1}$ ) was diluted with medium 1:1 and added to HeLa cells cultivated on a chamber slide for 2 days. The cells were incubated for 1 h at 37°C and washed twice with PBS. Then, FA/PPP-NH<sub>2</sub>-g-PEG polymer was added to the chamber slide and was incubated with cells for 2 h at 37°C. Afterwards, the cells were washed twice with PBS. In the final step, DAPI was added for the nuclei staining of intact cells. The treated cells were visualized via the fluorescence of the polymer and DAPI by using two filters (green emission; 515-550 nm, blue emission; 435-485 nm) under the fluorescence microscope.

#### **4.3 Conclusion**

The synthesis of PPP structure bearing PEG and amine group with high water solubility and stable fluorescence feature may lead new pathways in the bioconjugation field. The novel targeted fluorescence bio-probe was successfully synthesized and applied to both HeLa and A-549 cells for examination of differences of the cellular affinity between targeted and non-targeted samples. All of our results

demonstrated that the fluorescent property of synthesized PPP-NH<sub>2</sub>-*g*-PEG polymer can be appropriate for effective cell imaging application. In addition to that, the results showed that PPP-NH<sub>2</sub>-*g*-PEG polymer cannot diffuse into the HeLa and A549 cells when it is in non-conjugated form. The characteristic attributes of the polymer has shown to be a great model for the targeting systems. As a final addition, it was demonstrated that the PPP-NH<sub>2</sub>-*g*-PEG polymer is an excellent candidate for the targeting systems when it is appropriately functionalized.



## 5. CONCLUSIONS

In conclusion, we designed and demonstrated a facile and generally applicable technique for the formation of a novel multifunctional conjugated polymers bearing polypeptide, PEG and primary amine groups. Innovative approaches for the syntheses of polymeric structures bearing polypeptides or primary amines have received enormous interest in the fields of biomedicine, drug delivery, biomineralization, nanoscale self-assembly, and tissue engineering. Especially, the elaboration of polypeptides into polymeric structures opens new perspectives in the field of biotechnology as they are fascinating biomaterials mimicking natural proteins.

Polypeptides, possessing wonderful biocompatibility as well as remarkable mechanical and biological durability, are used to create an excellent platform in biosensor fabrication. Furthermore, polypeptides are assumed to exhibit a three-dimensional (3-D) conformation under certain conditions. Therefore, combining synthetic polymers with polypeptide segments becomes a promising approach in the field of enzyme immobilization. The resulting feature reveals compelling selfassembling behavior and new versatile functions are created through the synergistic effect of polymeric structures with polypeptide units. Thus, the novel design and synthesis of polypeptides containing conjugated polymers has attracted great interest.

The synthesis of polypeptide sequences were achieved by NCA-ROP technique based on transformation of  $\alpha$ -amino acids to urethane derivatives which have possibility to obtain polypeptides in the well-designed and desicive control of molecular weight with one spot intra-molecular cyclization reaction in the presence of primary amino functional initiators. We succesfully used the primary amino functional thiophene and phenyl compounds as NCA-ROP initiator to obtain macromonomers having electropolymerization ability and possibility to give Suzuki coupling polymerization.

Primary amino functional dibromobenzene and dibromothiophene possessing suitable functionalities for both polypeptide incorporation and Suzuki coupling processes was synthesized via Gabriel reaction. The substitution reaction with these alkyl halides derivatives and the conjugate base of phthalimide gave the corresponding *N*-alkyl phthalimide, The efficiency of the reaction was increased by using preformed potassium salt of phthalimide, instead of phthalimide, facilitating the reaction to be conducted in a polar protic solvent such as DMF under homogenous conditions. Treatment of the imide derivatives, with hydrazine in methanol results in the formation of phthalhydrazide and these primary amine initiators.

First part of this thesis discusses overall background information about the conjugated polymers and their recent novel applications, about the polypeptide preparation methods based on the ring-opening polymerization of the corresponding  $\alpha$ -amino acids of *N*-carboxyanhydrides (NCAs).

Second part of this thesis describes a simple and efficient approach for the electrochemical deposition of polypeptides as bio-based covering materials for surface design is described. The method involves *N*-carboxyanhydride (NCA) ring-opening polymerization from its precursor to form a thiophene-functionalized polypeptide macromonomer (T-Pala), followed by electropolymerization.

Third part of this thesis gives a detailed account of a novel approach for fabrication of multifunctional conjugated polymers, namely poly(*p*-phenylene)s (PPPs) possessing polypeptide (poly-L-lysine, PLL) and hydrophilic poly(ethylene glycol) (PEG) side chains. The approach is comprised of the combination of Suzuki coupling and *in situ* *N*-carboxyanhydride (NCA) ring-opening polymerization (ROP) processes.

Fourth part of this thesis involves an approach for bioconjugation associated with fluorescent conjugated polymer. A conjugated polymer, poly(*p*-phenylene) (PPP), with lateral substituents, namely primary amino groups and poly(ethylene glycol) (PEG) chains, as potential building block for polymer bioconjugates was synthesized and characterized.



## REFERENCES

- [1] **Y. Dai, M. Xu, J. Wei, H. Zhang & Y. Chen.** (2012). Surface modification of hydroxyapatite nanoparticles by poly(L-phenylalanine) via ROP of L-phenylalanine N-carboxyanhydride (Pha-NCA). *Applied Surface Science*, 258 (7), 2850-2855.
- [2] **Barbosa, M. E. M., Montembault, V., Cammas-Marion, S., Ponchel, G. & Fontaine, L.** (2007). Synthesis and characterization of novel poly( $\gamma$ -benzyl-L-glutamate) derivatives tailored for the preparation of nanoparticles of pharmaceutical interest. *Polymer International*, 56 (3), 317-324.
- [3] **Ling, J. Peng, H. & Shen, Z.** (2012). Deprotonation reaction of  $\alpha$ -amino acid N-carboxyanhydride at 4-CH position by yttrium tris(trimethylsilyl)amide. *Journal of Polymer Science Part a-Polymer Chemistry*, 50 (18), 3743-3749.
- [4] **Habraken, G. J. M., Peeters, M., Dietz, C. H. J. T., Koning, C. E. & Heise, A.** (2010). How controlled and versatile is N-carboxy anhydride (NCA) polymerization at 0 degrees C? Effect of temperature on homo-, block- and graft (co)polymerization. *Polymer Chemistry*, 1 (4), 514-524.
- [5] **Obeid, R. & Scholz, C.** (2011). Synthesis and Self-Assembly of Well-Defined Poly(amino acid) End-Capped Poly(ethylene glycol) and Poly(2-methyl-2-oxazoline). *Biomacromolecules*, 12 (10), 3797-3804.
- [6] **Ishikawa, K., & Endo, T.** (1988). Synthesis and polymerization of  $\gamma$ -trichloroethyl-L-glutamate N-carboxyanhydride: a polypeptide that can be functionalized with a nucleophilic agent. *Journal of the American Chemical Society*, 110 (6), 2016-2017.
- [7] **Koga, K., Sudo, A., Nishida, H. & Endo, T.** (2009) Convenient and Useful Synthesis of N-Carboxyanhydride Monomers through Selective Cyclization of Urethane Derivatives of  $\alpha$ -Amino Acids. *Journal of Polymer Science Part a-Polymer Chemistry*, 47 (15), 3839-3844.
- [8] **Robinson, J. W. & Schlaad, H.** (2012). A versatile polypeptoid platform based on N-allyl glycine. *Chemical Communications*, 48 (63), 7835-7837. **Sun, J. & Schlaad, H.** (2010). Thiol-Ene Clickable Polypeptides. *Macromolecules*, 43 (10), 4445-4448. **Krannig, K.-S. & Schlaad, H.** (2012). pH-Responsive Bioactive

Glycopolypeptides with Enhanced Helicity and Solubility in Aqueous Solution. *Journal of the American Chemical Society*, 134 (45), 18542-18545. **Aliferis, T., Iatrou, H. & Hadjichristidis, N.** (2004). Living Polypeptides. *Biomacromolecules*, 5 (5), 1653-1656. **Iatrou, H., Frielinghaus, H.; Hanski, S., Ferderigos, N., Ruokolainen, J., Ikkala, O., Richter, D., Mays, J. & Hadjichristidis, N.** (2007). Architecturally Induced Multiresponsive Vesicles from Well-Defined Polypeptides. Formation of Gene Vehicles. *Biomacromolecules*, 8 (7), 2173-2181. **Hadjichristidis, N., Iatrou, H., Pitsikalis, M. & Sakellariou, G.** (2009). Synthesis of Well-Defined Polypeptide-Based Materials via the Ring-Opening Polymerization of  $\alpha$ -Amino Acid N-Carboxyanhydrides. *Chemical Reviews*, 109 (11), 5528-5578.

- [9] **S. Yamada, K. Koga & T. Endo**, (2012). *J. Polym. Sci., Part A-1: Polym. Chem.*, 50, 2527.
- [10] **Fujita, Y., Koga, K., Kim, H.-K., Wang, X.-S., Sudo, A., Nishida, H. & Endo, T.** (2007). Phosgene-free synthesis of N-carboxyanhydrides of  $\alpha$ -amino acids based on bisarylcyanates as starting compounds. *Journal of Polymer Science Part A-Polymer Chemistry*, 45 (22), 5365-5369.
- [11] **Leuchs, H.** (1906). Ueber die Glycin-carbonsäure. *Berichte der deutschen chemischen Gesellschaft*, 39 (1), 857-861.
- [12] **Curtius, T., Hochschwender, K., Meier, H.; Lehmann, W., Benckiser, A., Schenck, M., Wirbatz, W., Gaier, J. & Mühlhäusser, W.** (1930). Umwandlung von alkylierten Malonsäuren in  $\alpha$ -Aminosäuren. *Journal für Praktische Chemie*, 125 (1), 211-302.
- [13] **Coleman, D. & Farthing, A. C.** (1950). 628. Synthetic polypeptides. Part II. Properties of oxazolidin-2 : 5-diones and an initial study of the preparation of polypeptides there-from. *Journal of the Chemical Society (Resumed)*, 0 (0), 3218-3222.
- [14] **Wilder, R. & Mobashery, S.** (1992). The use of triphosgene in preparation of N-carboxy  $\alpha$ -amino acid anhydrides. *The Journal of Organic Chemistry* 57 (9), 2755-2756.
- [15] **Katakai, R. & Iizuka, Y.** (1985). An improved rapid method for the synthesis of N-carboxy  $\alpha$ -amino acid anhydrides using trichloromethyl chloroformate. *The Journal of Organic Chemistry*, 50 (5), 715-716.
- [16] **Collet, H., Bied, C., Mion, L., Taillades, J. & Commeyras, A.** (1996). A new simple and quantitative synthesis of  $\alpha$ -amino acid-N-carboxyanhydrides (oxazolidin-2,5-dione). *Tetrahedron Letters*, 37 (50), 9043-9046.

- [17] **Kamei, Y., Sudo, A., Nishida, H., Kikukawa, K. & Endo, T.** (2008). Synthesis of polypeptides from activated urethane derivatives of  $\alpha$ -amino acids. *Journal of Polymer Science Part A: Polymer Chemistry*, 46 (7), 2525-2535.
- [18] **Kamei, Y., Nagai, A., Sudo, A., Nishida, H., Kikukawa, K. & Endo, T.** (2008). Convenient synthesis of poly( $\gamma$ -benzyl-L-glutamate) from activated urethane derivatives of  $\gamma$ -benzyl-L-glutamate. *Journal of Polymer Science Part A: Polymer Chemistry*, 46 (8), 2649-2657.
- [19] **Kamei, Y., Sudo, A., Nishida, H., Kikukawa, K. & Endo, T.** (2008). Synthesis of Polypeptide-Polyether Conjugates from an Activated Urethane Derivative of  $\gamma$ -Benzyl-L-glutamate as a Monomer. *Polym. Bull.*, 60 (5), 625-634.
- [20] **Koga, K., Sudo, A. & Endo, T.** (2010). Revolutionary phosgene-free synthesis of  $\alpha$ -amino acid N-carboxyanhydrides using diphenyl carbonate based on activation of  $\alpha$ -amino acids by converting into imidazolium salts. *Journal of Polymer Science Part A: Polymer Chemistry*, 48 (19), 4351-4355.
- [21] **Guenes, S., Neugebauer, H. & Sariciftci, N. S.** (2007). Conjugated polymer-based organic solar cells. *Chemical Reviews*, 107 (4), 1324-1338. **Kraft, A., Grimsdale, A. C. & Holmes, A. B.** (1998). Electroluminescent conjugated polymers - Seeing polymers in a new light. *Angewandte Chemie-International Edition*, 37 (4), 402-428. **McQuade, D. T., Pullen, A. E. & Swager, T. M.** (2000). Conjugated Polymer-Based Chemical Sensors. *Chemical Reviews*, 100 (7), 2537-2574.
- [22] **Coakley, K. M. & McGehee, M. D.** (2004). Conjugated Polymer Photovoltaic Cells. *Chemistry of Materials*, 16 (23), 4533-4542. **Roncali, J.** (1992). Conjugated poly(thiophenes): synthesis, functionalization, and applications. *Chemical Reviews*, 92 (4), 711-738. **Tour, J. M.** (1996). Conjugated Macromolecules of Precise Length and Constitution. Organic Synthesis for the Construction of Nanoarchitectures. *Chemical Reviews*, 96 (1), 537-554.
- [23] **De Paoli, M.-A., Waltman, R. J., Diaz, A. F. & Bargon, J.** (1985). An electrically conductive plastic composite derived from polypyrrole and poly(vinyl chloride). *Journal of Polymer Science: Polymer Chemistry Edition*, 23 (6), 1687-1698.
- [24] **Leclerc, M. & Faid, K.** (1997). Electrical and optical properties of processable polythiophene derivatives: Structure-property relationships. *Advanced Materials*, 9 (14), 1087-1094.
- [25] **McCullough, R. D.** (1998). The Chemistry of Conducting Polythiophenes. *Advanced Materials*, 10 (2), 93-116.

- [26] **Wang, H. L., Toppare, L. & Fernandez, J. E.** (1990). Conducting polymer blends: polythiophene and polypyrrole blends with polystyrene and poly(bisphenol A carbonate). *Macromolecules*, 23 (4), 1053-1059.
- [27] **Alkan, S., Toppare, L., Hepuzer, Y. & Yagci, Y.** (1999). Block copolymers of thiophene-capped poly(methyl methacrylate) with pyrrole. *Journal of Polymer Science Part A: Polymer Chemistry*, 37 (22), 4218-4225.
- [28] **Çirpan, A., Alkan, S., Toppare, L., Cianga, I. & Yagci, Y.** (2002). Synthesis and characterization of conducting copolymers of thiophene-3-yl acetic acid cholesteryl ester with pyrrole. *Journal of Materials Science*, 37 (9), 1767-1775.
- [29] **Stenger-Smith, J. D.** (1998). Intrinsically electrically conducting polymers. Synthesis, characterization, and their applications. *Progress in Polymer Science*, 23 (1), 57-79.
- [30] **Yildiz, H. B., Kiralp, S., Toppare, L., Yagci, Y. & Ito, K.** (2006). Synthesis of conducting copolymers of thiophene capped poly(ethylene oxide) with pyrrole and thiophene. *Materials Chemistry and Physics*, 100 (1), 124-127.
- [31] **Sahin, E., Camurlu, P., Toppare, L., Mercore, V. M., Cianga, I. & Yagci, Y.** (2005). Synthesis and characterization of thiophene functionalized polystyrene copolymers and their electrochemical properties. *Polymer International*, 54 (12), 1599-1605.
- [32] **Sahin, E., Camurlu, P., Toppare, L., Mercore, V. M., Cianga, I. & Yagci, Y.** (2005). Conducting copolymers of thiophene functionalized polystyrenes with thiophene. *Journal of Electroanalytical Chemistry*, 579 (2), 189-197.
- [33] **Ünür, E., Toppare, L., Yagci, Y. & Yilmaz, F.** (2005). Synthesis and characterization of thiophene-capped polytetrahydrofuran conducting copolymers. *Materials Chemistry and Physics*, 91 (2-3), 261-268.
- [34] **Kengne-Momo, R. P., Lagarde, F., Daniel, P., Pilard, J. F., Durand, M. J. & Thouand, G.** (2012). Polythiophene Synthesis Coupled to Quartz Crystal Microbalance and Raman Spectroscopy for Detecting Bacteria. *Biointerphases*, 7 (1-4).
- [35] **Lin, M., Cho, M. S., Choe, W. S. & Lee, Y.** (2009). Electrochemical analysis of copper ion using a Gly-Gly-His tripeptide modified poly(3-thiopheneacetic acid) biosensor. *Biosensors and Bioelectronics*, 25 (1), 28-33.

- [36] **Bhattacharyya, D. & Gleason, K. K.** (2011). Single-Step Oxidative Chemical Vapor Deposition of –COOH Functional Conducting Copolymer and Immobilization of Biomolecule for Sensor Application. *Chemistry of Materials*, 23 (10), 2600-2605.
- [37] **Wen, Y., Li, D., Xu, J., Wang, X. & He, H.** (2013). Electrosynthesis of Poly(thiophene-3-acetic Acid) Film in Ionic Liquids for Covalent Immobilization of Biologically Active Species. *International Journal of Polymeric Materials and Polymeric Biomaterials*, 62 (8), 437-443.
- [38] **Velayudham, S., Lee, C. H., Xie, M., Blair, D., Bauman, N., Yap, Y. K., Green, S. A. & Liu, H.** (2010). Noncovalent Functionalization of Boron Nitride Nanotubes with Poly(p-phenylene-ethynylene)s and Polythiophene. *ACS Applied Materials & Interfaces*, 2 (1), 104-110.
- [39] **A. Sassolas, L. J. Blum & B. D. Leca-Bouvier.** (2012). Immobilization strategies to develop enzymatic biosensors. *Biotechnol. Adv.*, 30, 489.
- [40] **Q. Gao, Y. Guo, J. Liu, X. Yuan, H. Qi & C. Zhang.** (2011). A biosensor prepared by co-entrapment of a glucose oxidase and a carbon nanotube within an electrochemically deposited redox polymer multilayer. *Bioelectrochemistry*, 81, 109.
- [41] **M. Tsai & Y. Tsai.** (2009). Adsorption of glucose oxidase at platinum-multiwalled carbon nanotube-alumina-coated silica nanocomposite for amperometric glucose biosensor. *Sens. Actuators, B*, 141, 592.
- [42] **B. Demir, M. Seleci, D. Ag, S. Cevik, E. E. Yalcinkaya, D. O. Demirkol, U. Anik & S. Timur.** (2013). Amine intercalated clay surfaces for microbial cell immobilization and biosensing applications. *RSC Adv.*, 3, 7513.
- [43] **C. Hea, J. Liua, Q. Zhanga & C. Wu.** (2012). A novel stable amperometric glucose biosensor based on the adsorption of glucose oxidase on poly(methyl methacrylate)–bovine serum albumin core–shell nanoparticles. *Sens. Actuators, B*, 166, 802.
- [44] **A. Eftekhari.** (2004). Electropolymerization of aniline onto passivated substrate and its application for preparation of enzyme-modified electrode. *Synth. Met.*, 2004, 145, 211.
- [45] **R. Antiochia & L. Gorton.** (2007). Development of a carbon nanotube paste electrode osmium polymer-mediated biosensor for determination of glucose in alcoholic beverages. *Biosens. Bioelectron.*, 22, 2611.

- [46] **T. Kong, Y. Chen, Y. Ye, K. Zhang, Z. Wang & X. Wang.** (2009). An amperometric glucose biosensor based on the immobilization of glucose oxidase on the ZnO nanotubes *Sens. Actuators, B*, 138, 344.
- [47] **L. Su, X. Qiu, L. Guo, F. Zhang & C. Tung.** (2004). Amperometric glucose sensor based on enzyme-modified boron-doped diamond electrode by cross-linking method. *Sens. Actuators, B*, 99, 499.
- [48] **J. Zhang, C. Wang, S. Chen, D. Yuan & X. Zhong.** (2013). Amperometric glucose biosensor based on glucose oxidase–lectin biospecific interaction. *Enzyme Microb. Technol.*, 52, 134.
- [49] **S. Cosnier, C. Gondran, A. Pellec & A. Senillou.** (2001). Controlled Fabrication of Glucose And Catechol Microbiosensors Via Electropolymerized Biotinylated Polypyrrole Films. *Anal. Lett.*, 2001, 34(1), 61.
- [50] **S. Demirci Uzun, N. Akbasoglu Unlu, M. Sendur, F. Ekiz Kanik, S. Timur & L. Toppare.** (2013). A novel promising biomolecule immobilization matrix: synthesis of functional benzimidazole containing conducting polymer and its biosensor applications. *Colloids Surf., B*, 112, 74.
- [51] **M. Kesik, F. Ekiz Kanik, G. Hızalan, D. Kozanoglu, E. Nalbant Esenturk, S. Timur & L. Toppare.** (2013). A functional immobilization matrix based on a conducting polymer and functionalized gold nanoparticles: Synthesis and its application as an amperometric glucose biosensor. *Polymer*, 54, 4463.
- [52] **C. L. Clark, M. R. Jacobs & P. C. Appelbaum, J. Clin.** (1998). Antipneumococcal Activities of Levofloxacin and Clarithromycin as Determined by Agar Dilution, Microdilution, E-Test, and Disk Diffusion Methodologies *Microbiol.*, 36, 3579.
- [53] **S. E Walsh, J. Y. Maillard, A. D Russell, C. E Catrenich, D. L Charbonneau & R. G. Bartolo.** (2003). Activity and mechanisms of action of selected biocidal agents on Gram-positive and -negative bacteria. *J. Appl. Microbiol.*, 94, 240.
- [54] **Lee, K., Povlich, L. K. & Kim, J.** (2007). Label-free and self-signal amplifying molecular DNA sensors based on bioconjugated polyelectrolytes. *Adv. Funct. Mater.* 17, 2580-2587.
- [55] **Ma, M., Guo, L., Anderson, D. G. & Langer, R.** (2013). Bio-Inspired Polymer Composite Actuator and Generator Driven by Water Gradients. *Science* 339, 186-189.
- [56] **Sirringhaus, H., Tessler, N. & Friend, R. H.** (1998). Integrated Optoelectronic Devices Based on Conjugated Polymers. *Science* 280, 1741-1744.

- [57] **Scott, J. C.** (1997). Conducting Polymers: From Novel Science to New Technology. *Science* 278, 2071-2072.
- [58] **Jager, E. W. H., Smela, E. & Inganäs, O.** (2000). Microfabricating Conjugated Polymer Actuators. *Science* 290, 1540-1545.
- [59] **Yu, J., Hu, D. & Barbara, P. F.** (2000). Unmasking Electronic Energy Transfer of Conjugated Polymers by Suppression of O<sub>2</sub> Quenching. *Science* 289, 1327-1330.
- [60] **Gross, M. et al.** (2000). Improving the performance of doped [pi]-conjugated polymers for use in organic light-emitting diodes. *Nature* 405, 661-665.
- [61] **Burroughes, J. H. et al.** (1990). Light-emitting diodes based on conjugated polymers. *Nature* 347, 539-541.
- [62] **Friend, R. H. et al.** (1999). Electroluminescence in conjugated polymers. *Nature* 397, 121-128.
- [63] **Kohler, A. et al.** (1998). Charge separation in localized and delocalized electronic states in polymeric semiconductors. *Nature* 392, 903-906.
- [64] **Lafferentz, L. et al.** (2009). Conductance of a Single Conjugated Polymer as a Continuous Function of Its Length. *Science* 323, 1193-1197.
- [65] **Thomas, S. W. & Swager, T. M.** (2005). Synthesis and Optical Properties of Simple Amine-Containing Conjugated Polymers. *Macromolecules* 38, 2716-2721.
- [66] **Ho Choi, S., Kim, B. & Frisbie, C. D.** (2008). Electrical Resistance of Long Conjugated Molecular Wires. *Science* 320, 1482-1486.
- [67] **Bakulin, A. A. et al.** (2012). The Role of Driving Energy and Delocalized States for Charge Separation in Organic Semiconductors. *Science* 335, 1340-1344.
- [68] **Jenekhe, S. A.** (1986). A class of narrow-band-gap semiconducting polymers. *Nature* 322, 345-347.
- [69] **Tessler, N., Denton, G. J. & Friend, R. H.** (1996). Lasing from conjugated-polymer microcavities. *Nature* 382, 695-697.
- [70] **Burn, P. L. et al.** (1992). Chemical tuning of electroluminescent copolymers to improve emission efficiencies and allow patterning. *Nature* 356, 47-49.

- [71] **Musa, I., Munindrasdasa, D. A. I., Amaratunga, G. A. J. & Eccleston, W.** (1998). Ultra-low-threshold field emission from conjugated polymers. *Nature* 395, 362-365.
- [72] **Cao, Y., Parker, I. D., Yu, G., Zhang, C. & Heeger, A. J.** (1999). Improved quantum efficiency for electroluminescence in semiconducting polymers. *Nature* 397, 414-417.
- [73] **Wohlgemant, M., Tandon, K., Mazumdar, S., Ramasesha, S. & Vardeny, Z. V.** (2001). Formation cross-sections of singlet and triplet excitons in [pi]-conjugated polymers. *Nature* 409, 494-497.
- [74] **Schon, J. H. et al.** (2001). Gate-induced superconductivity in a solution-processed organic polymer film. *Nature* 410, 189-192.
- [75] **Stucky, G. D.** (2001). Materials science: Polymers all in a row. *Nature* 410, 885-886.
- [76] **Perepichka, D. F. & Rosei, F.** (2009). Extending Polymer Conjugation into the Second Dimension. *Science* 323, 216-217.
- [77] **Bolinger, J. C., Traub, M. C., Adachi, T. & Barbara, P. F.** (2011). Ultralong-Range Polaron-Induced Quenching of Excitons in Isolated Conjugated Polymers. *Science* 331, 565-567.
- [78] **Bardeen, C.** (2011). Exciton Quenching and Migration in Single Conjugated Polymers. *Science* 331, 544-545.
- [79] **Kim, J. & Swager, T. M.** (2001). Control of conformational and interpolymer effects in conjugated polymers. *Nature* 411, 1030-1034.
- [80] **Turro, N. J., Ramamurthy, V. & Scaiano, J. C.** (2012). Modern Molecular Photochemistry of Organic Molecules. *Photochem. Photobiol.* 88, 1033-1033.
- [81] **Hong, J. W., Hemme, W. L., Keller, G. E., Rinke, M. T. & Bazan, G. C.** (2006). Conjugated-Polymer/DNA Interpolyelectrolyte Complexes for Accurate DNA Concentration Determination. *Adv. Mater.* 18, 878-882.
- [82] **Wosnick, J. H. & Swager, T. M.** (2000). Molecular photonic and electronic circuitry for ultra-sensitive chemical sensors. *Curr. Opin. Chem. Biol.* 4, 715-720.
- [83] **Akbulut, H. et al.** (2014). Electrochemical deposition of polypeptides: bio-based covering materials for surface design. *Polymer Chemistry* 5, 3929-3936.



- [84] **Colak, D. G. et al.** (2012). The synthesis and targeting of PPP-type copolymers to breast cancer cells: Multifunctional platforms for imaging and diagnosis. *Journal of Materials Chemistry* 22, 9293-9300.
- [85] **François, B., Widawski, G., Rawiso, M. & Cesar, B.** (1995). Block-copolymers with conjugated segments: Synthesis and structural characterization. *Synthetic Metals* 69, 463-466.
- [86] **Chemli, M., Haj Said, A., Fave, J.-L., Barthou, C. & Majdoub, M.** (2012). Synthesis and chemical modification of new luminescent substituted poly(p-phenylene) polymers. *J. Appl. Polym. Sci.* 125, 3913-3919.
- [87] **Ullrich, S. & Klaus, M.** (1997). in *Photonic and Optoelectronic Polymers Vol. 672 ACS Symposium Series* Ch. 24, 358-380 (American Chemical Society).
- [88] **Lauter, U., Meyer, W. H. & Wegner, G.** (1997). Molecular composites from rigid-rod poly(p-phenylene)s with oligo(oxyethylene) side chains as novel polymer electrolytes. *Macromolecules* 30, 2092-2101.
- [89] **Tour, J. M. & Lamba, J. J. S.** (1993). Synthesis of planar poly(p-phenylene) derivatives for maximization of extended .pi.-conjugation. *J. Am. Chem. Soc.* 115, 4935-4936.
- [90] **Sim, I. S., Kim, J. W., Choi, H. J., Kim, C. A. & Jhon, M. S.** (2001). Preparation and Electrorheological Characteristics of Poly(p-phenylene)-Based Suspensions. *Chem. Mater.* 13, 1243-1247.
- [91] **Cianga, I. & Yagci, Y.** (2004). New polyphenylene-based macromolecular architectures by using well defined macromonomers synthesized via controlled polymerization methods. *Prog. Polym. Sci.* 29, 387-399.
- [92] **Kesik, M. et al.** (2014). Synthesis and characterization of conducting polymers containing polypeptide and ferrocene side chains as ethanol biosensors. *Polym. Chem.* 5, 6295-6306.
- [93] **Duncan, R.** (2003). The dawning era of polymer therapeutics. *Nat Rev Drug Discov* 2, 347-360.
- [94] **Merdan, T., Kopeček, J. & Kissel, T.** (2002). Prospects for cationic polymers in gene and oligonucleotide therapy against cancer. *Adv. Drug. Deliv. Rev.* 54, 715-758.
- [95] **Luo, D. & Saltzman, W. M.** (2000). Synthetic DNA delivery systems. *Nat Biotech* 18, 33-37.
- [96] **Holmes, T. C.** (2002). Novel peptide-based biomaterial scaffolds for tissue engineering. *Trends in Biotechnology* 20, 16-21.

- [97] **Bertin, A., Hermes, F. & Schlaad, H.** (2010). in Polymer Membranes/Biomembranes Vol. 224 *Advances in Polymer Science* (eds W. P. Meier & W. Knoll) 167-195.
- [98] **Dai, Y., Xu, M., Wei, J., Zhang, H. & Chen, Y.** (2012). Surface modification of hydroxyapatite nanoparticles by poly(L-phenylalanine) via ROP of L-phenylalanine N-carboxyanhydride (Pha-NCA). *Appl. Surf. Sci.* 258, 2850-2855.
- [99] **Habraken, G. J. M., Peeters, M., Dietz, C. H. J. T., Koning, C. E. & Heise, A.** (2010). How controlled and versatile is N-carboxy anhydride (NCA) polymerization at 0 degrees C? Effect of temperature on homo-, block- and graft (co)polymerization. *Polym. Chem.* 1, 514-524.
- [100] **Barbosa, M. E. M., Montembault, V., Cammas-Marion, S., Ponchel, G. & Fontaine, L.** (2007). Synthesis and characterization of novel poly(gamma-benzyl-L-glutamate) derivatives tailored for the preparation of nanoparticles of pharmaceutical interest. *Polym. Int.* 56, 317-324.
- [101] **Pickel, D. L., Politakos, N., Avgeropoulos, A. & Messman, J. M.** (2009). A Mechanistic Study of alpha-(Amino acid)-N-carboxyanhydride Polymerization: Comparing Initiation and Termination Events in High-Vacuum and Traditional Polymerization Techniques. *Macromolecules* 42, 7781-7788.
- [102] **Koga, K., Sudo, A., Nishida, H. & Endo, T.** (2009). Convenient and Useful Synthesis of N-Carboxyanhydride Monomers through Selective Cyclization of Urethane Derivatives of alpha-Amino Acids. *J. Polym. Sci., Part A: Polym. Chem.* 47, 3839-3844.
- [103] **Guo, A.-r., Yang, W.-x., Yang, F., Yu, R. & Wu, Y.-x.** (2014). Well-Defined Poly(gamma-benzyl-L-glutamate)-g-Polytetrahydrofuran: Synthesis, Characterization, and Properties. *Macromolecules* 47, 5450-5461.
- [104] **Yamada, S., Koga, K. & Endo, T.** (2012). Useful Synthetic Method of Polypeptides with Well-Defined Structure by Polymerization of Activated Urethane Derivatives of alpha-Amino Acids. *Journal of Polymer Science Part a-Polymer Chemistry* 50, 2527-2532.
- [105] **Koga, K., Sudo, A. & Endo, T.** (2010). Revolutionary Phosgene-Free Synthesis of alpha-Amino Acid N-Carboxyanhydrides Using Diphenyl Carbonate Based on Activation of alpha-Amino Acids by Converting into Imidazolium Salts. *J. Polym. Sci., Part A: Polym. Chem.* 48, 4351-4355.

- [106] **Fujita, Y. et al.** (2007). Phosgene-free synthesis of N-carboxyanhydrides of alpha-amino acids based on bisarylcyanates as starting compounds. *J. Polym. Sci., Part A: Polym. Chem.* 45, 5365-5369.
- [107] **Hadjichristidis, N., Iatrou, H., Pitsikalis, M. & Sakellariou, G.** (2009). Synthesis of Well-Defined Polypeptide-Based Materials via the Ring-Opening Polymerization of alpha-Amino Acid N-Carboxyanhydrides. *Chem. Rev.* 109, 5528-5578.
- [108] **Aliferis, T., Iatrou, H. & Hadjichristidis, N.** (2004). Living polypeptides. *Biomacromolecules* 5, 1653-1656.
- [109] **Krannig, K.-S., Doriti, A. & Schlaad, H.** (2014). Facilitated Synthesis of Heterofunctional Glycopolypeptides. *Macromolecules* 47, 2536-2539.
- [110] **Robinson, J. W. & Schlaad, H.** (2012). A versatile polypeptoid platform based on N-allyl glycine. *Chemical Communications* 48, 7835-7837.
- [111] **Toy, P. H. & Tanda, K. D.** (2000). Soluble polymer-supported organic synthesis. *Accounts of Chemical Research* 33, 546-554.
- [112] **Dickerson, T. J., Reed, N. N. & Janda, K. D.** (2002). Soluble polymers as scaffolds for recoverable catalysts and reagents. *Chem. Rev.* 102, 3325-3343.
- [113] **Rafai Far, A. & Tidwell, T. T.** (1999). Soluble Polymer-Bound Allenecarboxylates: Useful  $\beta$ -Ketoester Equivalents. *J. Comb. Chem.* 1, 458-460.
- [114] **Gravert, D. J. & Janda, K. D.** (1997). Organic synthesis on soluble polymer supports: Liquid-phase methodologies. *Chem. Rev.* 97, 489-509.
- [115] **Feng, C. et al.** (2010). A Facile Synthesis of Tetrasubstituted 2,3-Dihydrofuran Derivatives Using Poly(ethylene glycol) as Soluble Support. *J. Heterocycl. Chem.* 47, 671-676.
- [116] **Arslan, M., Yilmaz, G. & Yagci, Y.** (2014). Synthesis of polystyrene-b-poly(ethylene glycol) block copolymers by radical exchange reactions of terminal RAFT agents. *Des. Monomers. Polym.* 17, 238-244.
- [117] **Okamoto, R. et al.** (2014). Total Chemical Synthesis and Biological Activities of Glycosylated and Non-Glycosylated Forms of the Chemokines CCL1 and Ser-CCL1. *Angewandte Chemie-International Edition* 53, 5188-5193.

- [118] **Dedola, S. et al.** (2014). Folding of Synthetic Homogeneous Glycoproteins in the Presence of a Glycoprotein Folding Sensor Enzyme. *Angewandte Chemie-International Edition* 53, 2883-2887.
- [119] **Izumi, M., Murakami, M., Okamoto, R. & Kajihara, Y.** (2014). Safe and efficient Boc-SPPS for the synthesis of glycopeptide-alpha-thioesters. *J. Pept. Sci.* 20, 98-101.
- [120] **Okamoto, R., Kimura, M., Ishimizu, T., Izumi, M. & Kajihara, Y.** (2014). Semisynthesis of a Post-Translationally Modified Protein by Using Chemical Cleavage and Activation of an Expressed Fusion Polypeptide. *Chemistry-a European Journal* 20, 10425-10430.
- [121] **Reuss, V. S., Obermeier, B., Dingels, C. & Frey, H.** (2012). N,N-Diallylglycidylamine: A Key Monomer for Amino-Functional Poly(ethylene glycol) Architectures. *Macromolecules* 45, 4581-4589.
- [122] **Fuertges, F. & Abuchowski, A.** (1990). The clinical efficacy of poly(ethylene glycol)-modified proteins. *J. Controlled Release* 11, 139-148.
- [123] **Brouwer, A. M.** (2011). Standards for photoluminescence quantum yield measurements in solution (IUPAC Technical Report). *Pure and Applied Chemistry* 83, 2213-2228.
- [124] **Hammick, D. L. & Locket, G. H.** (1922). CCLXXXIII.-Preparation of sodium and potassium phthalimide. *J. Chem. Soc., Trans.* 121, 2362-2363.
- [125] **Gibson, M. S. & Bradshaw, R. W.** (1968). The Gabriel Synthesis of Primary Amines. *Angew. Chem. Int. Ed.* 7, 919-930.
- [126] **Liu, Y.-X. et al.** (2008). Synthesis, herbicidal activities, and 3D-QSAR of 2-cyanoacrylates containing aromatic methylamine moieties. *J. Agric. Food. Chem.* 56, 204-212.
- [127] **Stals, P. J. M. et al.** (2012). Nitroxide-mediated controlled radical polymerizations of styrene derivatives. *J. Polym. Sci., Part A: Polym. Chem.* 50, 780-791.
- [128] **Pace, V., Hoyos, P., Fernandez, M., Sinisterra, J. V. & Alcantara, A. R.** (2010). 2-Methyltetrahydrofuran as a suitable green solvent for phthalimide functionalization promoted by supported KF. *Green Chem.* 12, 1380-1382.
- [129] **Kong, X. et al.** (2011). A Mesogenic Triphenylene-Perylene-Triphenylene Triad. *Org. Lett.* 13, 764-767.
- [130] **Pecher, J. & Mecking, S.** (2010). Nanoparticles of Conjugated Polymers. *Chemical Reviews* 110, 6260-6279.

- [131] **Kaeser, A. & Schenning, A. P. H. J.** (2010). Fluorescent Nanoparticles Based on Self-Assembled pi-Conjugated Systems. *Advanced Materials* 22, 2985-2997.
- [132] **Lutz, J.-F. & Boerner, H. G.** (2008). Modern trends in polymer bioconjugates design. *Progress in Polymer Science*, 33 (1), 1-39.
- [133] **Duncan, R.** (2003). The dawning era of polymer therapeutics. *Nat Rev Drug Discov* 2 (5), 347-360.
- [134] **Langer, R. & Tirrell, D. A.** (2004). Designing materials for biology and medicine. *Nature* 428 (6982), 487-492.
- [135] **Veronese, F. M.** (2001). Peptide and protein PEGylation: a review of problems and solutions. *Biomaterials* 22 (5), 405-417.
- [136] **Zalipsky, S.**(1995). Chemistry of polyethylene glycol conjugates with biologically active molecules. *Advanced Drug Delivery Reviews*, 16 (2-3), 157-182.
- [137] **Zhang, S. G.** (2003). Fabrication of novel biomaterials through molecular self-assembly. *Nature Biotechnology*, 21 (10), 1171-1178.
- [138] **Tu, R. S. & Tirrell, M.** (2004). Bottom-up design of biomimetic assemblies. *Advanced Drug Delivery Reviews*, 56 (11), 1537-1563.
- [139] **Niemeyer, C. M.** (2004). Living machinery. *Nature*, 429 (6995), 20-20.
- [140] **Hermanson, G. T.** (2013). Chapter 14 - Microparticles and Nanoparticles. In *Bioconjugate Techniques* (Third edition), Hermanson, G. T., Ed.; *Academic Press: Boston*, , pp 549-587.
- [141] **Hermanson, G. T.**, (2013). Front-matter. In *Bioconjugate Techniques* (Third edition), Ed.; *Academic Press: Boston*, , pp i-iii.
- [142] **Srivastava, A., O'Connor, I. B., Pandit, A. & Gerard Wall, J.** (2014). Polymer-antibody fragment conjugates for biomedical applications. *Progress in Polymer Science* 39 (2), 308-329.
- [143] **Mosiewicz, K. A., Kolb, L., van der Vlies, A. J., Martino, M. M., Lienemann, P. S., Hubbell, J. A.; Ehrbar, M. & Lutolf, M. P.** (2013). In situ cell manipulation through enzymatic hydrogel photopatterning. *Nat Mater* 12 (11), 1072-1078.
- [144] **Moazzen, E., Ebrahimzadeh, H., Amini, M. M. & Sadeghi, O.** (2013). A novel biocompatible drug carrier for oral delivery and controlled release of antibiotic drug: loading and release of clarithromycin as an antibiotic drug model. *Journal of Sol-Gel Science and Technology*, 66 (2), 345-351.

- [145] **Ramanathan, T., Fisher, F. T., Ruoff, R. S. & Brinson, L. C.** (2005). Amino-functionalized carbon nanotubes for binding to polymers and biological systems. *Chemistry of Materials* 17 (6), 1290-1295.
- [146] **Ayyadurai, N., Prabhu, N. S., Deepankumar, K., Jang, Y. J., Chitrapriya, N., Song, E., Lee, N.; Kim, S. K., Kim, B.-G., Soundrarajan, N., Lee, S., Cha, H. J., Budisa, N. & Yun, H.** (2011). Bioconjugation of L-3,4-Dihydroxyphenylalanine Containing Protein with a Polysaccharide. *Bioconjugate Chemistry* 22 (4), 551-555.
- [147] **Kesik, M.; Akbulut, H., Soylemez, S., Cevher, S. C., Hizalan, G., Udum, Y. A., Endo, T., Yamada, S., Cirpan, A., Yagci, Y. & Toppare, L.** (2014). Synthesis and characterization of conducting polymers containing polypeptide and ferrocene side chains as ethanol biosensors. *Polymer Chemistry*, 5 (21), 6295-6306.
- [148] **Sun, Y.; Cao, W., Li, S.; Jin, S., Hu, K., Hu, L., Huang, Y., Gao, X., Wu, Y. & Liang, X.-J.** (2013). Ultrabright and Multicolorful Fluorescence of Amphiphilic Polyethyleneimine Polymer Dots for Efficiently Combined Imaging and Therapy. *Scientific Reports* 3.
- [149] **Faure, A.-C., Hoffmann, C., Bazzi, R., Goubard, F., Pauthe, E., Marquette, C. A., Blum, L. J., Perriat, P., Roux, S. & Tillement, O.** (2008). Functionalization of Luminescent Aminated Particles for Facile Bioconjugation. *Acs Nano* 2 (11), 2273-2282.
- [150] **Parmar, R. G., Busuek, M., Walsh, E. S., Leander, K. R., Howell, B. J., Sepp-Lorenzino, L., Kemp, E., Crocker, L. S., Leone, A., Kochansky, C. J.; Carr, B. A., Garbaccio, R. M., Colletti, S. L. & Wang, W.** (2013). Endosomolytic Bio-reducible Poly(amido amine disulfide) Polymer Conjugates for the in Vivo Systemic Delivery of siRNA Therapeutics. *Bioconjugate Chemistry* 24 (4), 640-647.
- [151] **Audouin, F., Fox, M., Larragy, R., Clarke, P., Huang, J., O'Connor, B. & Heise, A.** (2012). Polypeptide-Grafted Macroporous PolyHIPE by Surface-Initiated N-Carboxyanhydride (NCA) Polymerization as a Platform for Bioconjugation. *Macromolecules* 45 (15), 6127-6135.
- [152] **Borase, T., Iacono, M., Ali, S. I., Thornton, P. D. & Heise, A.** (2012). Polypeptide core-shell silica nanoparticles with high grafting density by N-carboxyanhydride (NCA) ring opening polymerization as responsive materials and for bioconjugation. *Polymer Chemistry* 3 (5), 1267-1275.

- [153] **Yamada, S., Koga, K. & Endo, T.** (2012). Useful Synthetic Method of Polypeptides with Well-Defined Structure by Polymerization of Activated Urethane Derivatives of  $\alpha$ -Amino Acids. *Journal of Polymer Science Part a-Polymer Chemistry* 50 (13), 2527-2532.
- [154] **Yang, C., Ong, Z. Y., Yang, Y.-Y., Ee, P. L. R. & Hedrick, J. L.** (2011). Novel Biodegradable Block Copolymers of Poly(ethylene glycol) (PEG) and Cationic Polycarbonate: Effects of PEG Configuration on Gene Delivery. *Macromolecular Rapid Communications* 32 (22), 1826-1833.
- [155] **Toy, P. H. & Tanda, K. D.** (2000). Soluble polymer-supported organic synthesis. *Accounts of Chemical Research* 33 (8), 546-554.
- [156] **Yang, G., Chen, Z. X. & Zhang, H. Q.** (2003). Clean synthesis of an array of N-benzoyl-N'-aryl ureas using polymer-supported reagents. *Green Chemistry* 5 (4), 441-442.
- [157] **Dickerson, T. J., Reed, N. N. & Janda, K. D.** (2002). Soluble polymers as scaffolds for recoverable catalysts and reagents. *Chemical Reviews* 102 (10), 3325-3343.
- [158] **Reuss, V. S., Obermeier, B., Dingels, C. & Frey, H.** (2012). N,N-Diallylglycidylamine: A Key Monomer for Amino-Functional Poly(ethylene glycol) Architectures. *Macromolecules* 45 (11), 4581-4589.
- [159] **Huang, Y., Lu, C., Chen, Z. & Yang, G.** (2007). Traceless synthesis of quinazoline-2,4-diones by curtius rearrangement reaction using poly(ethylene glycol) as soluble polymeric support. *Journal of Heterocyclic Chemistry*, 44 (6), 1421-1424.
- [160] **Rafai Far, A. & Tidwell, T. T.** (1999). Soluble Polymer-Bound Allenecarboxylates: Useful  $\beta$ -Ketoester Equivalents. *Journal of Combinatorial Chemistry*, 1 (6), 458-460.
- [161] **Gravert, D. J. & Janda, K. D.** (1997). Organic synthesis on soluble polymer supports: Liquid-phase methodologies. *Chemical Reviews* 97 (2), 489-509.
- [162] **Feng, C., Lu, C., Chen, Z., Dong, N., Shi, J. & Yang, G.** (2010). A Facile Synthesis of Tetrasubstituted 2,3-Dihydrofuran Derivatives Using Poly(ethylene glycol) as Soluble Support. *Journal of Heterocyclic Chemistry* 47 (3), 671-676.
- [163] **Fuertges, F. & Abuchowski, A.** (1990). The clinical efficacy of poly(ethylene glycol)-modified proteins. *Journal of Controlled Release* 11 (1-3), 139-148.

- [164] Colak, D. G., Cianga, I., Demirkol, D. O., Kozgus, O., Medine, E. I., Sakarya, S., Unak, P., Timur, S. & Yagci, Y. (2012). The synthesis and targeting of PPP-type copolymers to breast cancer cells: Multifunctional platforms for imaging and diagnosis. *Journal of Materials Chemistry* 22 (18), 9293-9300.
- [165] Akbulut, H., Endo, T., Yamada, S. & Yagci, Y. (2015). Synthesis and characterization of polyphenylenes with polypeptide and poly(ethylene glycol) side chains. *Journal of Polymer Science Part A: Polymer Chemistry* DOI: 10.1002/pola.27621.
- [166] Demirel, A. L., Yurteri, S., Cianga, I. & Yagci, Y. (2005). Layered morphology of poly(phenylene)s in thin films induced by substitution of well-defined poly(epsilon-caprolactone) side chains. *Macromolecules* 38 (15), 6402-6410.
- [167] Cianga, I. & Yagci, Y. (2002). Synthesis and characterization of comb-like polyphenylenes via Suzuki coupling of polystyrene macromonomers prepared by atom transfer radical polymerization. *European Polymer Journal* 38 (4), 695-703.
- [168] Demirel, A. L., Yurteri, S., Cianga, I. & Yagci, Y. (2007). Synthesis and morphological characterization of poly(epsilon-caprolactone) and poly(2-methyloxazoline) substituted phenyl rings and phenylene oligomers. *Journal of Polymer Science Part a-Polymer Chemistry* 45 (11), 2091-2104.
- [169] Yuksel, M., Colak, D. G., Akin, M., Cianga, I., Kukut, M., Medine, E. I. Can, M., Sakarya, S., Unak, P., Timur, S. & Yagci, Y. (2012). Nonionic, Water Self-Dispersible "Hairy-Rod" Poly(p-phenylene)-g-poly(ethylene glycol) Copolymer/Carbon Nanotube Conjugates for Targeted Cell Imaging. *Biomacromolecules* 13 (9), 2680-2691.
- [170] Ag, D., Seleci, M., Bongartz, R., Can, M., Yurteri, S., Cianga, I., Stahl, F., Timur, S., Scheper, T. & Yagci, Y. (2013). From Invisible Structures of SWCNTs toward Fluorescent and Targeting Architectures for Cell Imaging. *Biomacromolecules* 14 (10), 3532-3541.
- [171] François, B., Widawski, G., Rawiso, M. & Cesar, B. (1995). Block-copolymers with conjugated segments: Synthesis and structural characterization. *Synthetic Metals* 69 (1-3), 463-466.
- [172] Scherf, U. & List, E. J. W. (2002). Semiconducting Polyfluorenes—Towards Reliable Structure–Property Relationships. *Advanced Materials* 14 (7), 477-487.
- [173] Chemli, M., Said, A. H., Fave, J.-L., Barthou, C. & Majdoub, M. (2012). Synthesis and chemical modification of new luminescent



substituted poly(p-phenylene) polymers. *Journal of Applied Polymer Science* 125 (5), 3913-3919.

- [174] **Ullrich, S. & Klaus, M.** (1997). Novel Conjugated Polymers: Tuning Optical Properties by Synthesis and Processing. In *Photonic and Optoelectronic Polymers*; American Chemical Society,; Vol. 672, pp 358-380.
- [175] **Lauter, U., Meyer, W. H. & Wegner, G.** (1997). Molecular composites from rigid-rod poly(p-phenylene)s with oligo(oxyethylene) side chains as novel polymer electrolytes. *Macromolecules* 30 (7), 2092-2101.
- [176] **Cianga, I. & Yagci, Y.** (2004). New polyphenylene-based macromolecular architectures by using well defined macromonomers synthesized via controlled polymerization methods. *Progress in Polymer Science* 29 (5), 387-399.
- [177] **Tour, J. M. & Lamba, J. J. S.** (1993). Synthesis of planar poly(p-phenylene) derivatives for maximization of extended .pi.-conjugation. *Journal of the American Chemical Society* 115 (11), 4935-4936.
- [178] **Sim, I. S., Kim, J. W., Choi, H. J.; Kim, C. A. & Jhon, M. S.** (2001). Preparation and electrorheological characteristics of poly(p-phenylene)-based suspensions. *Chemistry of Materials* 13 (4), 1243-1247.
- [179] **Fu Zhong, X. & Francois, B.** (1988). Synthesis of soluble polystyrene (PS)-poly(p-phenylene) (PPP) block copolymers: A new way towards pure PPP films. *Die Makromolekulare Chemie, Rapid Communications* 9 (6), 411-416.
- [180] **Pan, D., Turner, J. L. & Wooley, K. L.** (2003). Folic acid-conjugated nanostructured materials designed for cancer cell targeting. *Chemical Communications* (19), 2400-2401.
- [181] **Sudimack, J. & Lee, R. J.** (2000). Targeted drug delivery via the folate receptor. *Advanced Drug Delivery Reviews* 41 (2), 147-162.
- [182] **Stella, B., Arpicco, S., Peracchia, M. T., Desmaële, D., Hoebeke, J.; Renoir, M., D'Angelo, J., Cattell, L. & Couvreur, P.** (2000). Design of folic acid-conjugated nanoparticles for drug targeting. *Journal of Pharmaceutical Sciences* 89 (11), 1452-1464.
- [183] **Stals, P. J. M.; Phan, T. N. T., Gimes, D., Paffen, T. F. E., Meijer, E. W. & Palmans, A. R. A.** (2012). Nitroxide-mediated controlled radical polymerizations of styrene derivatives. *Journal of Polymer Science Part A: Polymer Chemistry* 50 (4), 780-791.

- [184] **Pace, V., Hoyos, P., Fernandez, M., Sinisterra, J. V. & Alcantara, A. R.** (2010). 2-Methyltetrahydrofuran as a suitable green solvent for phthalimide functionalization promoted by supported KF. *Green Chemistry* 12 (8), 1380-1382.
- [185] **Kim, J. M., Bogdan, M. A. & Mariano, P. S.** (1993). Mechanistic analysis of the 3-methylflavin-promoted oxidative deamination of benzylamine. A potential model for monoamine oxidase catalysis. *Journal of the American Chemical Society* 115 (23), 10591-10595.
- [186] **Hammick, D. L. & Locket, G. H.** (1922). CCLXXXIII.-Preparation of sodium and potassium phthalimide. *Journal of the Chemical Society, Transactions* 121 (0), 2362-2363.
- [187] **Nigh, W. G.** (1975). The Gabriel synthesis of benzylamine: An undergraduate organic experiment. *Journal of Chemical Education* 52 (10), 670.
- [188] **Gibson, M. S. & Bradshaw, R. W.** (1968). The Gabriel Synthesis of Primary Amines. *Angewandte Chemie International Edition in English* 7 (12), 919-930.
- [189] **Liu, Y.-X., Wei, D.-G., Zhu, Y.-R., Liu, S.-H., Zhang, Y.-L., Zhao, Q.-Q., Cai, B.-L., Li, Y.-H., Song, H.-B., Liu, Y., Wang, Y., Huang, R.-Q. & Wang, Q.-M.** (2008). Synthesis, herbicidal activities, and 3D-QSAR of 2-cyanoacrylates containing aromatic methylamine moieties. *Journal of Agricultural and Food Chemistry* 56 (1), 204-212.
- [190] **Kong, X., He, Z., Zhang, Y., Mu, L., Liang, C., Chen, B., Jing, X. & Cammidge, A. N.** (2011). A Mesogenic Triphenylene-Perylene-Triphenylene Triad. *Organic Letters* 13 (4), 764-767.
- [191] **Neises, B. & Steglich, W.** (1978). Simple Method for the Esterification of Carboxylic Acids. *Angewandte Chemie International Edition in English* 17 (7), 522-524.
- [192] **Miyaura, N. & Suzuki, A.** (1995). Palladium-Catalyzed Cross-Coupling Reactions of Organoboron Compounds. *Chemical Reviews* 95 (7), 2457-2483.
- [193] **Fahnenstich, U., Koch, K.-H. & Müllen, K.** (1989). Polynaphthylenes, 1. Synthesis of soluble poly(3,7-di-tert-butyl-1,5-naphthylene) via palladium-catalyzed coupling. *Die Makromolekulare Chemie, Rapid Communications* 10 (11), 563-569.
- [194] **Ito, K., Tomi, Y. & Kawaguchi, S.** (1992). Poly(ethylene oxide) macromonomers. 10. Characterization and solution properties of the regular comb polymers with polystyrene main chains and

poly(ethylene oxide) side chains. *Macromolecules* 25 (5), 1534-1538.

- [195] **Pecher, J. & Mecking, S.** (2010). Nanoparticles of Conjugated Polymers. *Chemical Reviews* 110 (10), 6260-6279.
- [196] **Kaaser, A. & Schenning, A. P. H. J.** (2010). Fluorescent Nanoparticles Based on Self-Assembled  $\pi$ -Conjugated Systems. *Advanced Materials* 22 (28), 2985-2997.
- [197] **Ag, D., Bongartz, R., Dogan, L. E., Selici, M., Walter, J.-G., Demirkol, D. O., Stahl, F., Ozcelik, S., Timur, S. & Scheper, T.** (2014). Biofunctional quantum dots as fluorescence probe for cell-specific targeting. *Colloids and Surfaces B: Biointerfaces* 114 (0), 96-103.
- [198] **Low, P. S. & Kularatne, S. A.** (2009). Folate-targeted therapeutic and imaging agents for cancer. *Current Opinion in Chemical Biology* 13 (3), 256-262.
- [199] **Saul, J. M., Annapragada, A. & Natarajan, J. V.; Bellamkonda, R. V.** (2003). Controlled targeting of liposomal doxorubicin via the folate receptor in vitro. *Journal of Controlled Release* 92 (1-2), 49-67.



## CURRICULUM VITAE



**Name Surname:** Hüseyin AKBULUT

**Place and Date of Birth:** Fatih-1985

**E-Mail:** zeferan@gmail.com

**University and College Degrees obtained:**

**2012 – 2015** Philosophy of Doctorate

Chemistry, Istanbul Technical University, Graduate School of Science  
Engineering and Technology

**2009 – 2011** Master of Science

Chemistry, Istanbul Technical University, Graduate School of Science  
Engineering and Technology

**2003 – 2007** Bachelor of Science

Chemistry, Faculty of Art and Sciences, Ataturk University

**Publications from thesis:**

- **Akbulut, H.**, Yavuz, M., Guler, E., Demirkol, D. O., Endo, T., Yamada, S., Timur, S. & Yagci, Y. (2014). Electrochemical deposition of polypeptides: bio-based covering materials for surface design. *Polymer Chemistry* 5 (12), 3929-3936.
- **Akbulut, H.**; Endo, T., Yamada, S. & Yagci, Y. (2015). Synthesis and characterization of polyphenylenes with polypeptide and poly(ethylene glycol) side chains. *Journal of Polymer Science Part a-Polymer Chemistry*, 53 (15), 1785-1793.
- **Akbulut, H.**; Guler, B., Timur, S. & Yagci, Y. (2015). Synthesis, characterization and targeted cell imaging applications of poly(p-phenylene)s with amino and poly(ethylene glycol) substituents. *RSC Advances*, 5 (75), 60861-60869.

**Publications:**

- Yucel, B., Sanli, B., Soylemez, H. & **Akbulut, H.** (2012). Palladium-catalyzed reaction of 2-iodoferrocenyl alcohols with internal alkynes: Synthesis of functionally 1,2-disubstituted ferrocenes and ferroceno-pyrans. *Journal of Organometallic Chemistry* 704, 49-64.
- Yucel, B.; Sanli, B., **Akbulut, H.**, Ozbey, S. & Benniston, A. C. (2012). Colour-responsive fluorescent oxy radical sensors. *Organic & Biomolecular Chemistry* 10 (9), 1775-1784.
- Kesik, M., **Akbulut, H.**, Soylemez, S., Cevher, S. C., Hizalan, G., Udum, Y. A., Endo, T., Yamada, S., Cirpan, A., Yagci, Y. & Toppare, L. (2014). Synthesis and characterization of conducting polymers containing polypeptide and ferrocene side chains as ethanol biosensors. *Polymer Chemistry* 5 (21), 6295-6306.